SU, M2 GEOP, 2018

Petroleum systems :
links with tectonic evolution

Olivier LACOMBE

Petroleum systems in fold-and-thrust belts

Hydrocarbon discoveries in FTBs date back to oil exploration in the late 19th and early 20th.

The primary reason for these discoveries was that early drilling focused on structurally simple anticlines that could be mapped using the surface geology, which mimicked the subsurface structure at the reservoir level.
This ultimately led to the discovery of super-giant oilfields in the Zagros (Iran-Iraq) in the early 20th century.

However, 80% of the giant fields were discovered after 1950 because of the challenges of exploring in structurally complex terrain. For example, in Wyoming the first discovery was in 1900, but it was not until the late 1970s that the first giant field (Whitney Canyon-Carter Creek) was discovered.

Structural complexity is a major problem when exploring many FTBs because the surface structural expression is commonly decoupled from the subsurface structural geometry at the reservoir level.

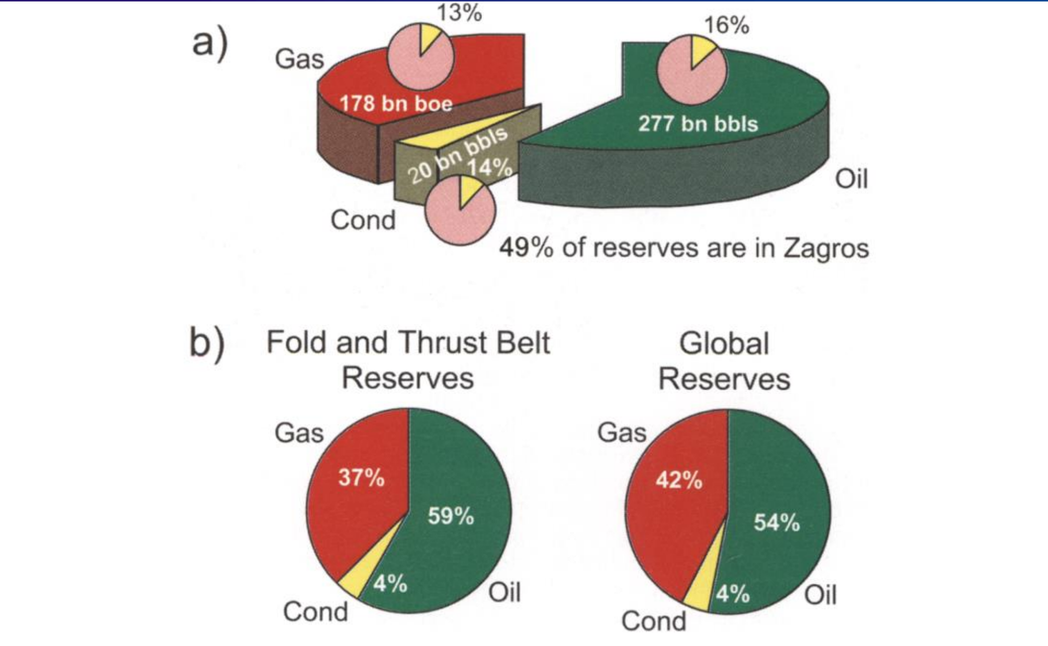

(a) Distribution of hydrocarbon type in fold and thrust belts; total volumes are indicated on the pie chart segments. The yellow segments of the smaller pie charts indicate the proportions of global reserves in fold and thrust belts for each hydrocarbon type with the actual percentage labelled. (b) Comparison of hydrocarbon type split between fold and thrust belts and all global reserves.

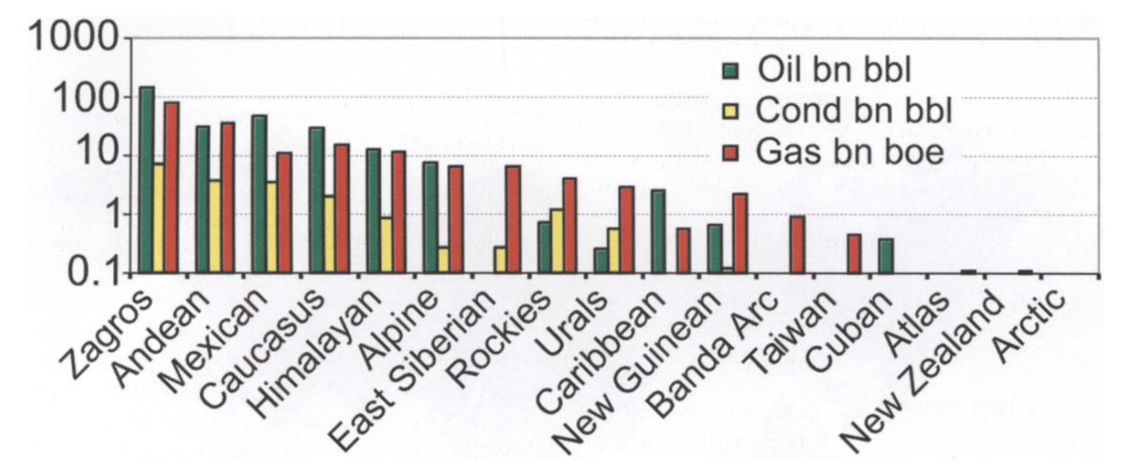

Logarithmic graph of the distribution of hydrocarbon reserves in fold and thrust belts grouped by orogenic belt (Table 1), in order of decreasing total reserves. Green, oil in bn bbls; yellow, condensate in bn bbl; red, gas in bn boe.

(Cooper, 2007)

Influence of the age of the onset of the last phase of deformation

The Pliocene age deformation of the Zagros is dominant.

The Miocene and Palaeocene are the second and third most important times of hydrocarbon-rich FTB development. All other times are volumetrically insignificant by comparison.

The preservation potential of a FTB is enhanced when it is relatively young.

As the age of deformation becomes progressively greater, there is more chance of the FTB being uplifted and eroded (e.g. Appalachians) or buried to uneconomic depths beneath a later passive margin (e.g. the Variscan FTB beneath the European Atlantic margin).

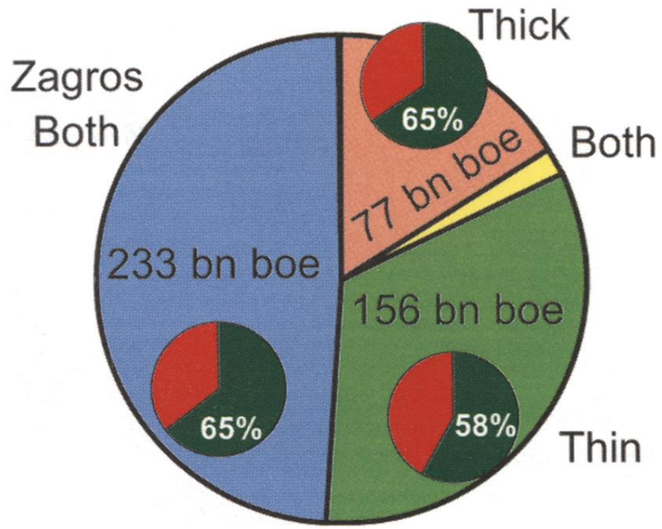

Fig. 10. Graph of the distribution of hydrocarbon reserves in fold and thrust belts grouped by thin- or thick-skinned deformation style (Table 1). The pie chart shows the total reserves for each grouping of deformation style; total volumes are labeled on the pie chart segments. The smaller pie charts indicate the proportions of oil and condensate to gas for each deformation style with the percentage of oil and condensate labelled. Green, oil and condensate; red, gas.

Influence of the tectonic style

Thin-skinned deformation accounts for c. 60% of reserves in FTBs excluding the Zagros (that shows both thick- and thin-skinned deformation.

Thick-skinned FTBs have a slightly higher oil:gas ratio in comparison with thin-skinned FTBs, but neither differs significantly from the overall oil:gas ratio in FTBs.

(Cooper, 2007)

Influence of late burial of FTBs

some FTBs have been buried by either syn- or post-depositional sediments (e.g., Northern Apennines). Normally, thrusting is associated with elevation and the simple structures of the frontal zones form last and will post-date the significant loading and hydrocarbon generation.

Burial, however, encourages maturation of the source after trap formation if the source was either immature or early mature during the deformation.

Influence of occurrence of salt decollement

The presence of a salt has a strong influence on the deformation style, tending to favour thin-skinned structures as a result of the efficiency of the decollement.
The Zagros is problematic in this analysis, the Cambrian Hormuz Salt is present only in the SE part of the Zagros, which is less petroliferous.

FTBs with no salt decollement dominate the reserves, excluding the Zagros; in FTBs with no salt decollement the oil:gas ratio is c. 50:50, in contrast to FTBs with a salt decollement, where the oil:gas ratio is about 80:20.

This could be due to the salt decollement inhibiting the migration of gas from secondary deeper and more mature source rock horizons beneath the salt decollement into the traps located above the decollement.

Where to look for hydrocarbons in FTBs ?

Predictably, oil and gas fields are aligned parallel to the structural trend.

The most prospective are for hydrocarbons is the external foothills belt between the leading thrust of the internal zone and the limit of thrusting in the foreland basin, whether emergent or buried, i.e., a band along the external fringe of the thrust belt.

This is because normally the generation and expulsion front moves ahead of the deformation front and the normal asymmetry of the basin encourages migration into the foreland. As a result, there is a stronger possibility of the frontal thrust creating a giant field than for structures further back from the thrust front.

In contrast :

-toward the hinterland the reservoir horizons tend to be breached and flushed, older source rocks may be overmature, and younger source rocks, present in the clastic foredeep, may be absent.

-toward the foreland, the reservoir horizons tend to be depositionally thinner, the source rocks may be immature, the young source rocks may overlie the reservoir, and the structural traps may be small or absent.

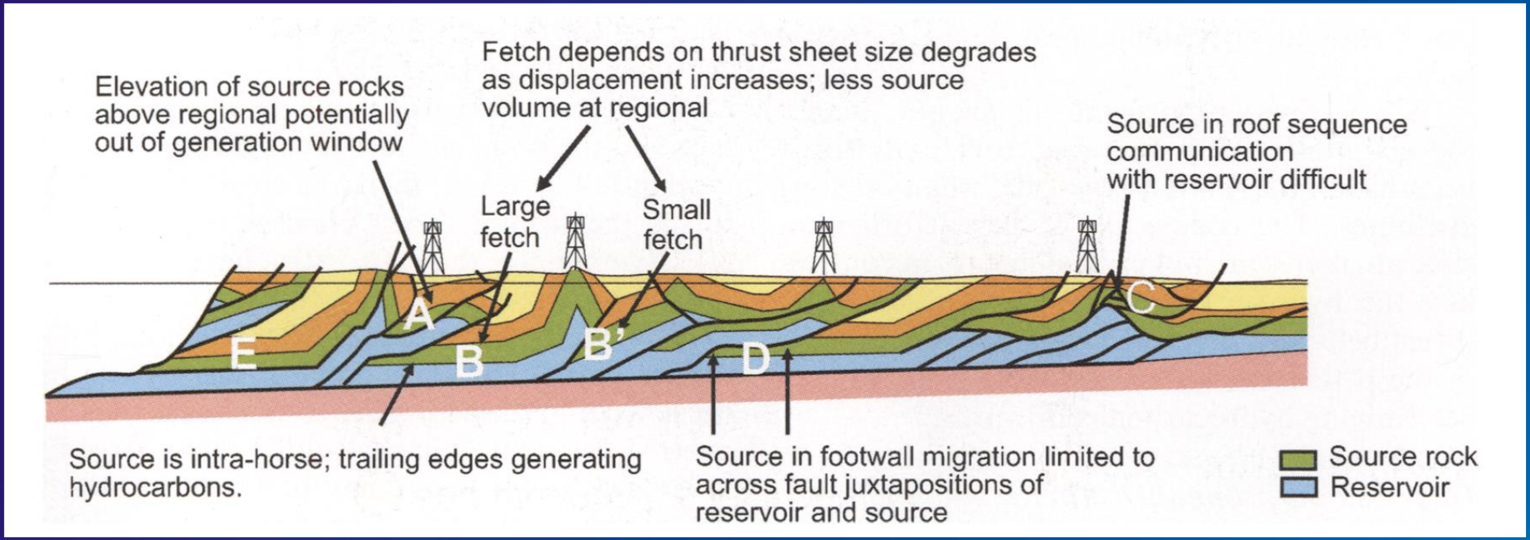

A : Thrust systems elevate rocks above their regional elevation, thus potentially removing the source rocks from the generating window

C : If the source is in the roof sequence communication with the reservoir may be difficult to achieve.

D : If the source is in the footwall similar problems apply but in addition migration pathways will be limited by the availability of across-fault juxtaposition of reservoir and source.

The system works if :
- subsequent burial of the thrust belt by syn-orogenic sediments puts the entire system, including source and traps, in the maturity window. In this case, traps predate the generation and migration of hydrocarbons.
- thrusting is synchronous with, or shortly post-dated rapid burial by foreland basin sediment. The loading effect of the thrust belt creates the accommodation space in the foreland basin, which is then progressively cannibalized by the prograding thrust system. In this case, the structures develop as the source rocks are in the maturity window; much of the early charge may migrate into the foreland basin but the later charge is trapped.
- thrusting pushes the source into the generation window (E).

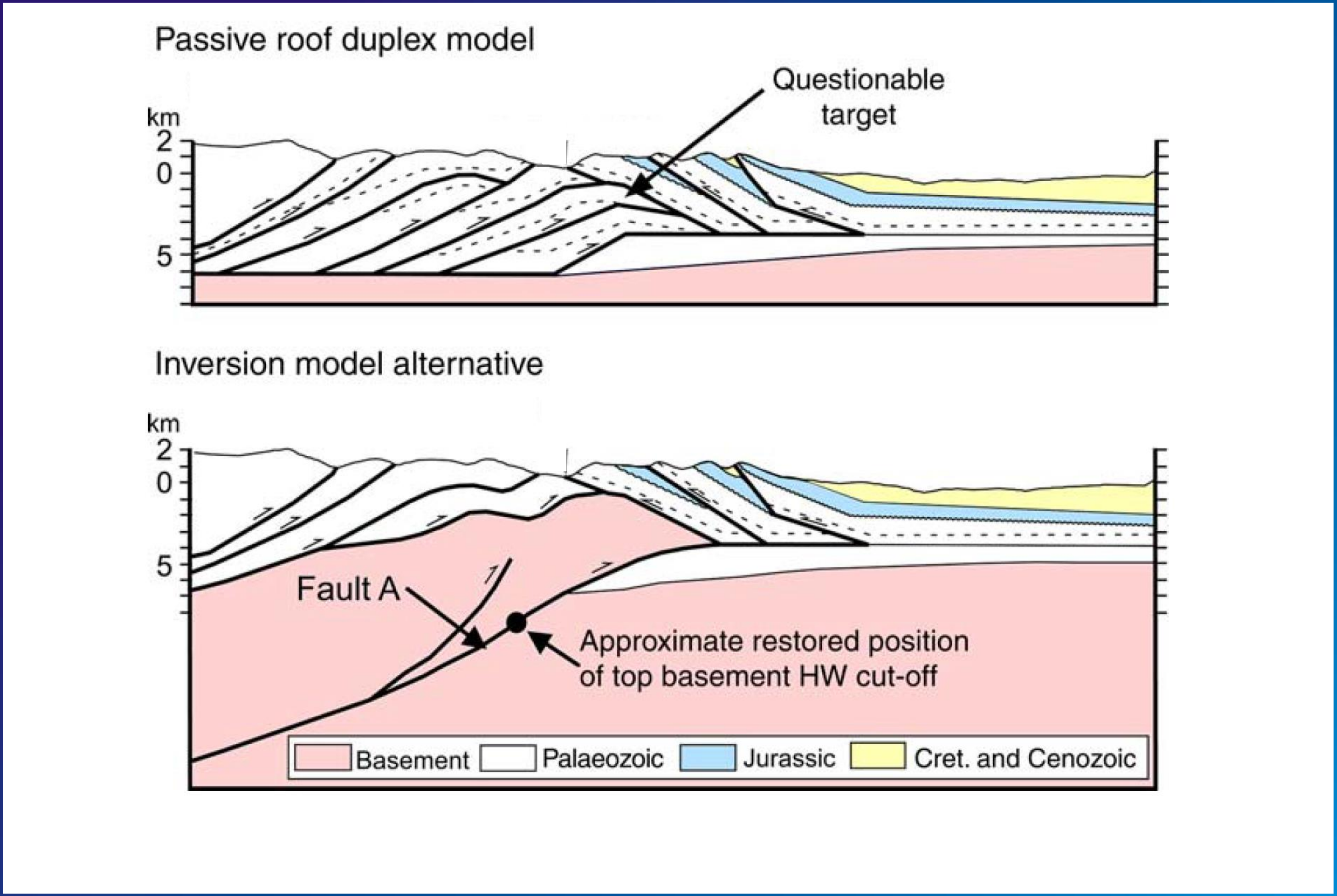

(Cooper and Warren, 2010)

Defining the structural style of fold–thrust belts and understanding the controlling factors are necessary steps to assess their potential in terms of hydrocarbon exploration.

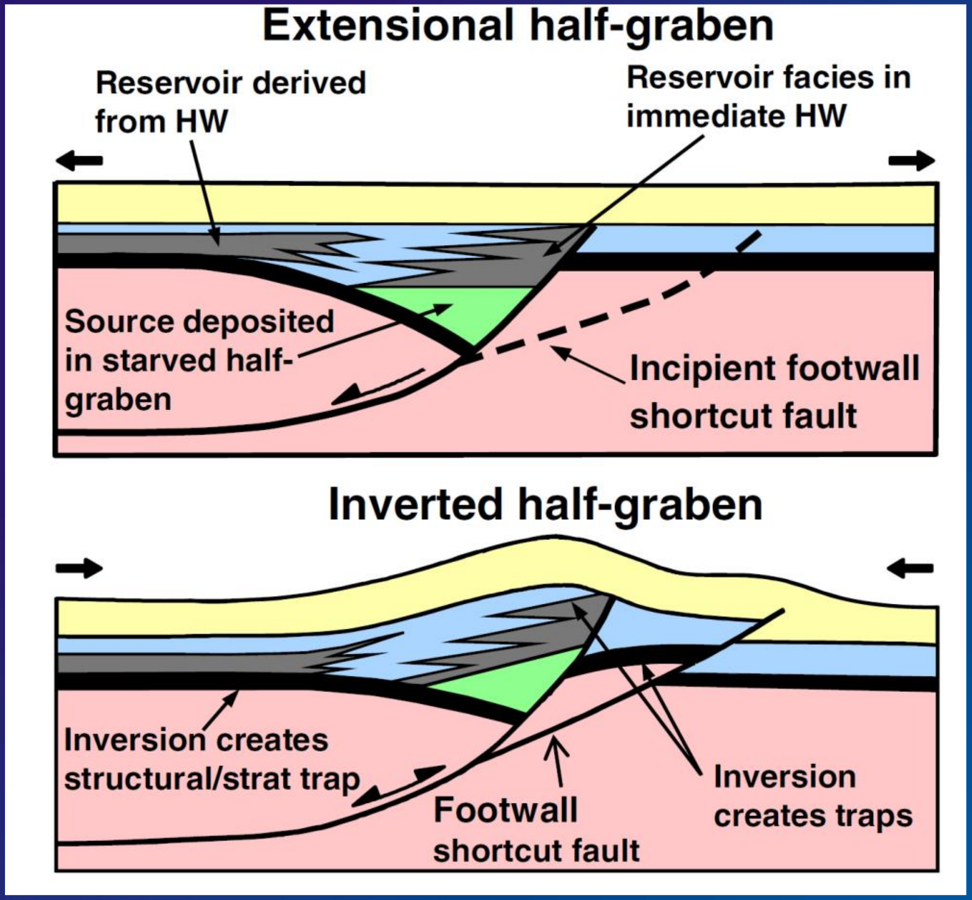

(Cooper and Warren, 2010)

The precursor extensional fault commonly controls reservoir distribution and deposition in the hanging wall of the fault system : as accommodation space is created during extensional faulting the extensional fault geometries and in particular transfer zones and relay ramps will strongly control sediment dispersion pathways into the developing basin, This is a major factor in controlling where reservoir facies will be deposited.

Extensional faulting can also control seal distribution, e.g., intraformational shales that commonly separate reservoir sands.

The accommodation space created during extension can also control source rocks distribution, particularly in situations where the evolving basin is starved of sediment and anoxic conditions develop due to restricted circulation.

Extensional faulting can also control source maturation in the fault-controlled depocentre,

The extensional faulting can also create structural trap geometries in both the footwall and hanging wall of the fault.

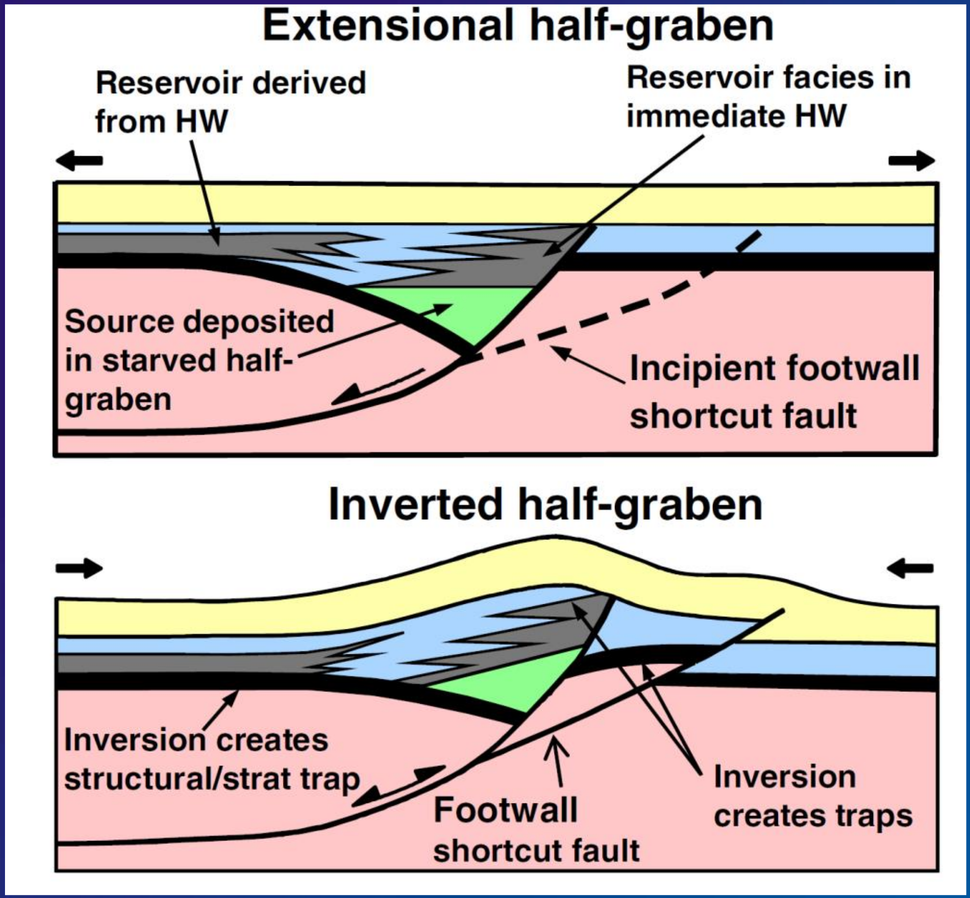

The compressional inversion of the extensional fault system will principally affect structural trap configurations, creating new trap geometries such as footwall shortcut structures and the inversion anticline.

The inversion can also modify older structural trap geometries which could result in the re-migration of pre-inversion hydrocarbon accumulations.

Inversion can also create new trap geometries by turning a facies change from reservoir to seal in a down dip direction into a viable stratigraphic trap that occurs in an updip direction.

However, the uplift above regional elevation that is a product of inversion, if significant, can result in erosion of one or more critical components of the petroleum system.

(Cooper and Warren, 2010)

Petroleum systems in fold-and-thrust belts : the Albania case study

Related to alpine orogeny between Hellenides and Dinarides

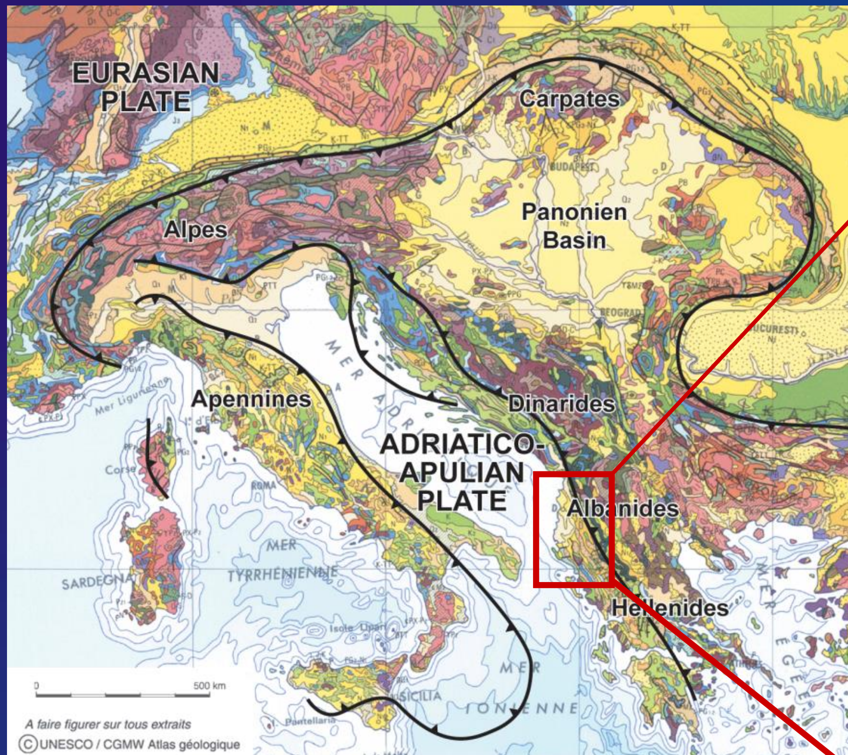

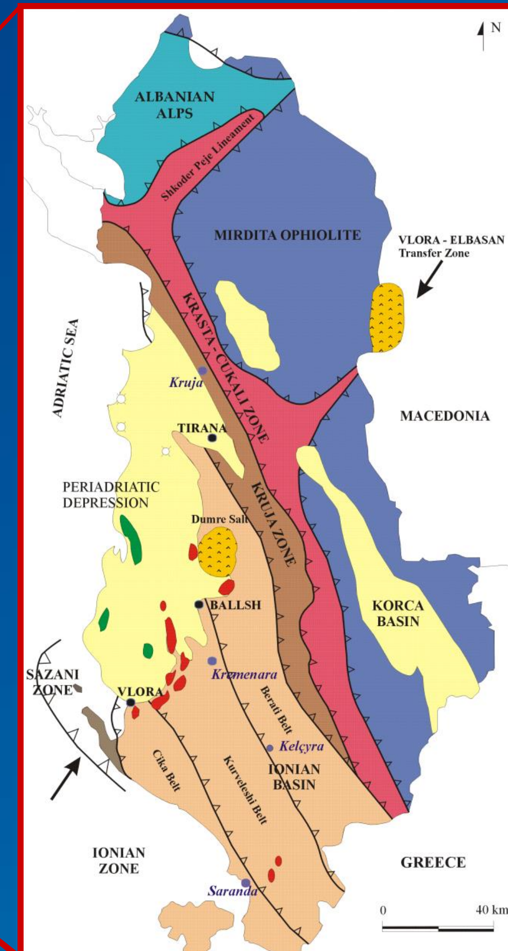

The Outer Albanides constitute one of the European foredeep basins in which the synorogenic series are the best preserved. Because of these unusual conditions, it is possible to constrain the kinematics of the deformation and trace the burial and thermal evolution of potential source rocks and reservoirs.

The northern part of the Outer Albanides comprises two distinct domains :

(1) the Peri-Adriatic Depression, where only the Neogene molasse of the foredeep crops out at the surface;

(2) the Kruja Zone which comprises thrust anticlines of Mesozoic platform carbonates.

The southern part of the Outer Albanides is almost entirely made up of Mesozoic-Paleogene basinal units of the Ionian Zone, detached from its former substratum along an intra-Triassic evaporitic series.

The Triassic evaporite constitutes the main decollement in the Ionian Basin, although Toarcian Posidonia Schist and Oligocene flysch are likely to provide secondary decoupling horizons.

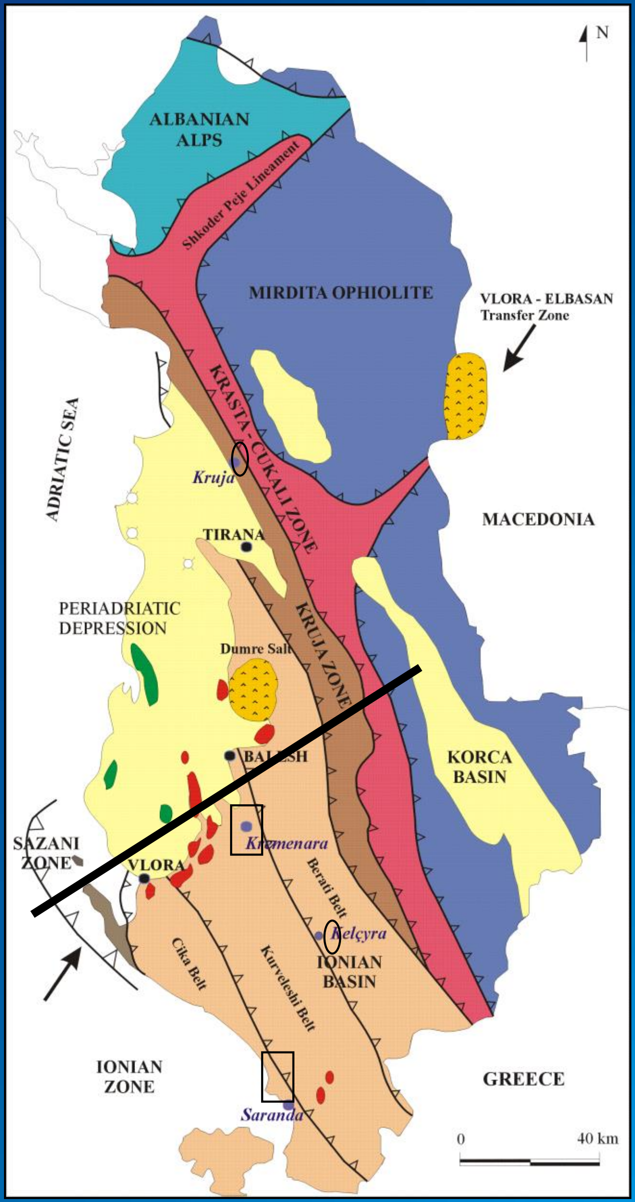

Kruja: ridge with mainly shallow water lst.

Ionian - a broad furrow (deep marine pelagic lst.)

Sazani - shallow water lst.

Peri-Adriatic depression – siliciclastic (7Km)

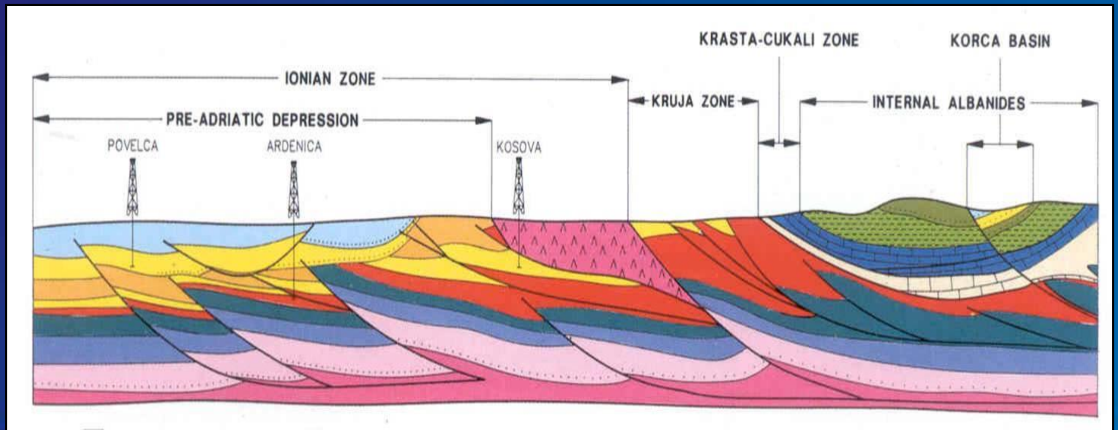

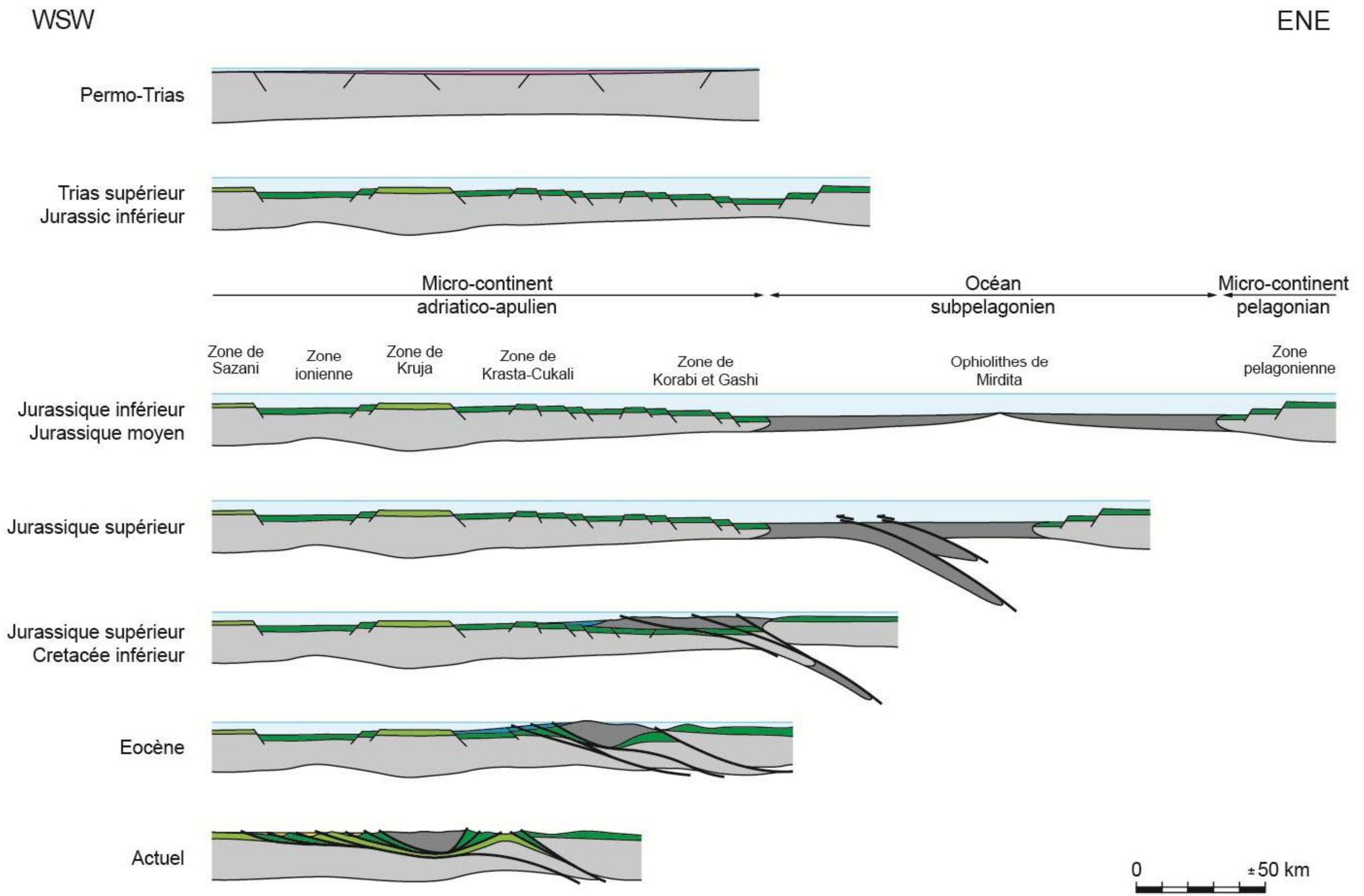

(Barrier et al, 2003)

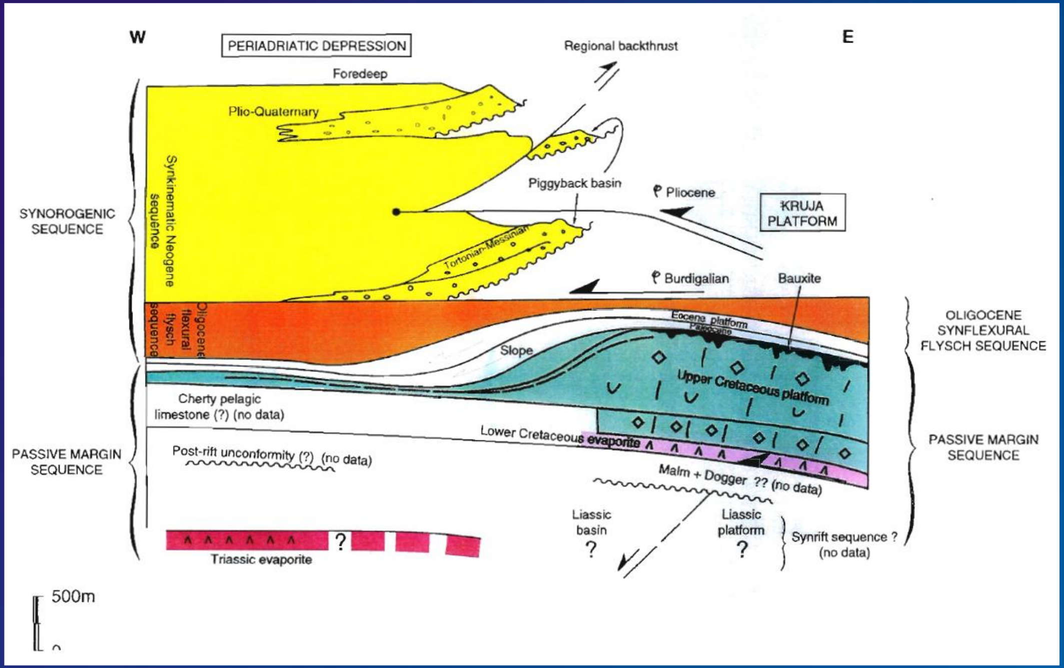

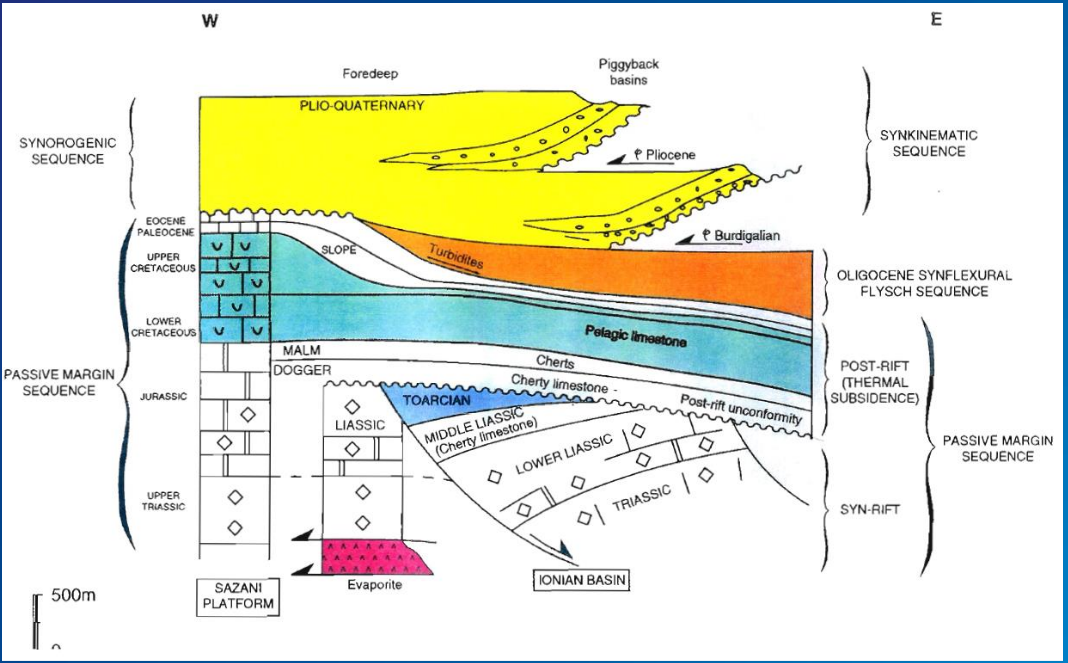

(Roure et al, 2004)

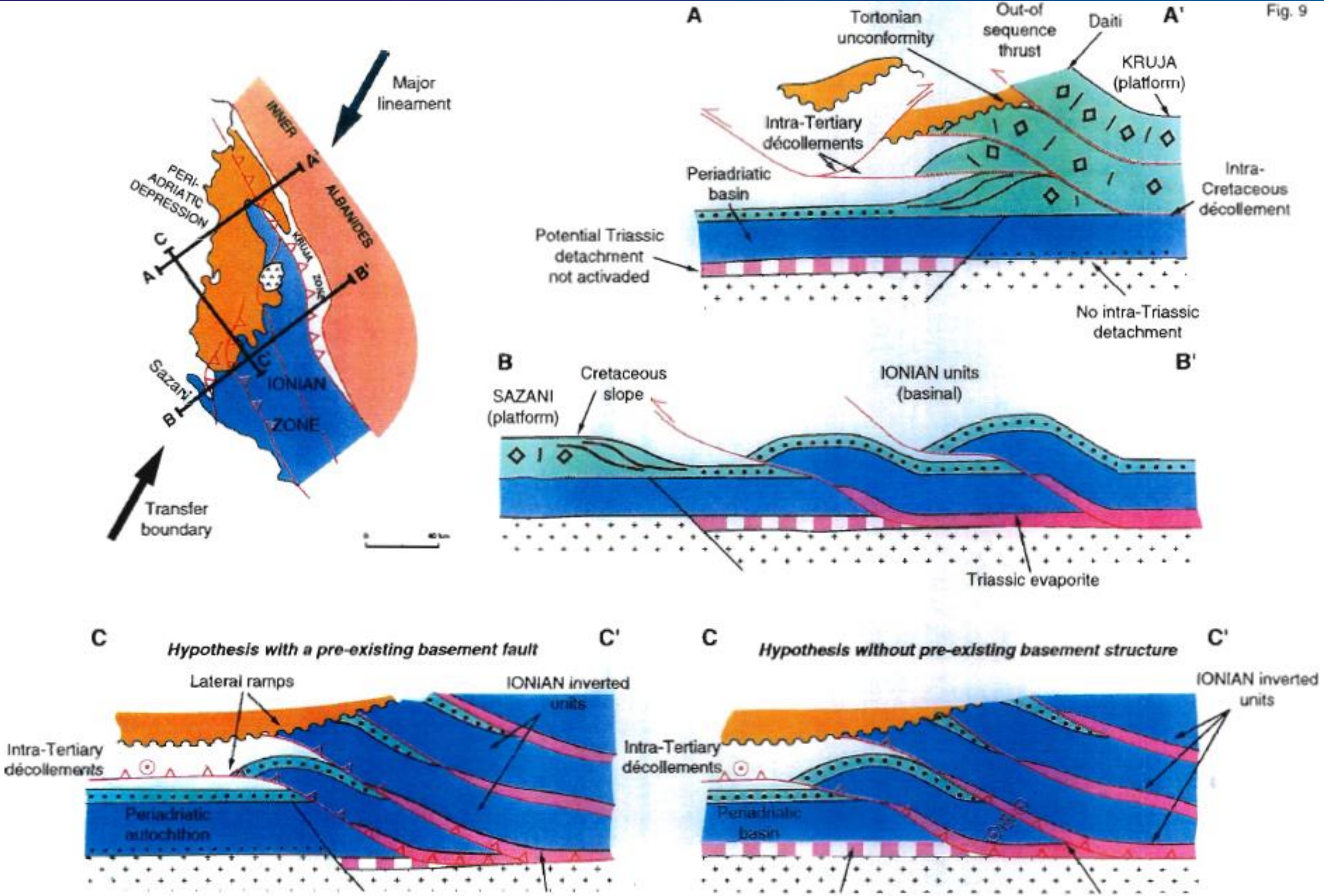

(Roure et al, 2004)

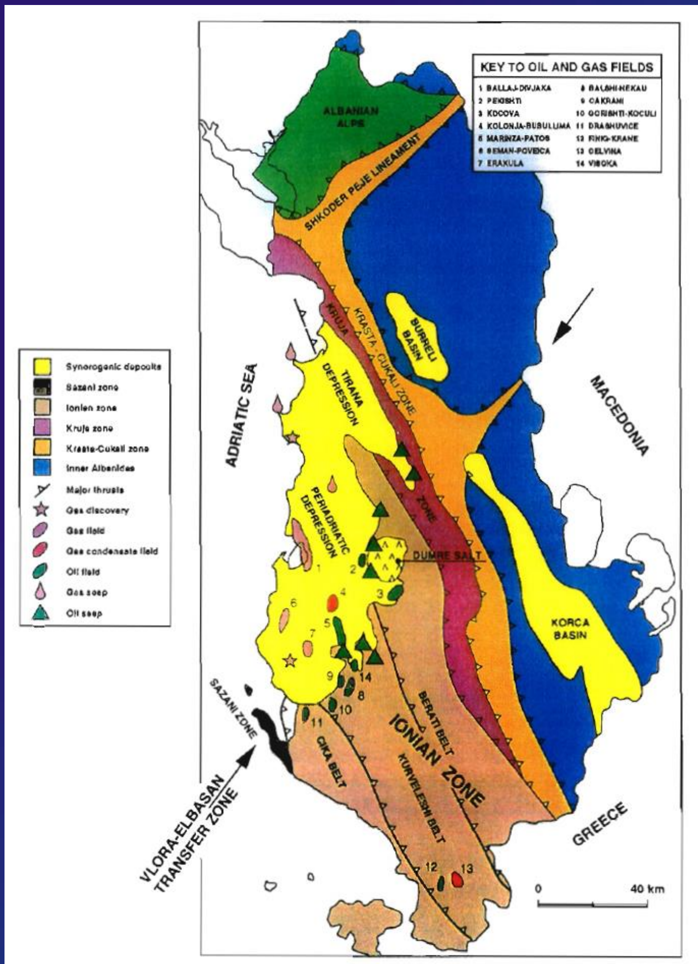
KEY TO OIL AND GAS FIELDS
1 BALLAJ-DIVJAKA
2 PEKISHTI
3 KOCOVA
4 KOLONJA-BUBULLIMA
5 MARINZA-PATOS
6 SEMAN-POVELCA
7 ERAKULA
8 BALSHI-HEKAU
9 CAKRANI
10 GORISHTI-KOCULI
11 DRASHUVICE
12 FINIQ-KRANE
13 DELVINA
14 VISOKA
Synorogenic deposits
Sazani zone
Ionian zone
Kruja zone
Krasta-Cukali zone
Inner Albanides
Major thrusts
Gas discovery
Gas field
Gas condensate field
Oil field
Gas seep
Oil seep
ALBANIAN ALPS
SHKODER PEJE LINEAMENT
KRUJA
KRASTA-CUKALI ZONE
BURRELI BASIN
ADRIATIC SEA
TIRANA DEPRESSION
PERIADRIATIC DEPRESSION
MACEDONIA
DUMRE SALT
KORCA BASIN
SAZANI ZONE
BERATI BELT
IONIAN ZONE
CIKA BELT
KURVELESHI BELT
VLORA-ELBASAN TRANSFER ZONE
GREECE
0
40 km

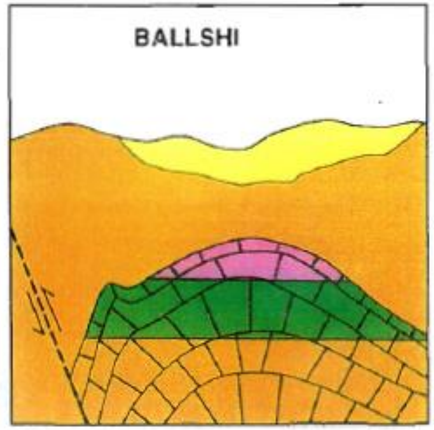
BALLSHI

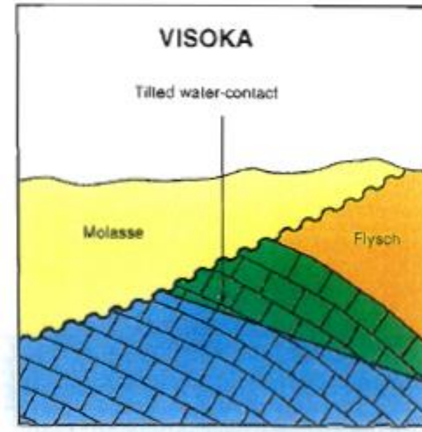
VISOKA
Tilted water-contact
Molasse
Flysch

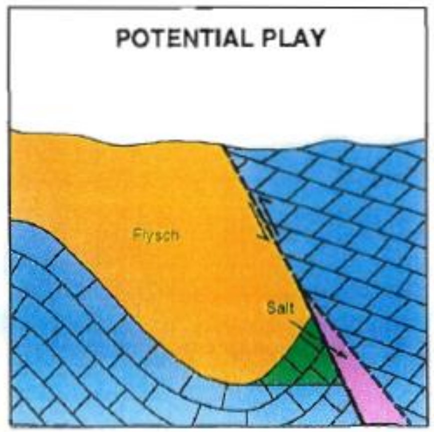
POTENTIAL PLAY
Flysch
Salt

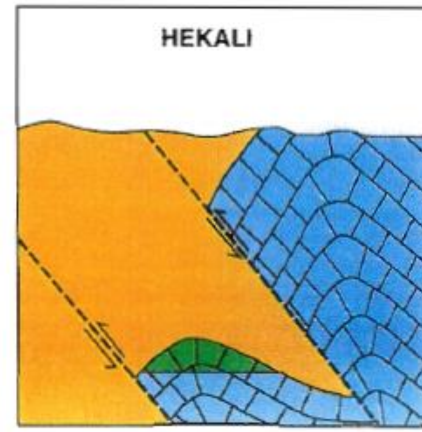
HEKALI

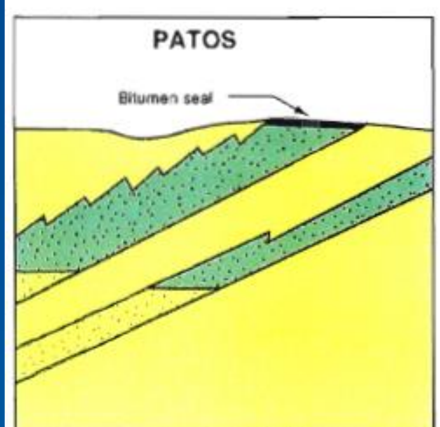
PATOS
Bitumen seal

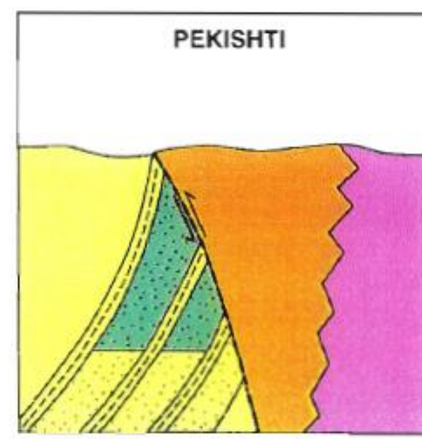
PEKISHTI

WORFLOW FOR PETROLEUM MODELING

Subsurface Data (Wells And Seismic) and Selection of the Modeled Transects

* seismic coverage mostly continuous and of sufficient quality, and reasonable number of calibration wells

Calibration, Interpretation and Depth Conversion of the Seismic Profiles

Cross-section Balancing

* Restoration of structural sections using the Locace software, with a line-length balance and constant thickness hypothesis.

Construction of Forward Kinematic Models Using the Thrustpack Software

*Once restored, the initial geometries were used as the initial template in the Thrustpack forward kinematic modeling. These initial sections provided the requisite thickness values to simulate the former Mesozoic to Eocene passive-margin series, prior to their burial beneath the Oligocene flexural and Neogene synkinematic series, and also provided the spacing of future thrusts.

Incremental deformation was applied successively to the various thrust faults identified with coeval activation of synorogenic sedimentation, erosion, and flexure, to account for the geometries and unconformities observed on seismic profiles and in structural sections. Using a trial-and-error procedure, it was possible to achieve a realistic kinematic model. When the resulting geometries were reasonably similar to the modern seismic imagery and thus, they were considered representative of the burial history of potential source-rock and reservoir intervals

Zone/belt	Age	Rock Type	Sample Type	Depth of Well Samples (m)	Source Bed thickness (m)	TOC %	HI mgHC/g org.C	Tmax	Kerogen Type	Ro	No. Data Pts
Kruia	Eocene	Black Sh	Outcrop	–	NM	3.95	197	428	I/II	0.46	1
	U.Cret	Dol	Outcrop	–	19.0	0.52	530	425	I	NM	30
Kurveleshi	U/L Cret	Shale	Outcrop	–	NM	26.01	700	413	I	0.48	11
		Shale	Well	2313	NM	1.61	521	413	Inert I	0.53	1
	U Jur	Shale	Outcrop	–	NM	1.50	520	480	I	0.51	10
	M Jur	Shale	Outcrop	–	NM	5.25	508	482	I	0.52	8
		Arg Lst	Well	2923-2924	NM	2.00	505	424	Inert I	0.57	1
	Toarcian	Shale	Outcrop	–	NM	4.00	588	482	I/III	0.55	6
	L Jur	Dol Shale	Outcrop	–	NM	15.66	450	434	I/II	0.55	7
Cika	U/L Cret	Shale	Outcrop	–	0.5	15.38	666	424	I	NM	5
	UTrias/LJur	Dol	Outcrop	–	2.5	29.16	778	409	I	0.65	15
	U Trias	Dol Shale	Outcrop	–	15.2	4.96	617	416	I	0.70	21
Sazani	U Trias	Shale	Well	3822-3822	10	0.16	162	424	Inert I	0.87	2

Table 1 Summary of source bed data informations supplied by the Geologcal Institute, Fieri. (NM = not measured)

Distribution and Characteristics of the Potential Source Rocks

Triassic Source Rocks
*the oldest potential source-rock intervals are located within Upper Triassic series
Ro values are between 0.7 and 0.9, thus indicating a mature source rock. Because they relate to surface samples, these values attest to an early maturation of the Triassic series, which eventually reached the oil window and started to expel hydrocarbons long before the onset of thrusting

These observed maturity likely results from sedimentary burial, the maximum thickness of sediments probably being recorded prior to the late Oligocene-Aquitanian orogenic event—that is, during deposition of the lower Oligocene synflexural flysch.

	SAZANI Z.	IONIAN Z.	PERI-ADRIATIC Z.	KRUJA Z.	Tectonic events	Thrustpack stages
Pliocene-Quaternary	erosion	erosion	molasse R	erosion	mud diapirs late shortening	**Stage 5** 5 Ma (B.P.)
Messinian Tortonian Langhian-Serravallian Burdigalian Aquitanian	turbidite? calcarenite	molasse R local emersion	turbidite R S deep water?	molasse emersion	Messinian evaporitic seal continuous shortening growth anticlines	5 Ma **Stage 4** 10 Ma **Stage 3** 15 Ma **Stage 2**
Oligocene	emersion	flysch **Seal**	flysch **S?**	flysch **Seal**	onset foreland flexure	20 Ma **Stage 1** 30 Ma
Eocene Paleocene	emersion bauxite	R		emersion bauxite		30 Ma **Stage 0** 70 Ma
Upper Cretaceous Lower Cretaceous	**R ?** Platform	**R** carbonate turbidite **S**	no data	**S ? R ?** Platform **S ?**	salt diapirs passive margin	
Upper Jurassic Middle Jurassic Lower Jurassic	Platform	basinal sequence Posidonia source **S - Seal**	no data	no data	synrift extension	
Triassic	**S** dolomite salt ?	**S** dolomite **R** basal salt	no salt?			
Hercynian basement	no data	no data	no data	no data		

Jurassic Source Rocks

*At least four organic-rich intervals within the Ionian Jurassic series, including the Toarcian Posidonia Schist.
PS well exposed in the Mali Gjere unit of the Ionian Basin.Toarcian series can locally exceed 300 m in thickness, and they constitute the most prolific source-rock interval of the Ionian Basin
Ro lower than 0.55 : rocks are immature. The preservation of such low-maturity at the surface precludes their deep former burial beneath the Oligocene to Neogene flexural sequence as is currently imaged for coeval series in the Peri-Adriatic Depression. This instead suggests that most Ionian structures started to develop as growth anticlines very early during the foothills evolution, most likely before or during the late Oligocene. In contrast, the same source-rock intervals are likely to have reached the oil window locally in subthrust domains, during subsequent Neogene episodes of tectonic burial.

Cretaceous Source Rocks

*bituminous shales and carbonates have been found at the boundary between Lower and Upper Cretaceous intervals
In the Kruja Zone, TOC reaches 4%, and Ro lower than 0.5. These source-rock horizons of the Peri-Adriatic Depression are still deeply buried and attached to the autochthonous foreland. Therefore, their maturity has increased constantly during Neogene sedimentary and tectonic burial.

	SAZANI Z.	IONIAN Z.	PERI-ADRIATIC Z.	KRUJA Z.	Tectonic events	Thrustpack stages
Pliocene-Quaternary	erosion	erosion	molasse **R**	erosion	mud diapirs late shortening	**Stage 5** 5 Ma (B.P.)
Messinian Tortonian Langhian-Serravalian Burdigalian Aquitanian	turbidite? calcarenite	molasse **R** local emersion	turbidite **R** **S** deep water?	molasse emersion	Messinian evaporitic seal continuous shortening growth anticlines	5 Ma **Stage 4** 10 Ma **Stage 3** 15 Ma **Stage 2**
Oligocene	emersion	flysch **Seal**	flysch **S?**	flysch **Seal**	onset foreland flexure	20 Ma **Stage 1** 30 Ma
Eocene Paleocene	emersion bauxite	**R**		emersion bauxite		30 Ma **Stage 0**
Upper Cretaceous Lower Cretaceous	**R ?** Platform	**R** carbonate turbidite **S**	no data	**S ? R ?** Platform **S ?**	salt diapirs passive margin	70 Ma
Upper Jurassic Middle Jurassic Lower Jurassic	Platform	basinal sequence Posidonia source **S - Seal**	no data	no data	synrift extension	
Triassic	**S** dolomite salt ?	**S** dolomite **R** basal salt	no salt?			
Hercynian basement	no data	no data	no data	no data		

Cenozoic Source Rocks

*display a terrestrial signature with a type-III kerogen. Mostly immature (Ro between 0.3 and 0.5) and considered to be good only for generating biogenic gas samples collected within the Neogene molasses of the Peri-Adriatic Depression. Nevertheless, because of the extremely wide range of burials recorded by these series, and despite the low geothermal gradients measured in the Peri-Adriatic Depression, part of the Neogene strata are probably already in the oil window.

Age	Formation member	Matrix Porosity %	Permeability (md)	Remarks
Western Mollasse Belt				
Pliocene	Helmesi Formation	16-32	2-35	Ballaj-Divjaka Gas Field
Tortonian to Messinian	Frakulla & Divjaka formations	13-28	7-45	Divjaka. Frakulla Povelca Gas Fields
Eastern Transgressive Belt				
Messinian	Kucova member	25-30	500-2000	Marinza. Kucova Kolonja Oil Fields
	Gorani member	17-30	500-600	
	Druza member	25-32	Upto 200	
	Marinza member	21-26	600-2000	
	Bubullima member	10-25	200-400	

Table 3 : Petrophysical charateristics of major reservoirs of the synorogenic sequence

Age	Formation/Facies	Effective Porosity %		Permeability	Remarks
		Matrix+Vuggy	Fracture		
KRUJA ZONE					
Paleocene/Eocene	Organogenic Lst	5.0-8.0	1.0-3.0	30-800 md	Well and outcrop samples
U. Cretaceous	Dolomites/Limestone	NM	NM	NM	No wells Outcrop only
IONIAN ZONE					
U. Cretaceous to Eocene	Organogenic Limestone	0.7-4.2	0.1-1.5	44-224 md	Gorishti, Cakrani and Ballshi Oilfields
M. Jurassic/ L. Cretaceous	Chert beds. Green Lst, Porcellanic Lst	1.5-2.3	0.1-0.3	NM	Gorishti, Cakrani Oilfields
U. Triassic/L.Jurassic	Breccia Dolomite Cika and Delvina Facies	1.0-7.0	0.5-3.0	md to darcies	Outcrop samples

Table 2 · Principal reservoir intervals in Triassic to Eocene carbonates. (NM = not measured)

(Roure et al, 2004)

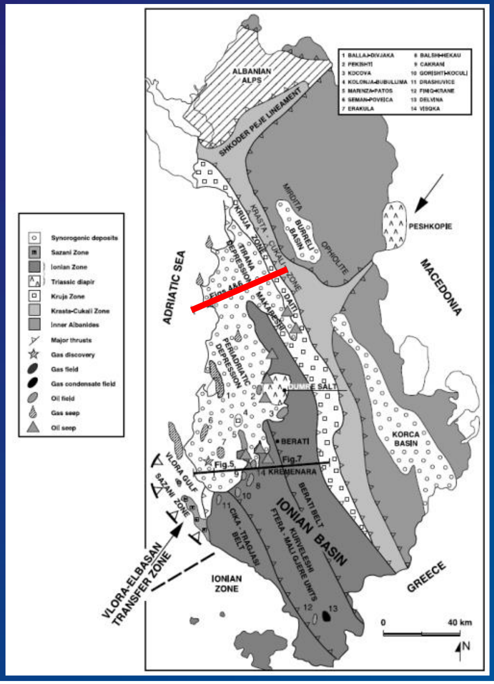

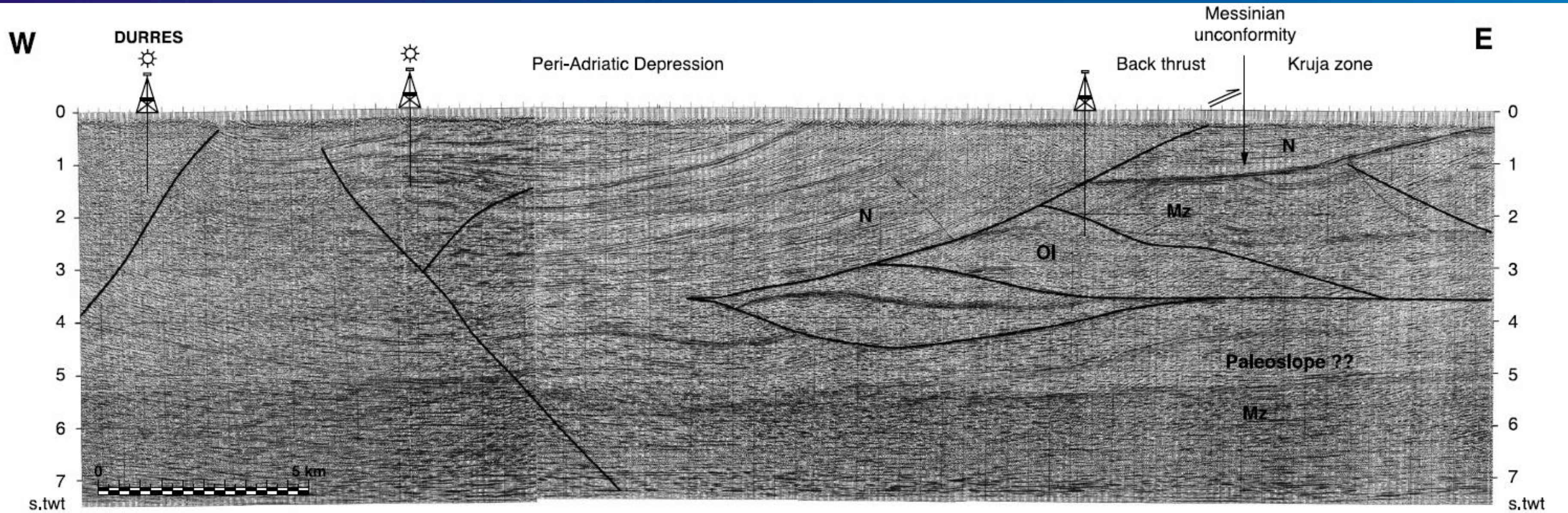

FIGURE 4. Seismic profile used for the construction of the northern transect (time section). Note the deep reflections imaged beneath the Kruja allochthon. Mz = Mesozoic; Ol = Oligocene flysch; N = Neogene.

(Roure et al, 2004)

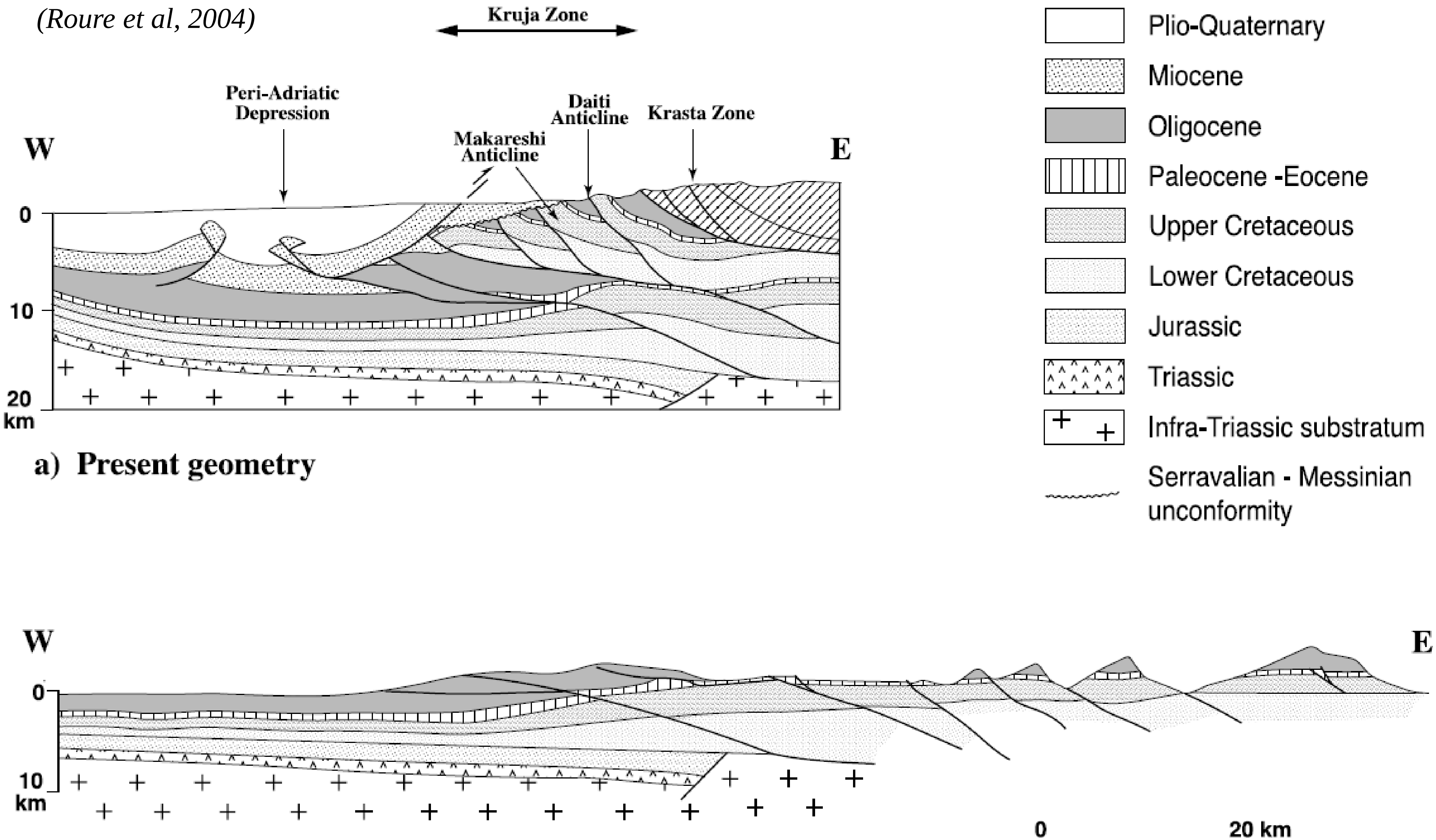

b) Restored geometry

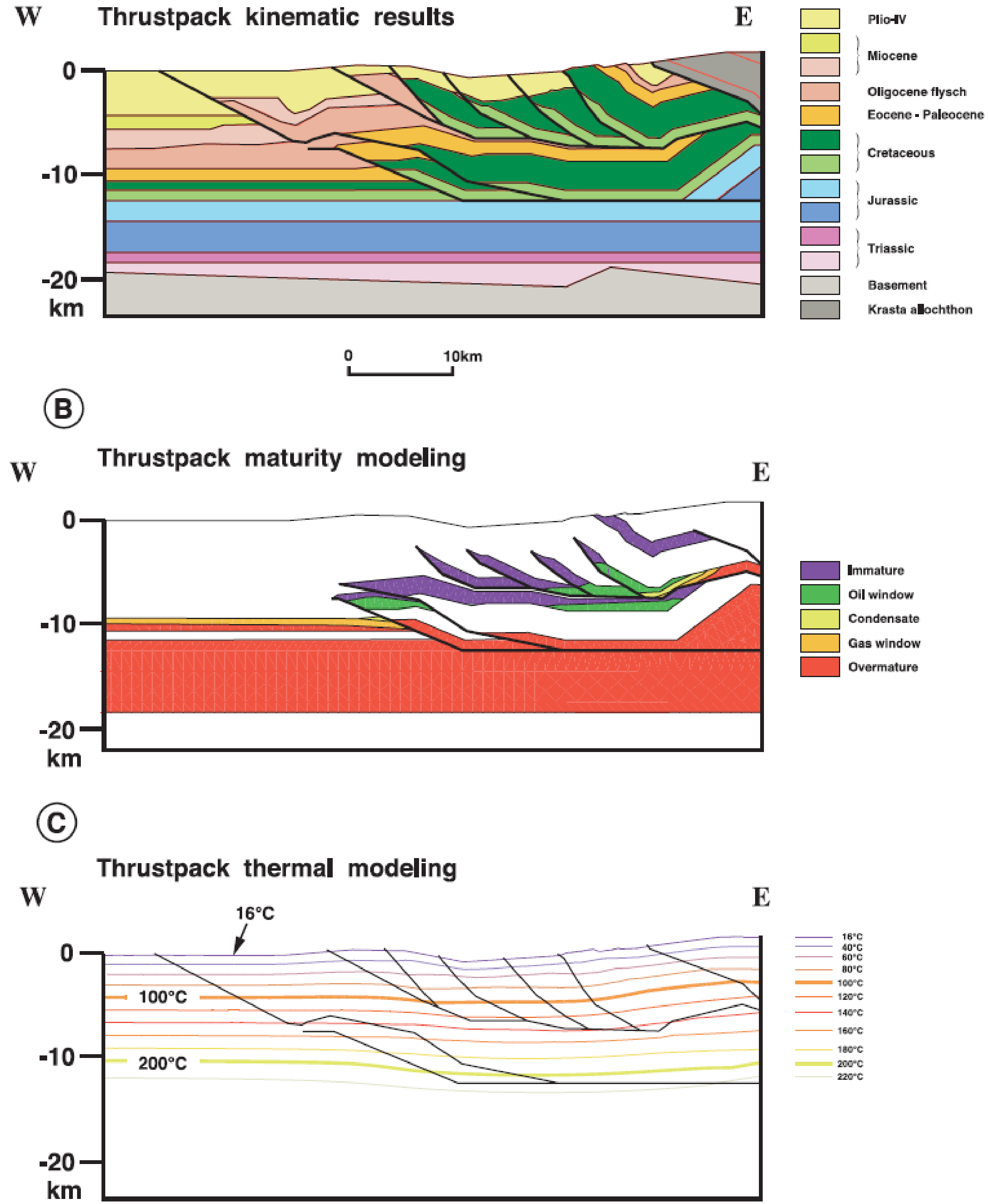

(Roure et al, 2004)

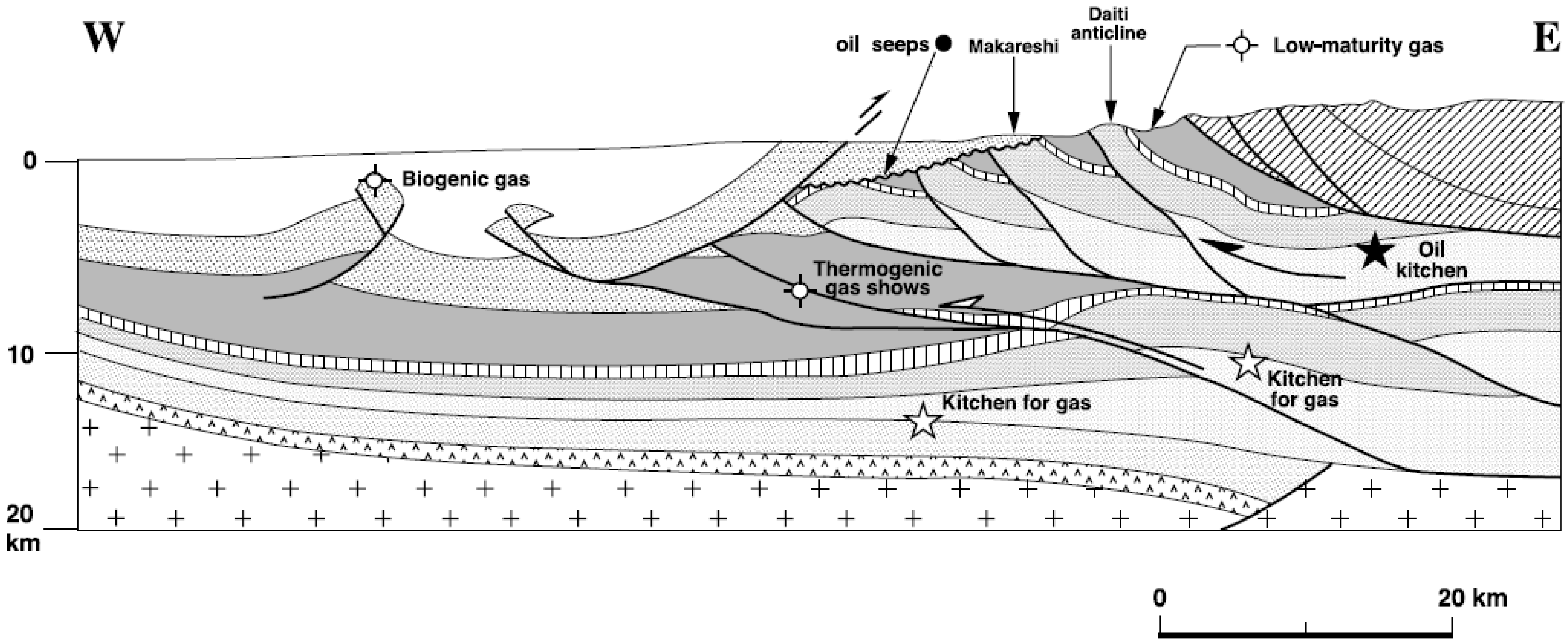

(Roure et al, 2004)

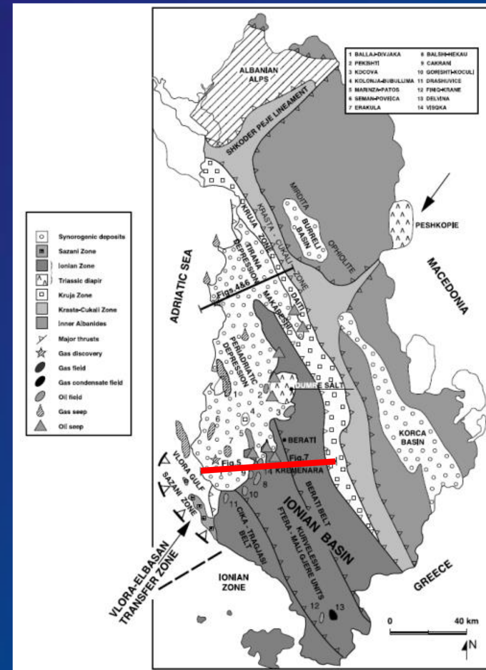

(Roure et al, 2004)

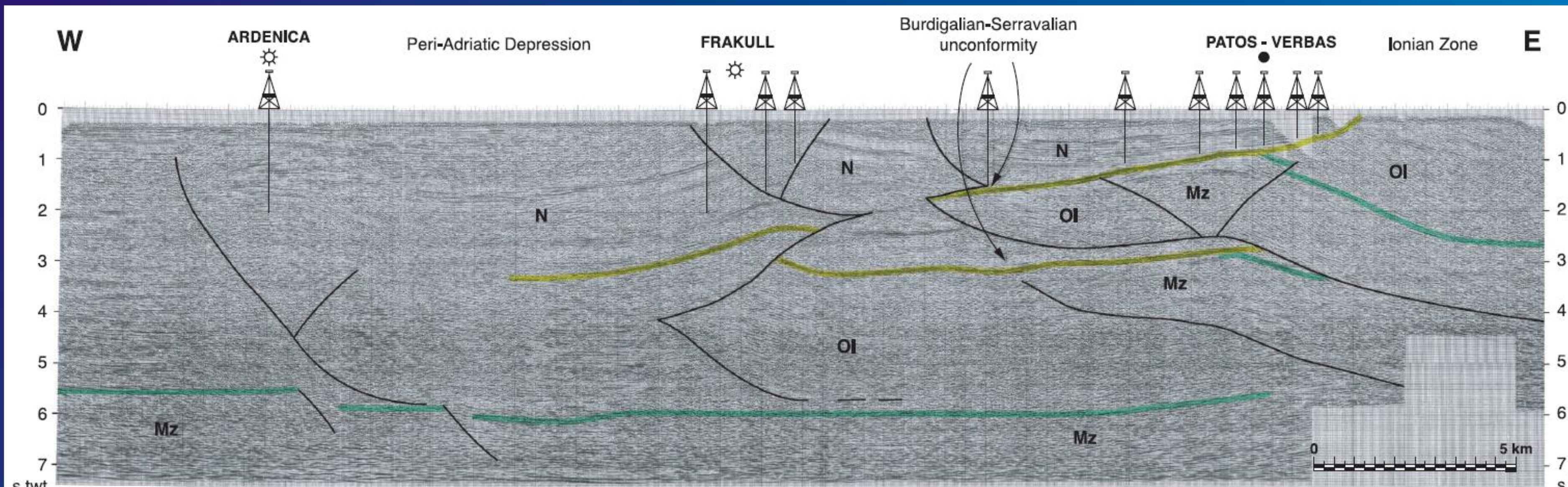

FIGURE 5. Western part of the seismic profile used for the construction of the southern transect (time section). Note the disruption of the Burgigalian-Serravalia unconformity, as a result of Pliocene-Quaternary fault reactivation. Mz = Mesozoic; Ol = Oligocene flysch; N = Neogene.

(Roure et al, 2004)

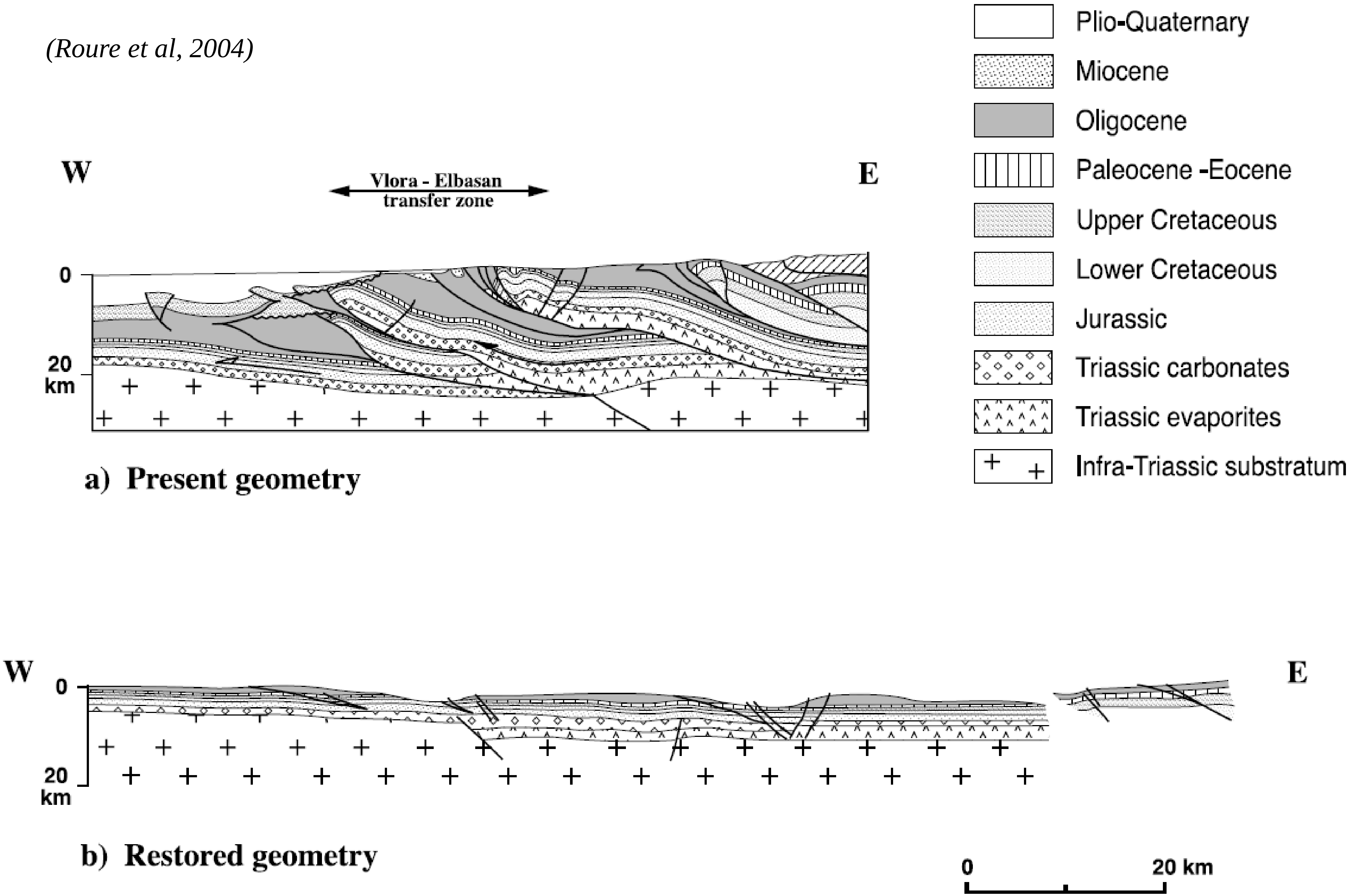

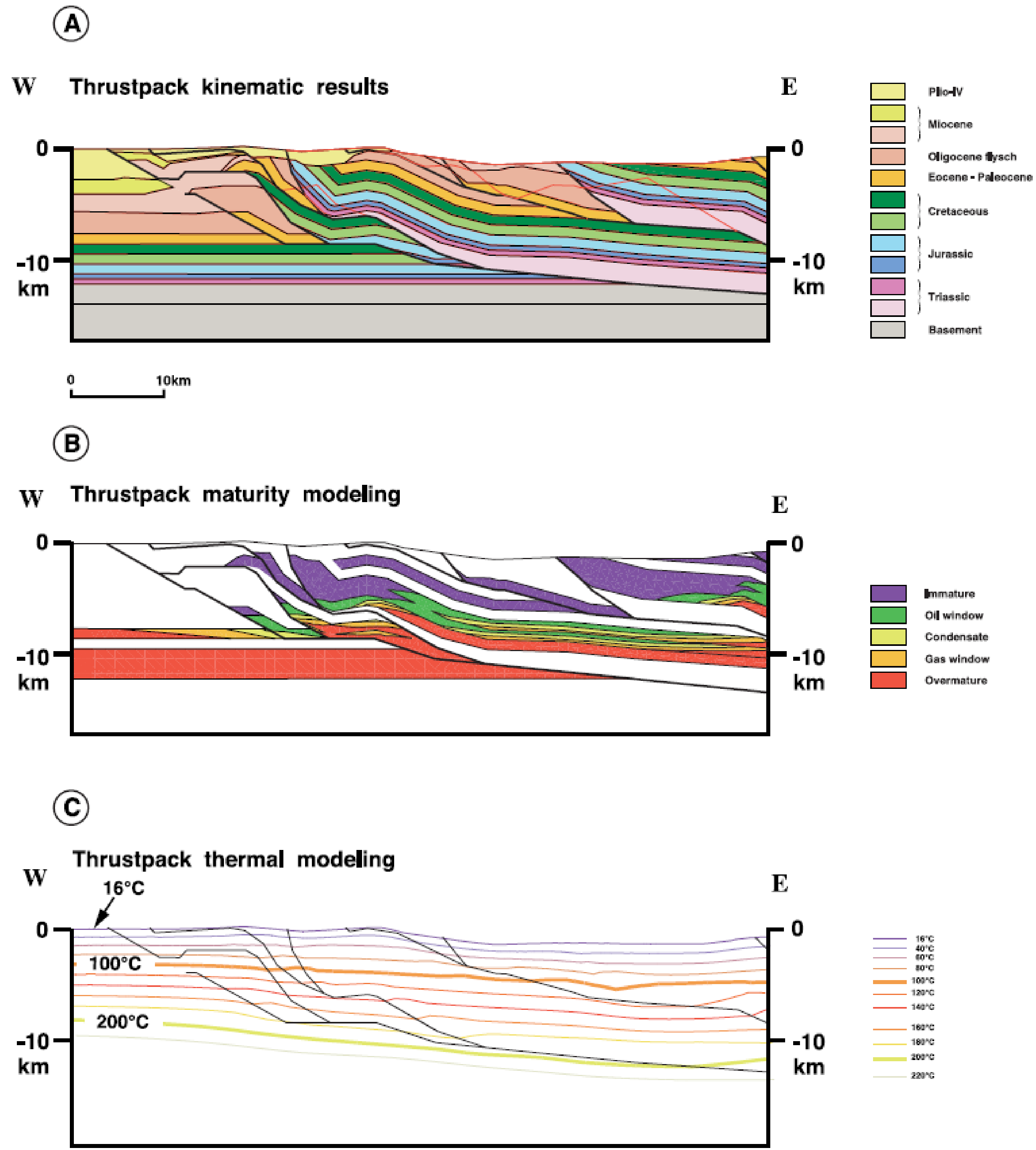

(Roure et al, 2004)

(Roure et al, 2004)

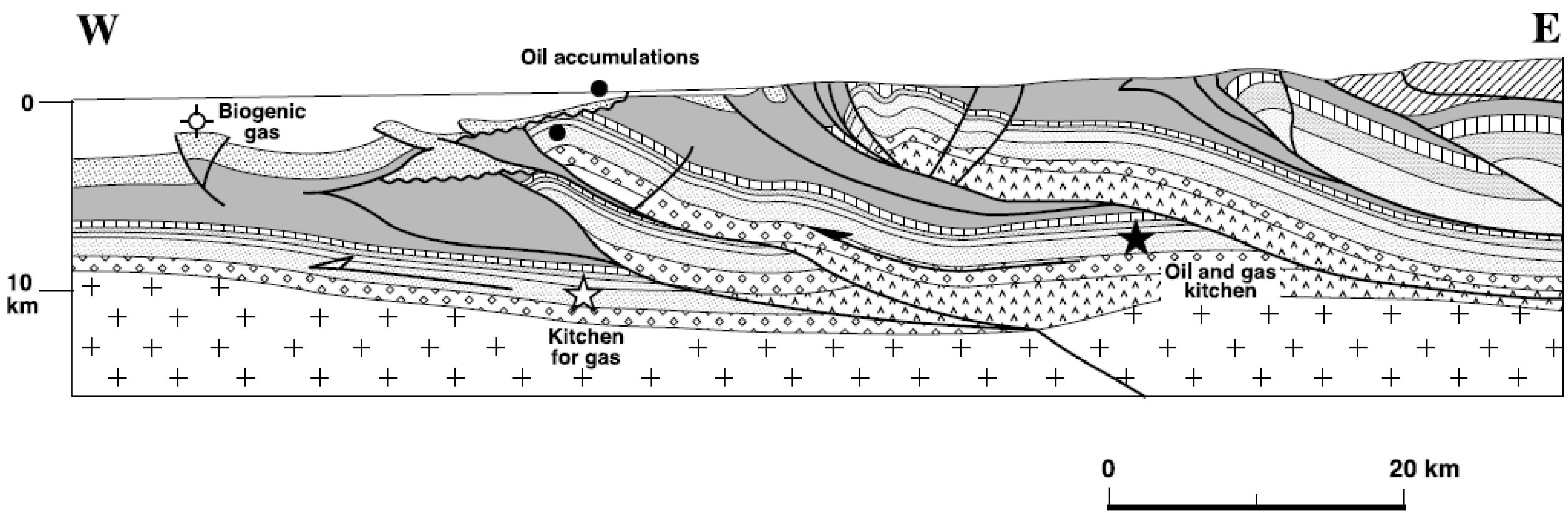

The easiest migration pathway for the hydrocarbons would be lateral migration, with east-dipping Mesozoic series directly connecting the syncline kitchens with adjacent productive anticlines.

However, an alternative is to also consider vertical migration from the footwall, across or along the intervening thrust planes. In such a case, future exploration should consider not only the shallower Cretaceous-Eocene carbonate reservoirs, but also the deeper Triassic-Liassic dolomite, if very good seals can be documented in the intervening Posidonia Schist and other Jurassic and Cretaceous shaly intervals.

A large amount of hydrocarbons generated in the Peri-Adriatic Depression probably migrated across the Adriatic Basin, along the regional foreland flexure. However, late thermogenic gas and light oil are also likely to be entrapped locally in growth anticlines of the Peri-Adriatic Depression itself, thus providing an additional, not-yet documented target for exploration in Albania, in an area where only biogenic gas has been found to date.

Paleo-burial estimates in fold-and-thrust belts

The problem of estimating the eroded rock thickness in FTBs : Combining paleo-thermo-barometers and coupled thermal, fluid flow and pore fluid pressure modelling for hydrocarbon and reservoir prediction in FTBs

If crustal thickness remained relatively constant and only limited erosion occurred, vitrinite reflectance (Ro) and Rock-Eval (Tmax) values measured along vertical profiles (wells) are usually sufficient, when combined with 1D well modelling (burial v. time curves), to derive realistic values for the palaeo-thermicity,

Large uncertainties are recorded when addressing petroleum modelling in FTBs, basically because of the lack of controls on the paleo-burial estimates in areas which have been strongly affected by erosion, and where it is challenging to solve for each time interval and for each cell of the model two unknowns (T and burial).

Use of hydrocarbon-bearing fluid inclusions in paleo-burial reconstructions

Th measurements in syngenetic FI in minerals are mainly used in reservoir studies to estimate Tmin of diagenetic fluids at the time of cementation of fractures in carbonate reservoirs.

This T should be corrected by a factor relative to the composition of the fluid and the P at time of fluid entrapment. This correction is often neglected in basin modelling of petroleum occurrences because of low salinities aqueous systems (0–3 wt%) with high CH4 in solution and relatively low P (300b) attained in sedimentary basins.

In FTBs, using Th data provides only valuable information for calibrating petroleum modelling at different scales when P is high and tectonically dependent and basinal fluids are involved. However, the minimum paleo-T reached by a given sample does not tell directly when this T was reached, nor at which paleo-burial, making the P estimate and then the correction factor unknown, implying errors on T.

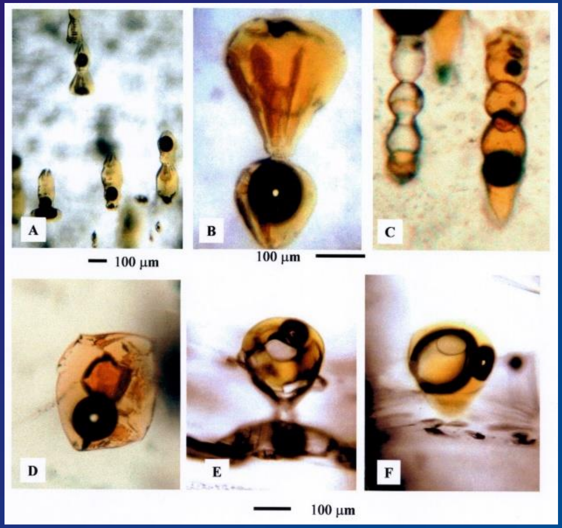

Because of great immiscibility of oil and aqueous phases, aqueous FI can develop synchronously (same P and T) with hydrocarbon-bearing FI in cements, thus providing a means for solving both the paleo-T and paleo-Pf circulating in the reservoir at the time of cementation. The technique applied to derive T and P values from these two types of FI in the same set relies on the different thermodynamic properties of the two fluids. PT isochoric modelling can be addressed, provided density and composition of aqueous and hydrocarbon phases can be defined individually by joint micro-thermometry and FTIR (Fourier Transform Infra-Red spectrometry) in situ analysis. For a specific composition and density, the intersection of the hydrocarbon isochore at the aqueous fluid Th or in some case (low dissolved CH4) with the aqueous isochore, provides an accurate estimate of both P and T at the time of FI trapping and then T and P values of the natural system at the time of crystallization/cementation.

Cretaceous –Paleocene
Laramide compression

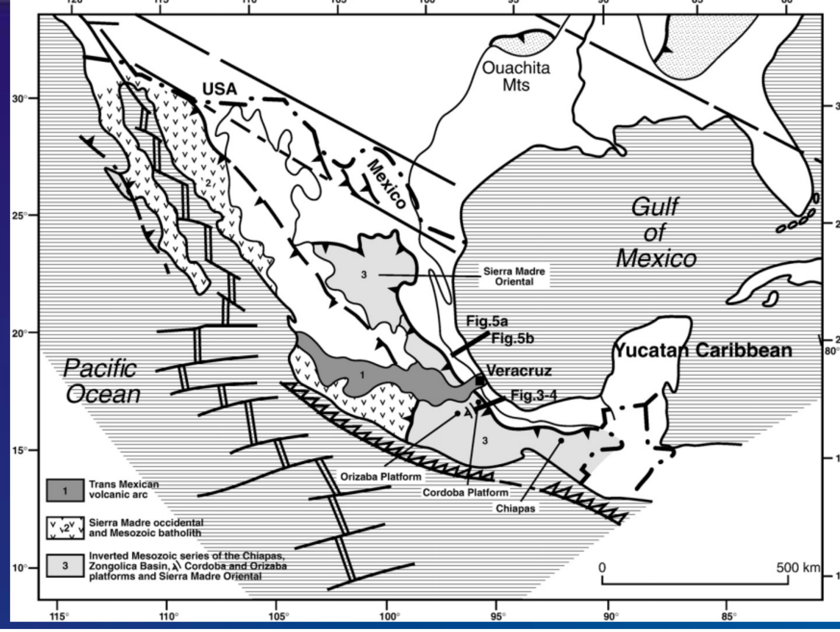

(Roure et al., 2009)

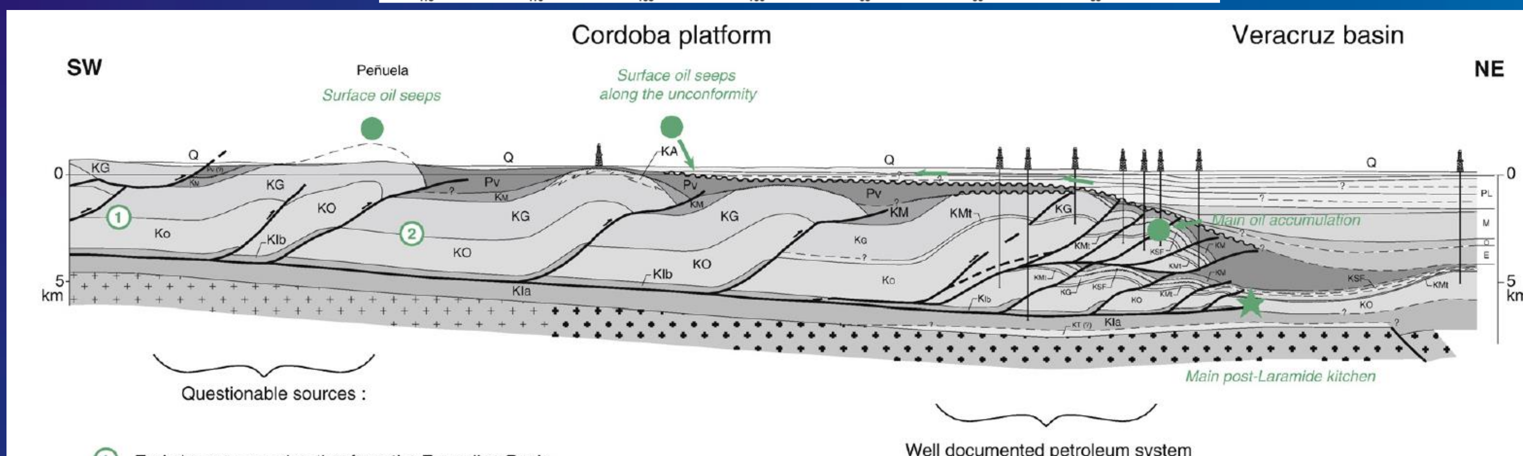

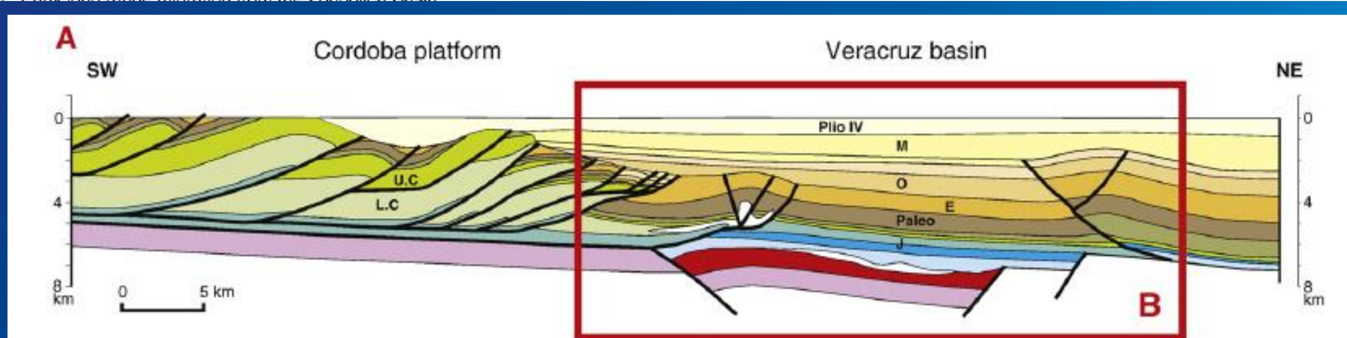

The Cretaceous platform carbonates of the Cordoba Allochthon, in the southeasternmost part of the North American Cordillera in Mexico, are almost devoid of synflexural or synorogenic sediments. Only limited outcrops document the gradual changes from shallow water Cenomanian carbonates towards deep water Late Cretaceous–Paleocene turbidites. The initial thickness of these flysch deposits is unknown.

Furthermore, seismics documents a surprising present east-dipping attitude of the crystalline basement beneath these allochthonous Mesozoic carbonates.

While few Tmax and Ro data were available in the allochthon due to the lack of organic-rich outcrops, diagenetic quartz from cemented fractures of the carbonate was used as a paleo-thermo-barometer

Unexpectedly, the P–T path derived from isochores documents a few km (4,5 km) of unroofing of the Cretaceous carbonate platform, which is best explained by the post-Laramide erosional removal of a similar thickness of Late Cretaceous–Paleocene synflexural flysch.

The restoration of the missing flexural sequence requires generation of a coeval space at basin scale to accommodate such sedimentary thickness at the top of the well-known carbonate sequence, which is best explained by assuming an initial west-dipping configuration of the foreland.

(Roure et al., 2010)

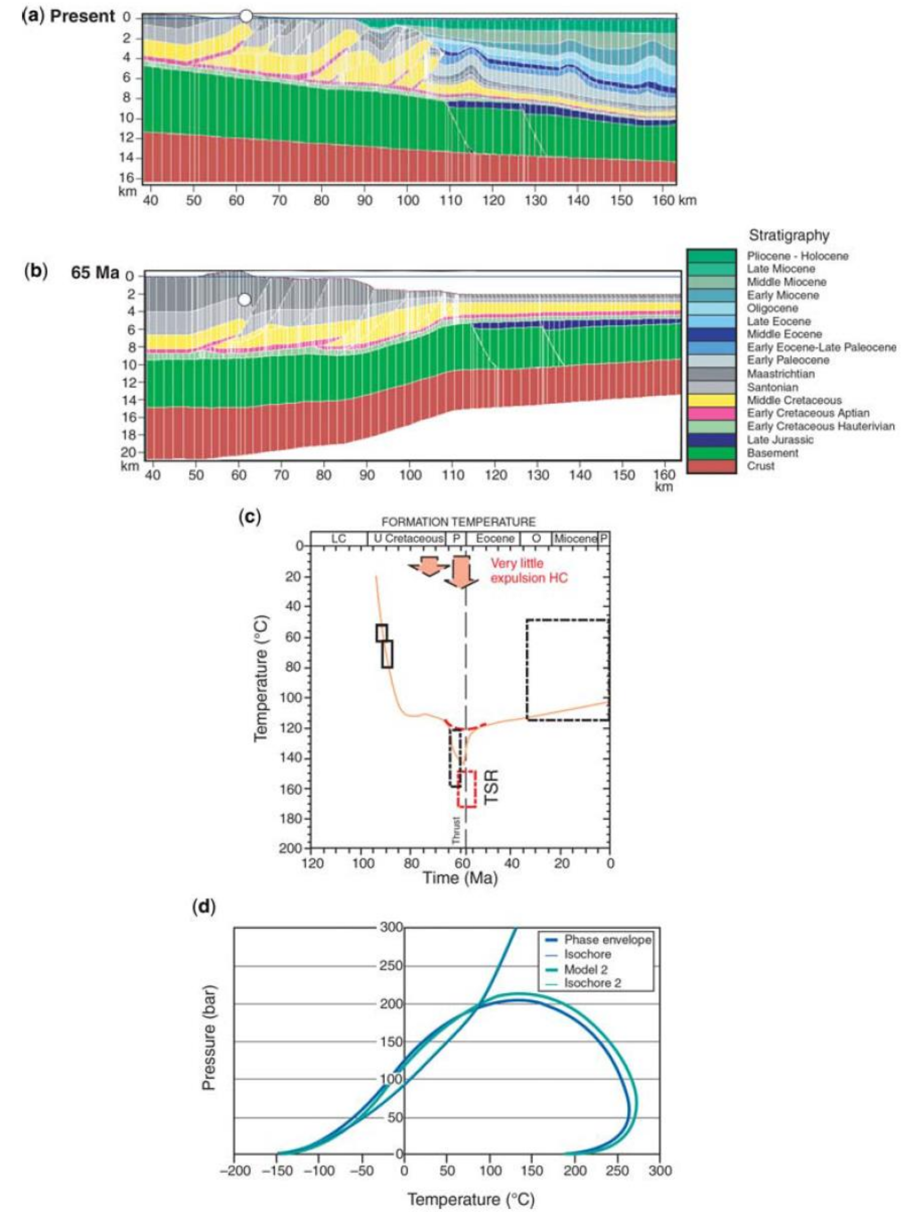

Fluid inclusions data and PVT modelling as constraints for palaeo-burial reconstructions along a regional transect across the Cordoba Platform (Eastern Mexico; modified after Roure *et al.* 2009*a*; Ferket *et al.* 2003, 2010). (**a**) Top section: Present architecture of the transect, with an east-dipping attitude of the basement. (**b**) Central section Laramide deformation stage, the basement being restored to accommodate the 4.5 km of Late Cretaceous–Paleocen flexural sequence, which have been subsequently removed by erosion, but are required to account for the PVT modellin of fluid inclusions taken from cements at the top of the Cretaceous platform carbonates in the inner (western) part of th section. (**c**) Burial v. depth plot of Mesozoic carbonates in eroded anticlines (indicated by a white circle in the sections). (**d**) Bottom: results of the PVT modelling on fluid inclusions from Mesozoic carbonates.

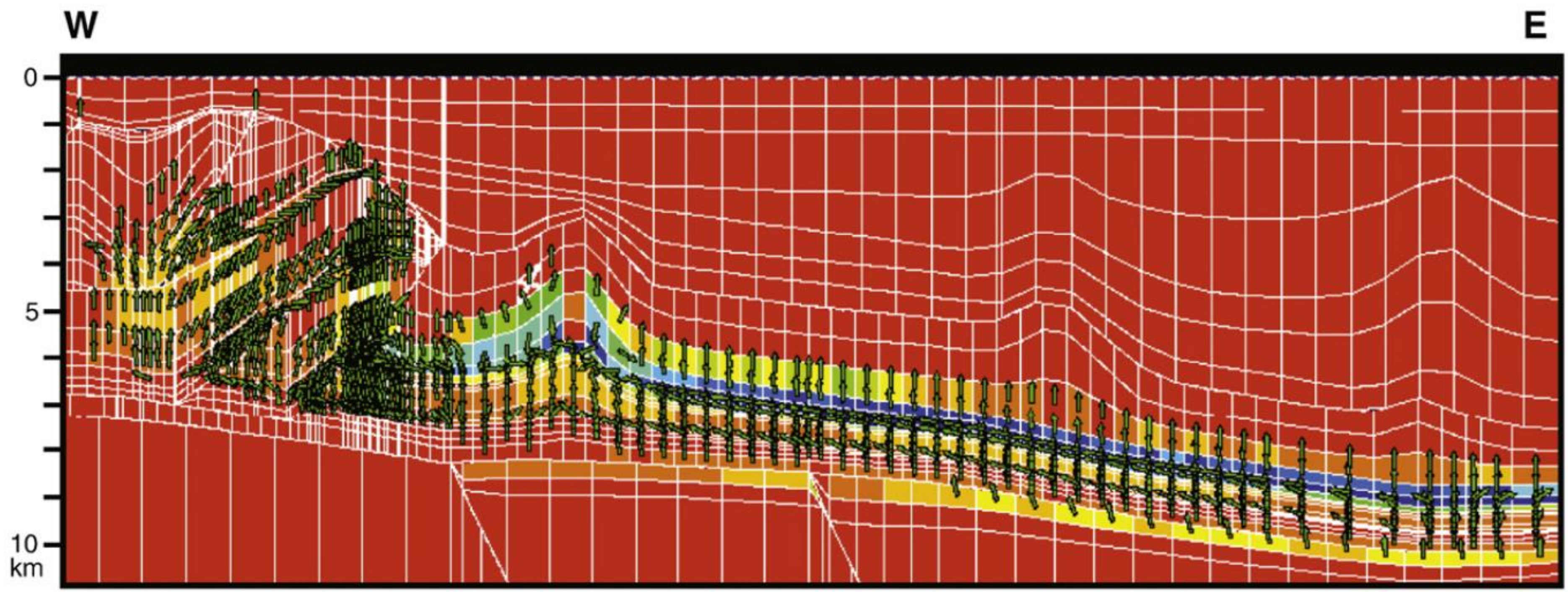

Themis flow modeling

All the oil currently produced in the frontal duplexes is derived from the adjacent Veracruz Basin.
Jurassic source rocks remained immature until the end of the Cordilleran orogeny.
They entered subsequently into the oil window during Oligocene–Neogene episodes of increasing burial.
Lateral migration toward the structural traps of the frontal duplexes was clearly enhanced by the progressive post-orogenic tilt of the basement

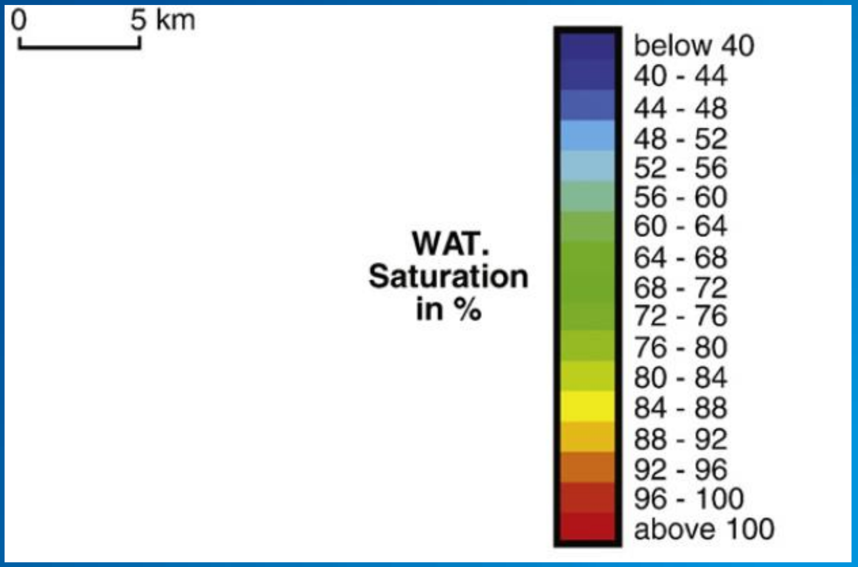

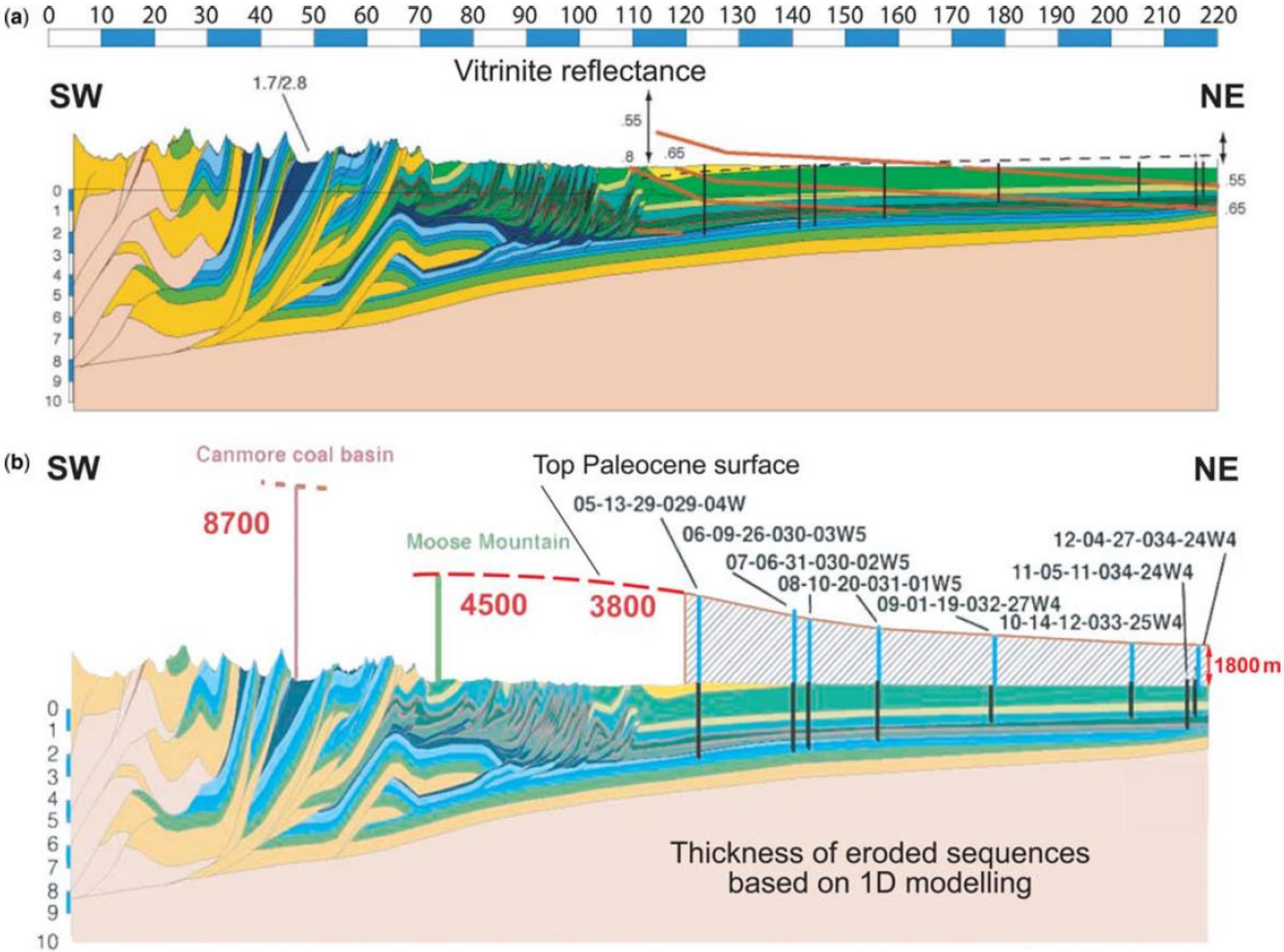

Erosional profile along the Banff–Calgary transect, recording the effect of post-Laramide asthenospheric rise and related thermal doming and unroofing of the former orogen. (**a**) present distribution of vitrinite reflectance (Ro) data; (**b**) thickness of eroded sediments derived from 1D modelling of selected wells.

(Roure et al., 2010)

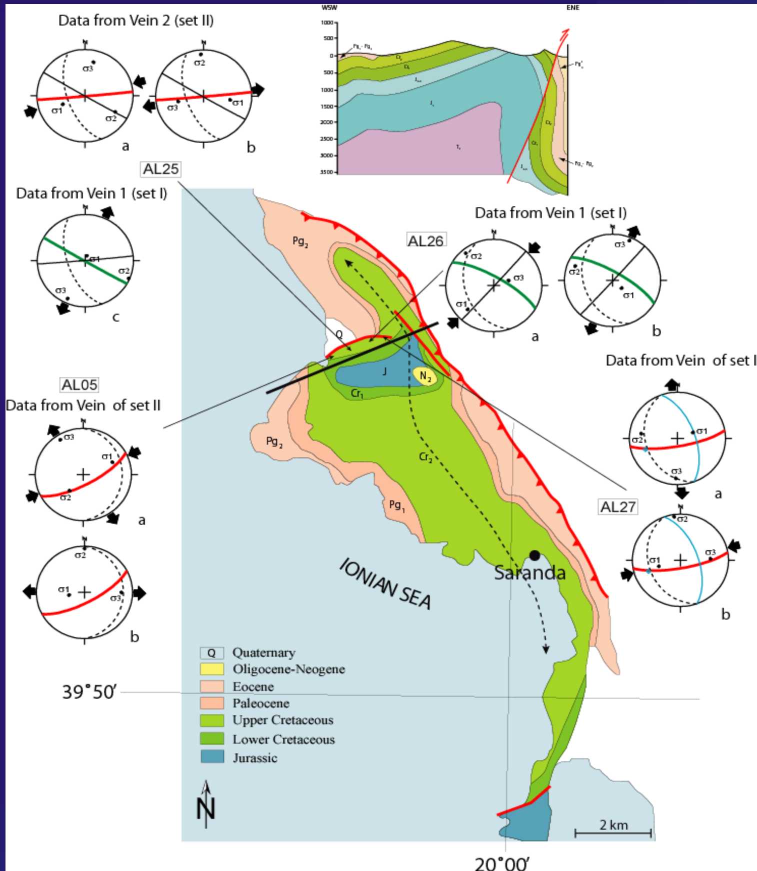

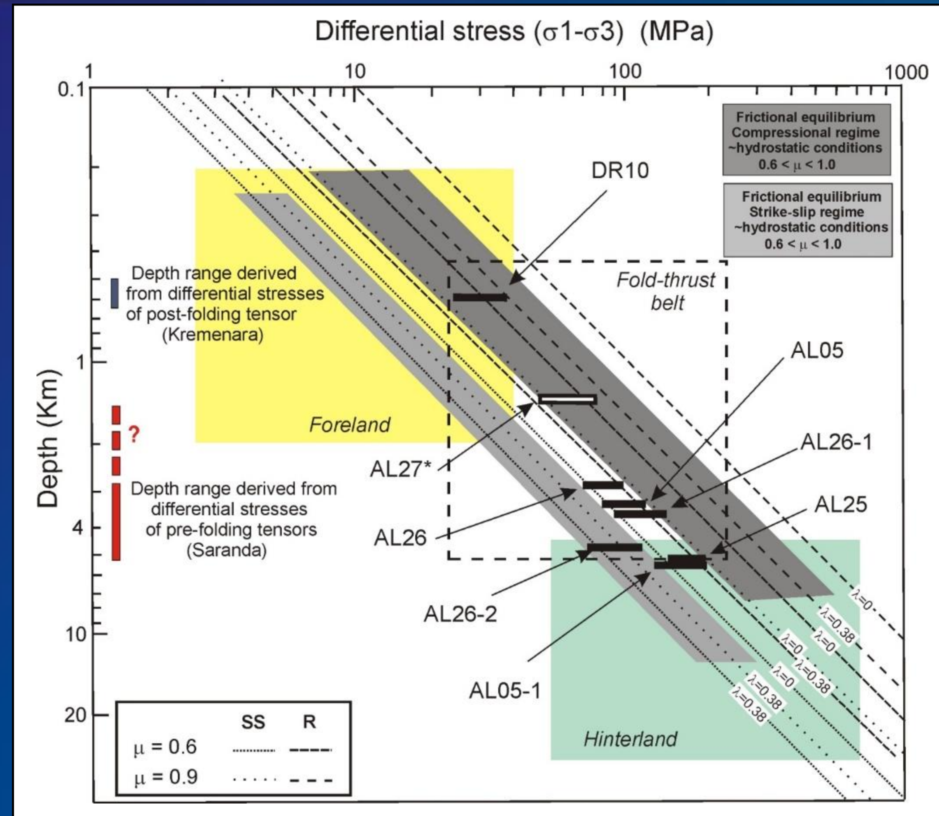

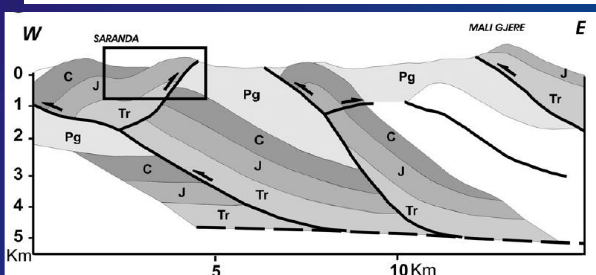

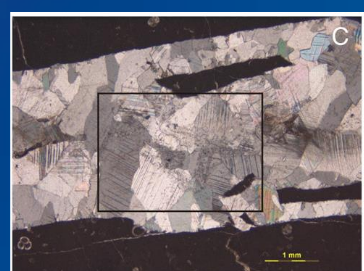

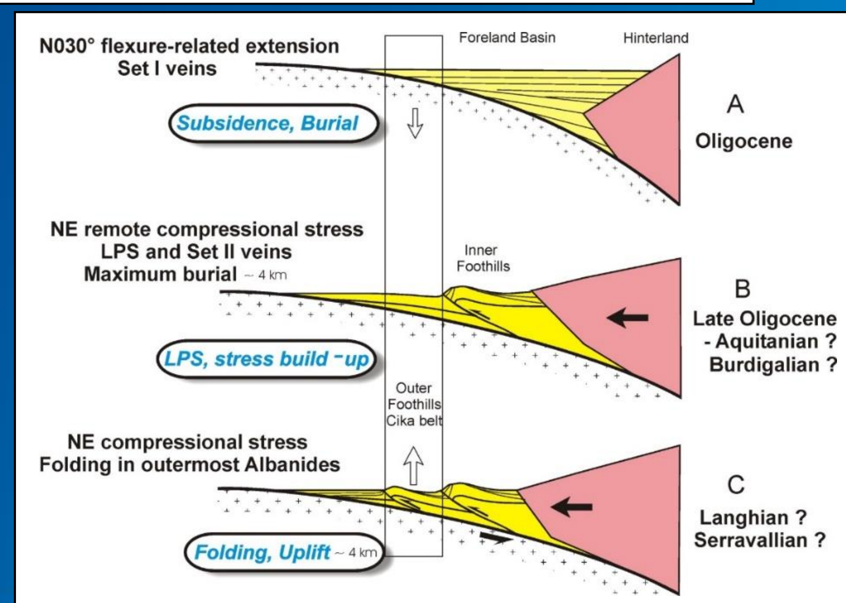

Calcite twins provide estimates of pre-folding paleoburial consistent with independent estimates from micro-thermometry of fluid inclusions, maturity of organic matter and results of 1D thermal modeling.

Fluid overpressures in petroleum systems

Fluid overpressures in FTBs

FTBs share many similarities with offshore accretionary wedges (modes of thrust emplacement and structural style).
However, boundary conditions are rather different in terms of porosity/ permeability distributions and fluid flow regimes.

This is due to (1) the age of the accreted series (usually restricted to the relatively young syn-flexural sequences in accretionary wedges, against dominantly pre-orogenic passive margin sequences in FTB), and (2) the origin of the fluids (mixing of sedimentary fluids with meteoric water in FTB, against entirely marine or basinal fluids in offshore accretionary wedges).

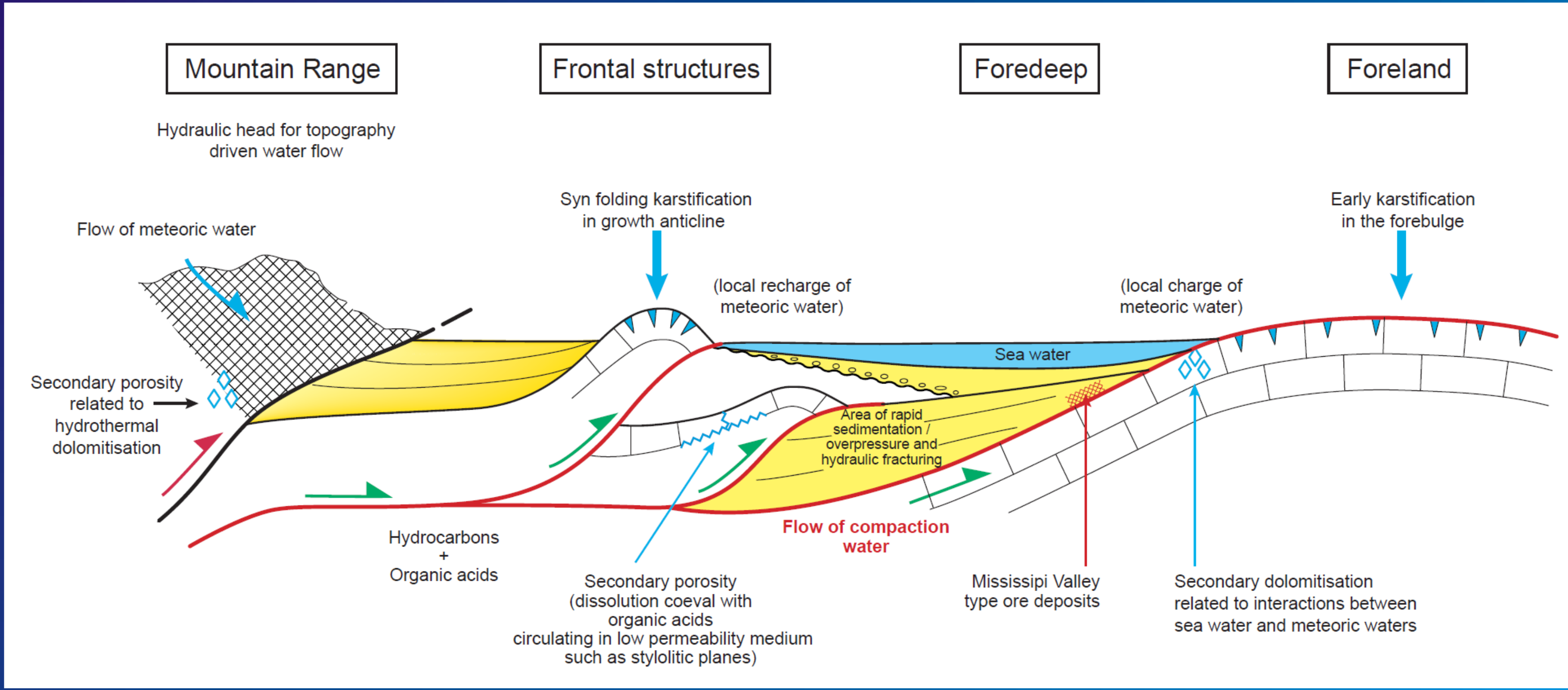

(Roure et al., 2004)

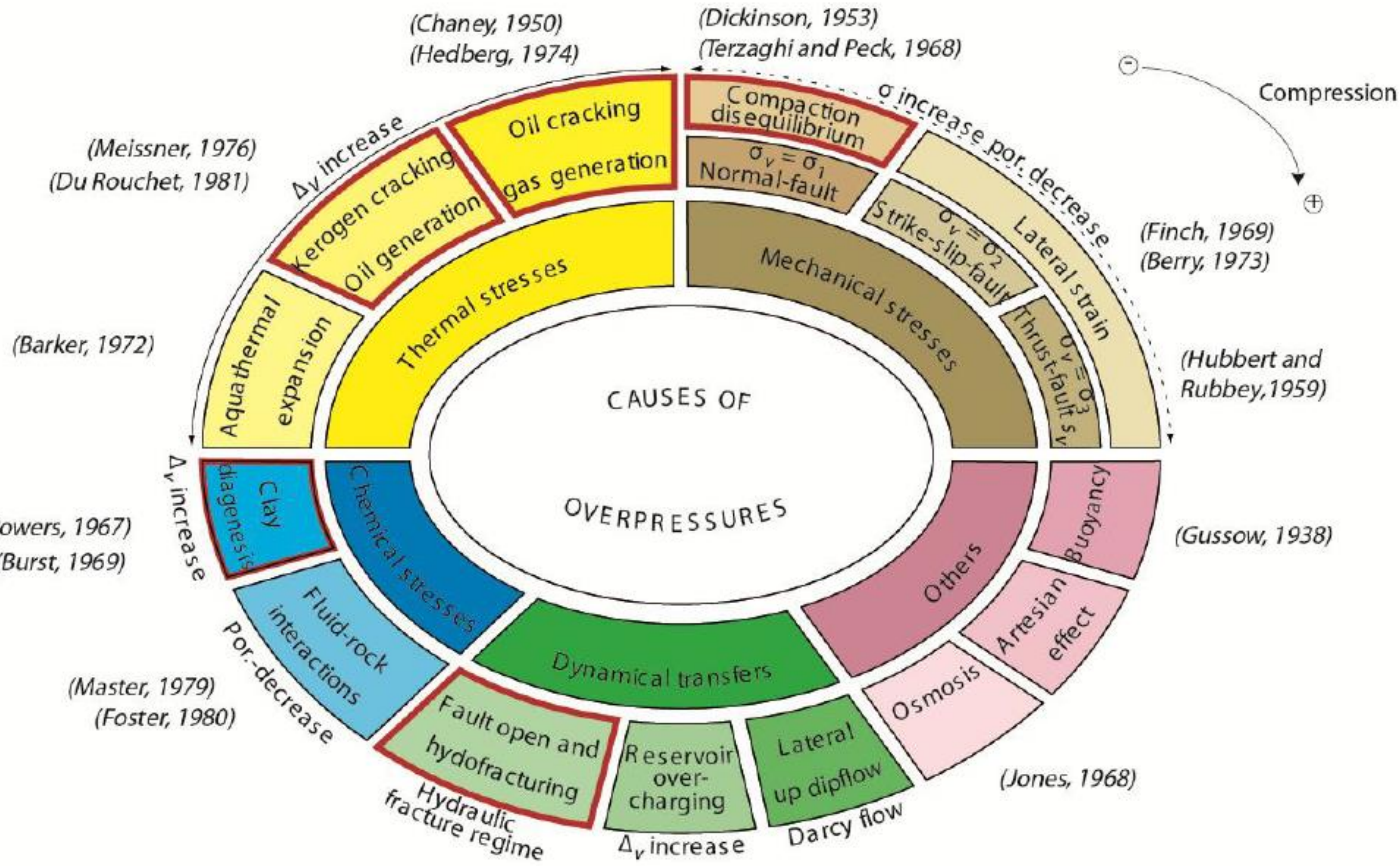

Δ_v = fluid volume differential
σ = total stress
σ_v = vertical stress

por. = porosity
σ_1 = maximum principal stress
σ_2 = intermediate principal stress
σ_3 = minimum principal stresss

The increasing load of syn-flexural sediments deposited in foredeep basins results in a vertical escape of formation water and a progressive mechanical compaction of the sedimentary pile where pore-fluid pressures remain dominantly hydrostatic.

This process ultimately induces a velocity increase of seismic waves from the surface down to a depth where the vertical permeability reaches a minimum, precluding any further escape of underlying fluids toward the seafloor.

Undercompacted sediments occur beneath this compaction-induced regional seal, being characterized by slower seismic velocities and overpressures.

Unlike offshore accretionary wedges, FTB are not only characterized by fluid flow controlled by lateral permeability barriers but also by the topography-driven, gavitational flow of meteoric water, which operates from the positive relief of the hinterland towards the adjacent low lands and is mostly confined to the shallow horizons of the foreland, that is above the compaction-induced permeability barrier.

What about LPS ?

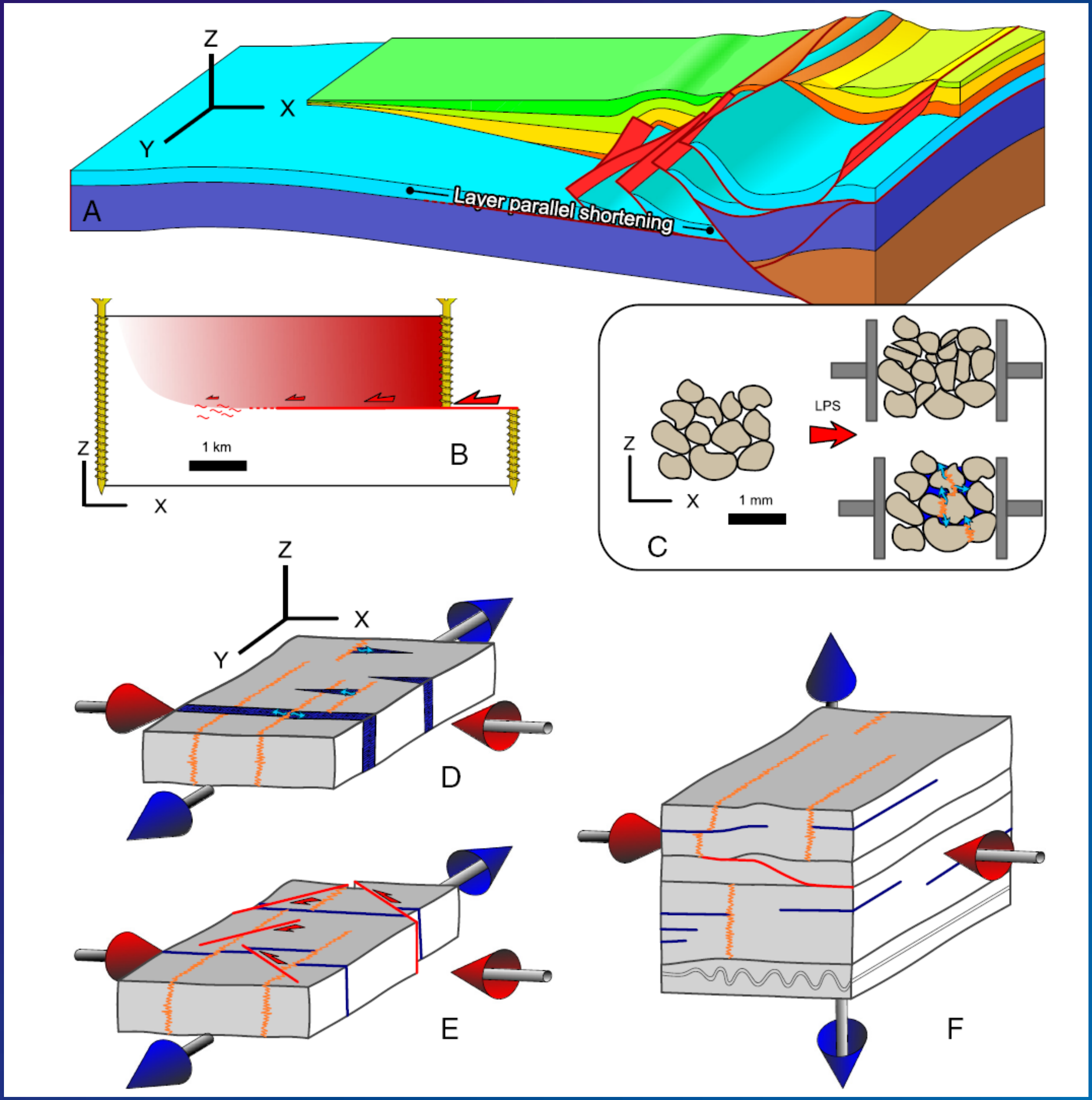

LPS stimulates pressure-solution, inducing lateral changes in the compaction, decrease in porosity and permeability.

LPS contributes to the development of overpressures and tectonically controlled squeegee episode of forelandward expulsion of compaction water.

The main episode of LPS occurs in the footwall of frontal thrusts at the time of their nucleation, when the evolving thrust belt and its foreland are mechanically strongly coupled.

(Tavani et al., ESR, 2015)

The build-up of horizontal tectonic stresses in the foreland induced LPS at reservoir scale, involving pressure-solution at detrital grain contacts, causing in situ mobilization of silica, rapid reservoir cementation by quartz-overgrowth and coeval porosity and permeability reductions
--> killing the porosity = deterioration of sandstone reservoir quality

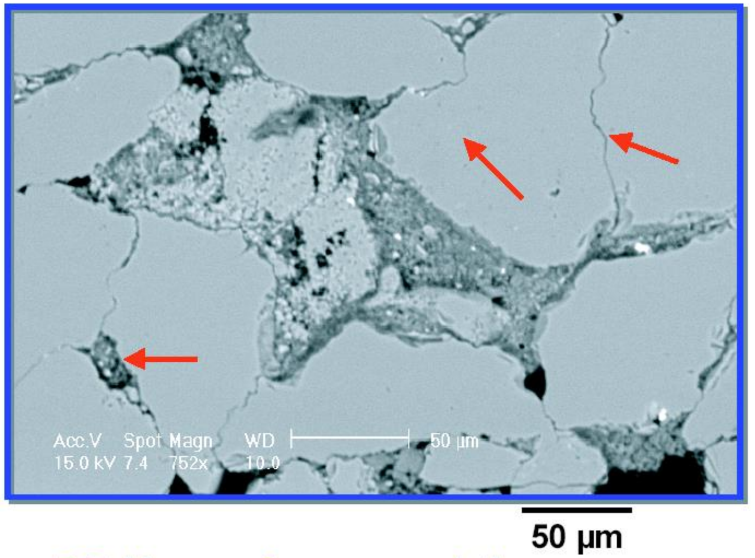

B Evidences of pressure-solution processes

The age and duration of such quartz-cementation episodes can be roughly determined by combining micro-thermometric fluid inclusion studies with 1D and 2D basin modelling.

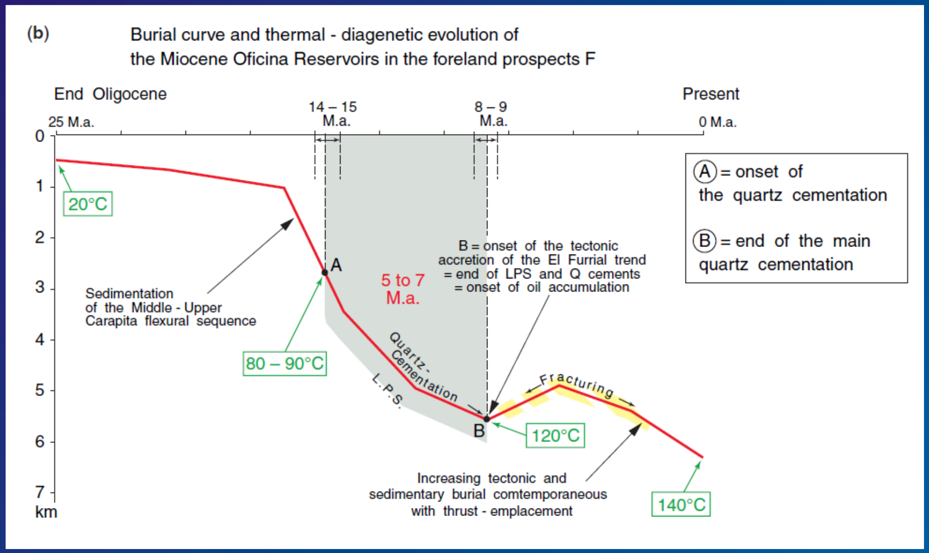

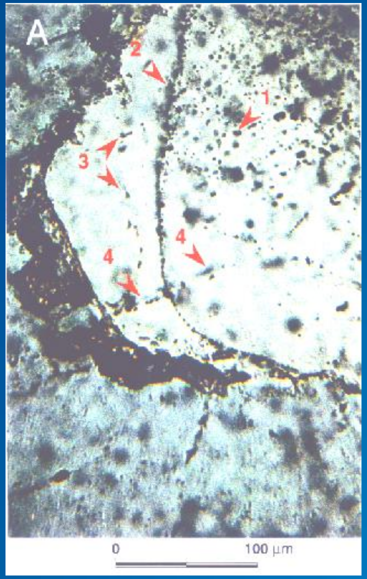

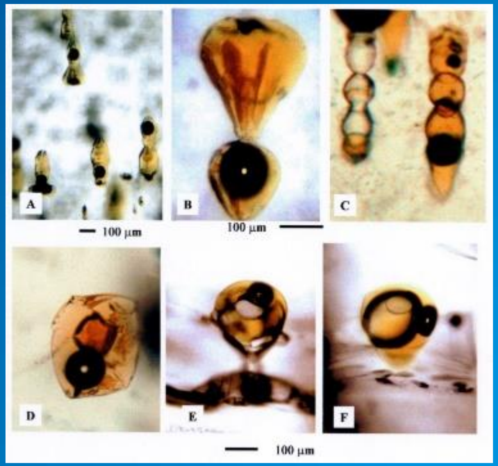

Generally first host-rock buffered fluids are squeezed out, then chemical compaction forms LPS stylolites.

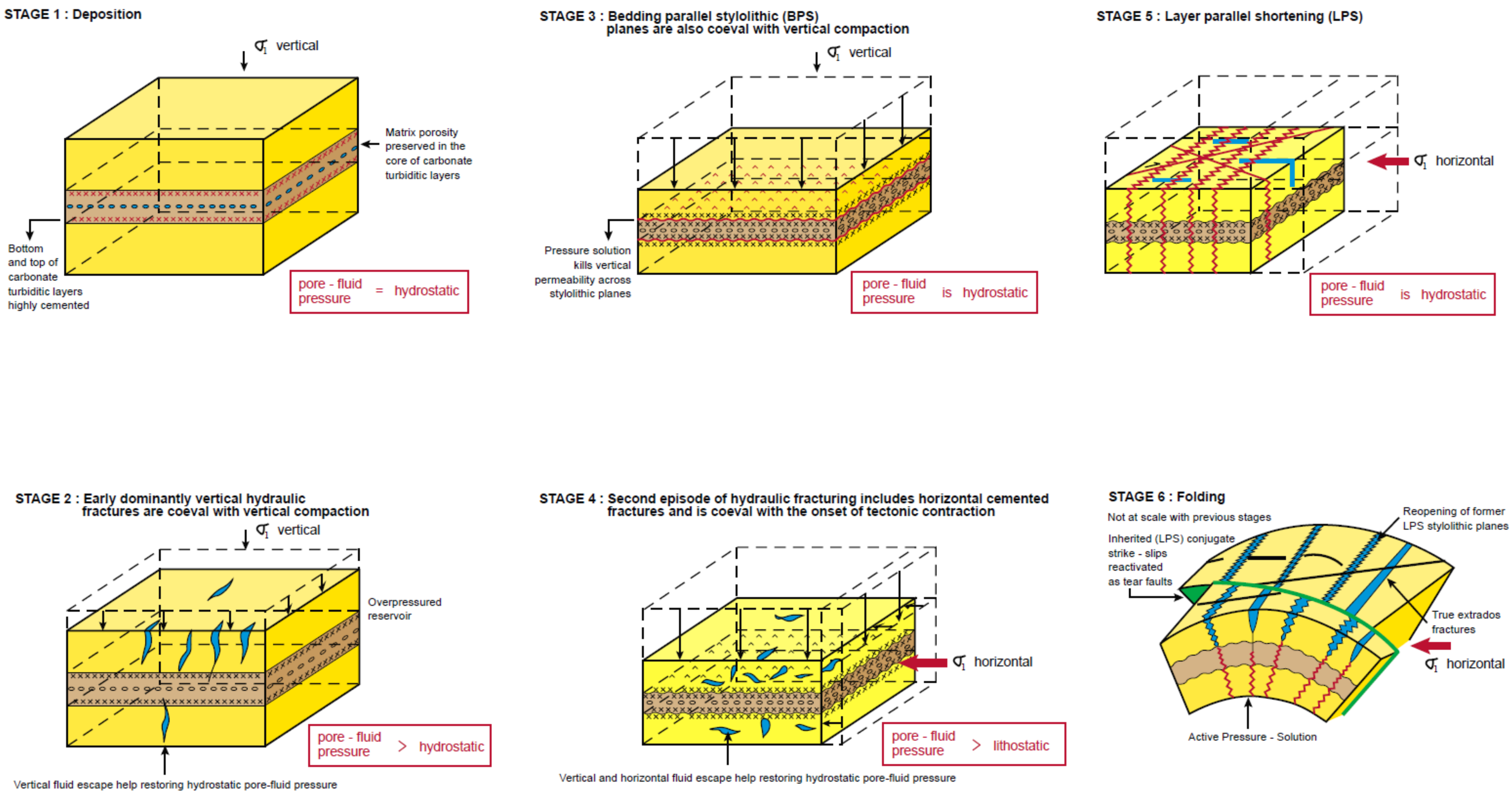

Later non-equilibrium fluids circulate through reopened structures. Palaeo-stress evolution reveals that the engine must be hydrofracturing.

Fluid overpressures and decollements

- *Orogène d'âge Cénozoïque*
- *Orogéne d'âge Paléozoïque ou Mesozoïque*
- *Prisme deltaïque*
- *Prisme d'accrétion océanique*

(1) Cooper et al, 2004
(2) Mackay, 2015
(3) Aydin et Engelder, 2014
(4) Deville et al, 2010
(5) Schneider et al, 2003
(6) Cobbold et al, 2004
(7) Moretti et al, 1998; Echavarria et al, 2003; Rocha et al, 2015
(8) Cobbold et al, 1999; Zanella et al, 2015
(9) Zanella et al, 2014
(10) Cobbold et al, 2009
(11) Deville et Sassi, 2006
(12) Roure et al, 1995
(13) Weng et al, 2013
(14) Hansberry et al, 2015
(15) Morley et al, 2011

] Localisation et type de système géologique dans laquelle des décollements ont pu être observés dans les formations roches-mères.

(Berthelon, thèse, 2015)

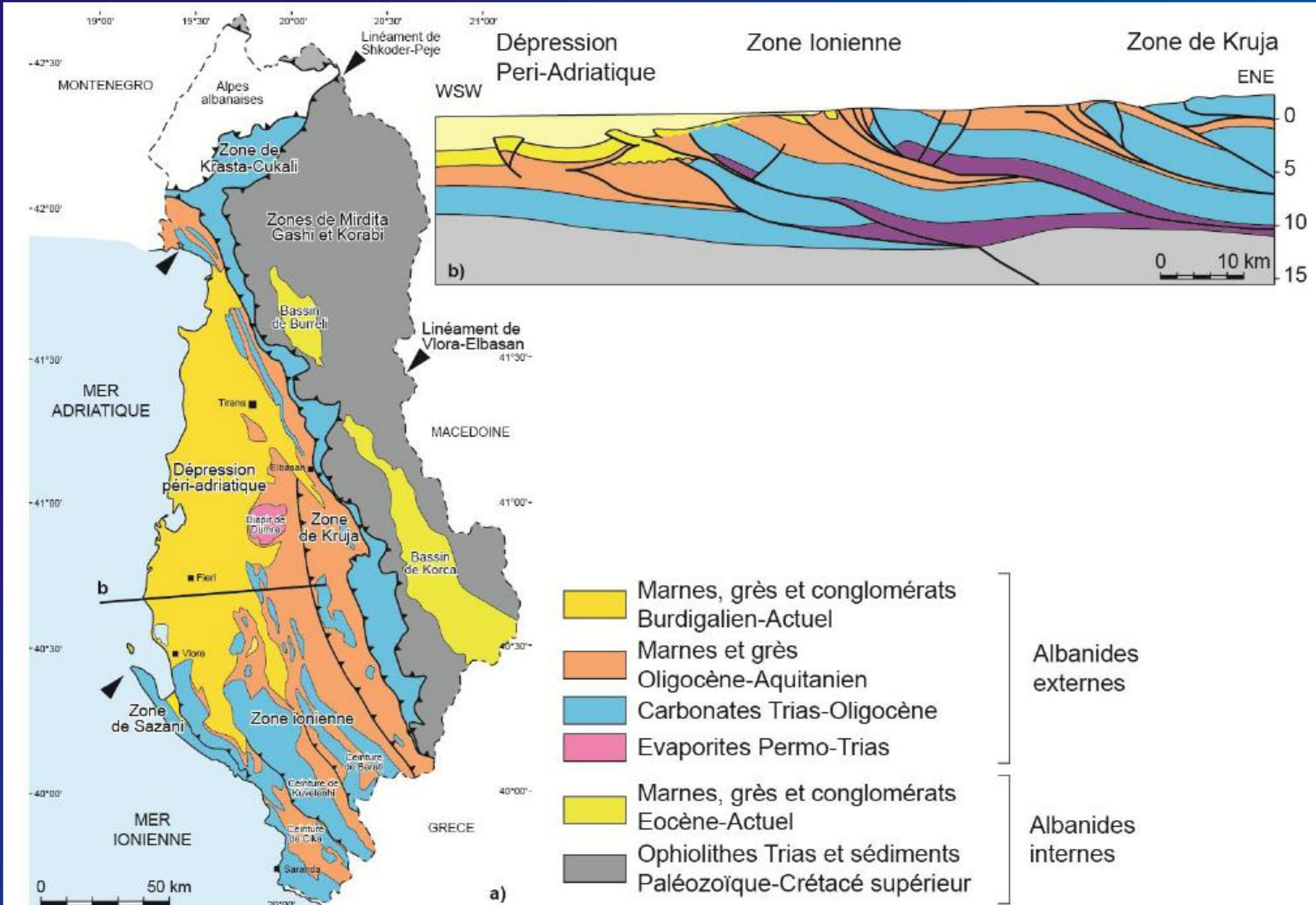

Dépression Peri-Adriatique
Zone Ionienne
Zone de Kruja
WSW
ENE
0
5
10
15
0
10 km
b)
MONTENEGRO
Alpes albanaises
Linéament de Shkoder-Peje
Zone de Krasta-Cukali
Zones de Mirdita Gashi et Korabi
Bassin de Burreli
Linéament de Vlora-Elbasan
MER ADRIATIQUE
Tirana
MACEDOINE
Dépression péri-adriatique
Elbasan
Diapir de Dumre
Zone de Kruja
Bassin de Korca
b
Fieri
Vlora
Zone de Sazani
Zone ionienne
Ceinture de Berati
Ceinture de Kurveleshi
Ceinture de Cika
MER IONIENNE
GRECE
Saranda
0
50 km
a)
Marnes, grès et conglomérats Burdigalien-Actuel
Marnes et grès Oligocène-Aquitanien
Carbonates Trias-Oligocène
Evaporites Permo-Trias
Albanides externes
Marnes, grès et conglomérats Eocène-Actuel
Ophiolithes Trias et sédiments Paléozoïque-Crétacé supérieur
Albanides internes

a) Toarcian Posidonia Schist, Mali i Gjërë, Albania

(Berthelon, thèse, 2015)

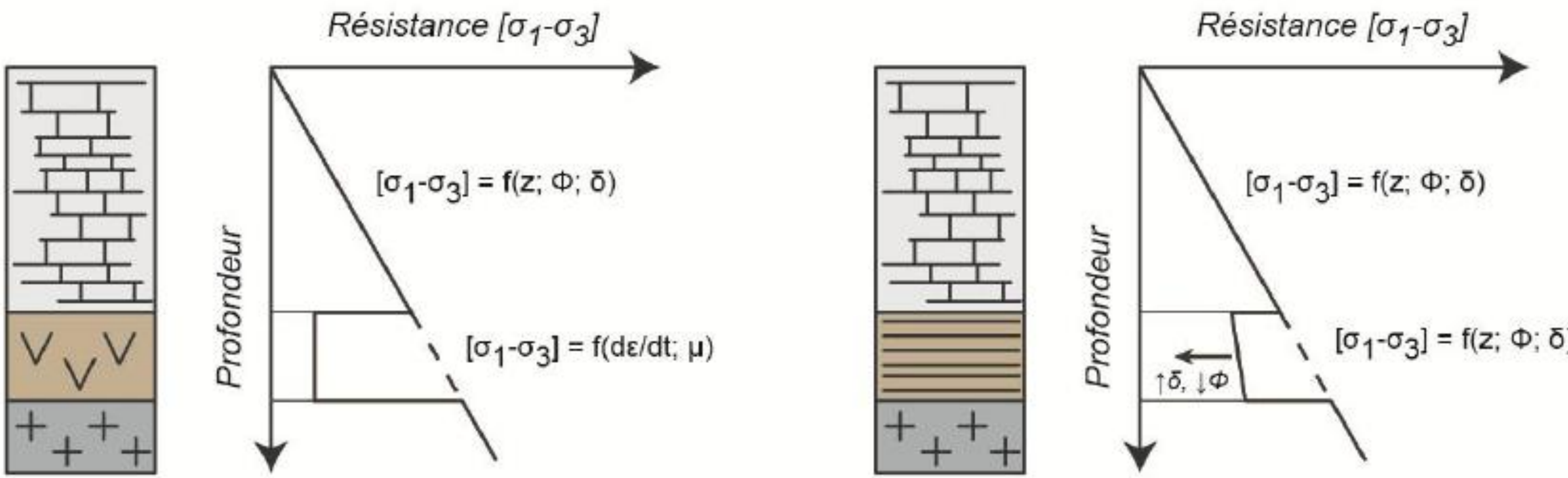

a) Profil de résistance typique d’une colonne sédimentaire détachée sur un niveau salifère

Le comportement du sel est controlé par sa viscosité et par le taux de déformation

b) Profil de résistance typique d’une colonne sédimentaire détachée sur un niveau argileux

Le comportement du décollement argileux est controlé par ses propriétés de frictions, par la profondeur de décollement et par la pression de fluides

(Berthelon, thèse, 2015)

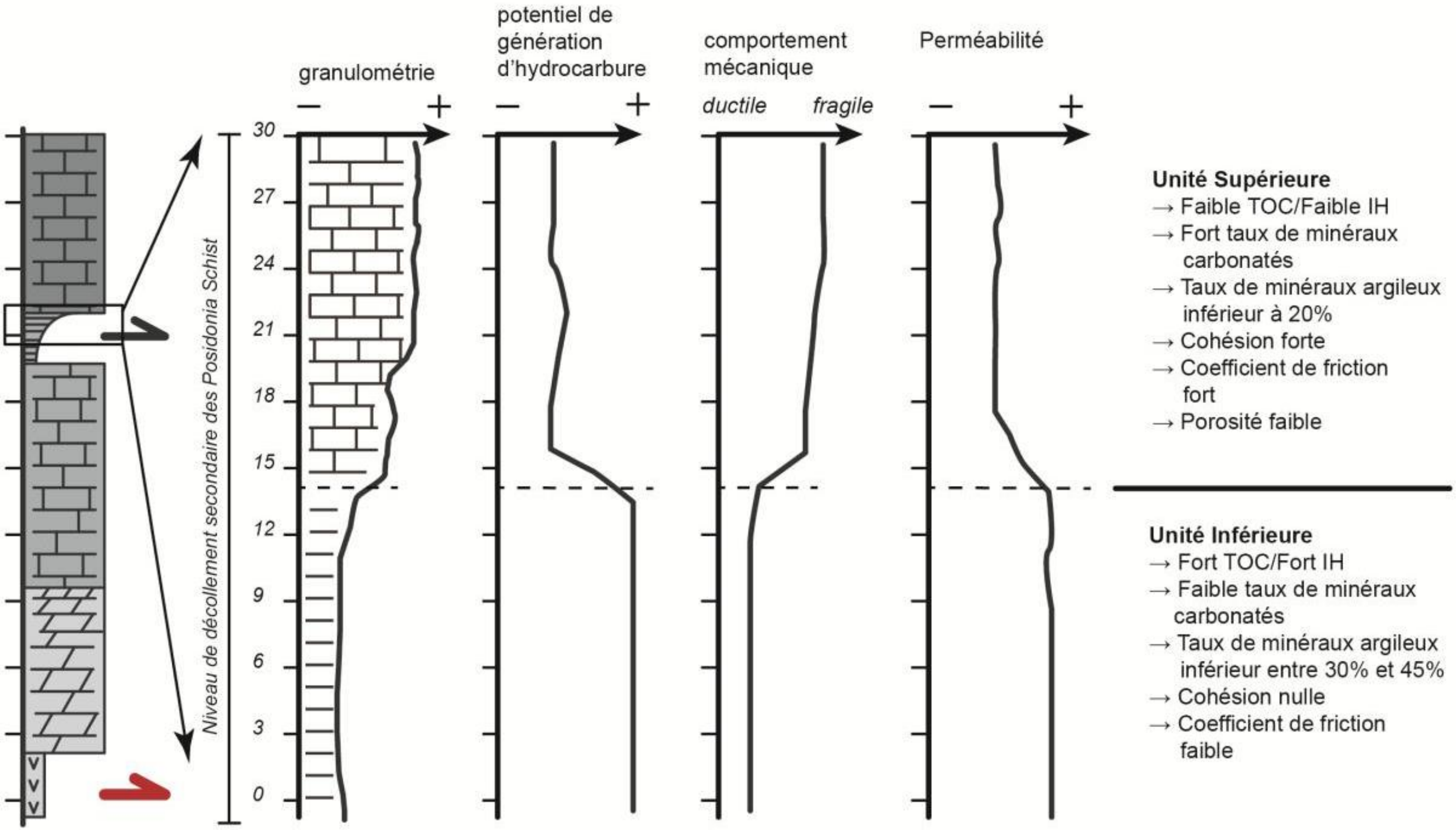

Colonne straitgraphique du Trias et du Jurassique inférieure et moyen du Mali i Gjerë

(Berthelon, thèse, 2015)

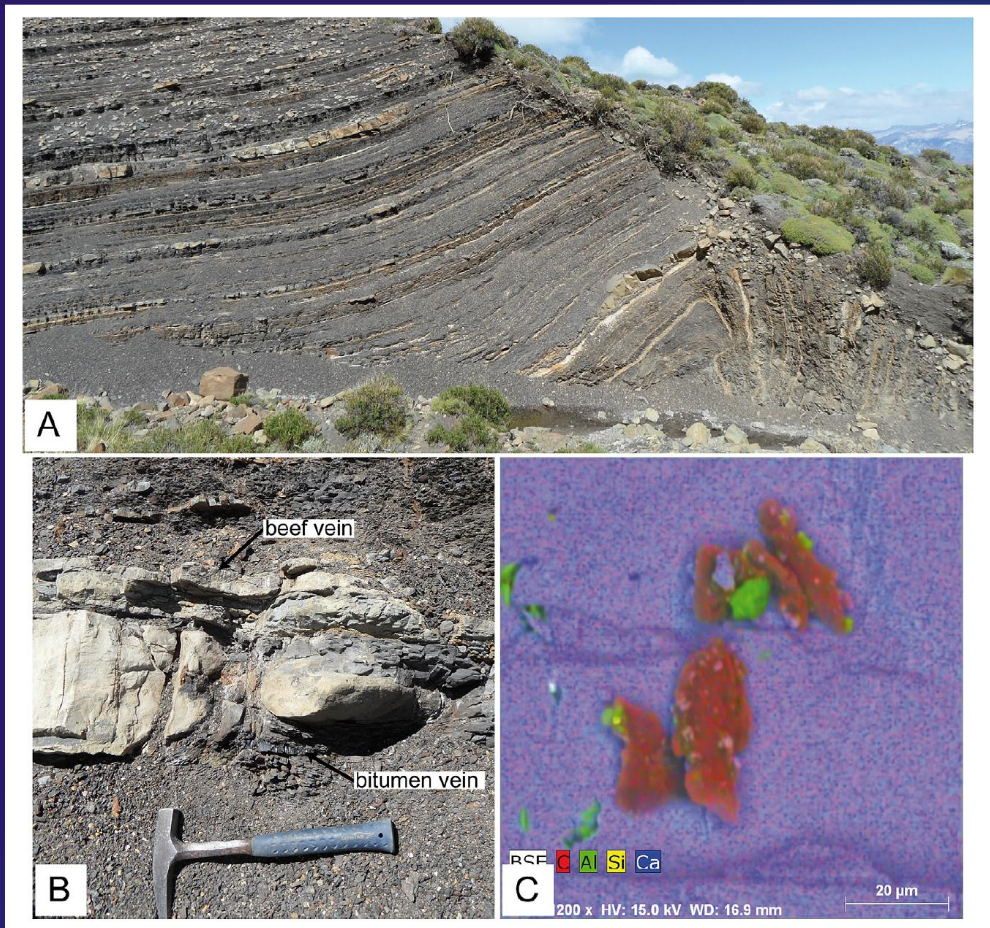

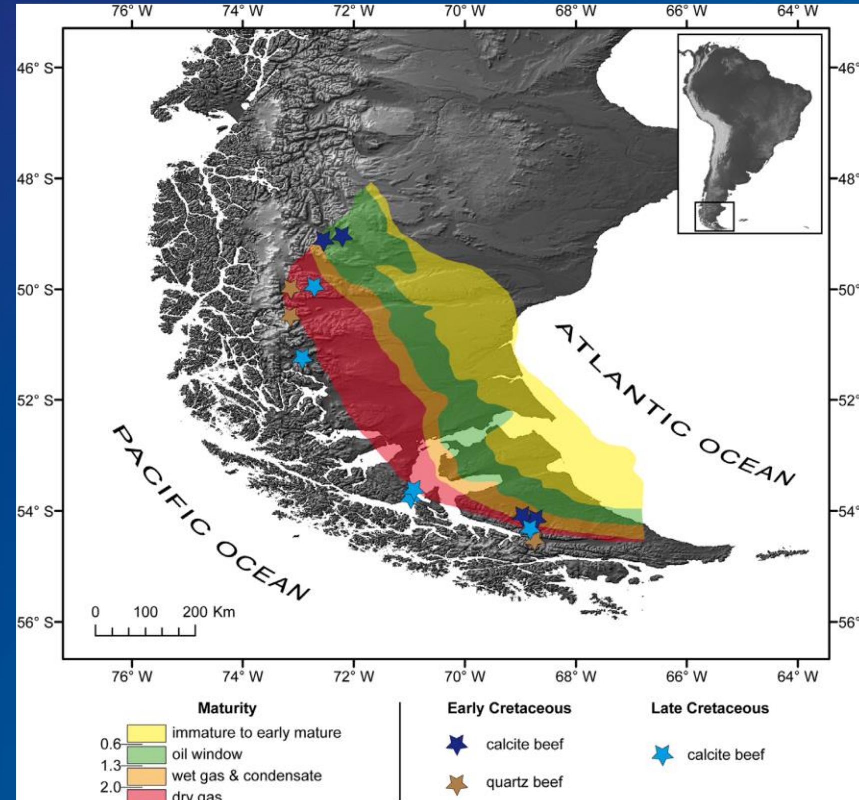

Calcite beef occurs in mudstone source rocks, together with thrust detachments, which are visible at the surface and on subsurface data. Beef contains solid inclusions of bitumen, or fluid inclusions of oil or gas. This provides evidence for overpressure during hydrocarbon migration.

Hydrocarbon generation in the Magallanes-Austral Basin has led to overpressure as a result of chemical compaction and load transfer, or volume changes during hydrocarbon generation, or both.

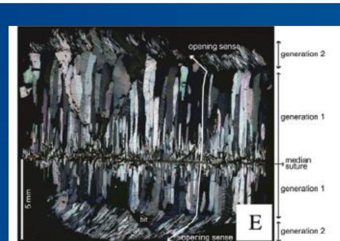

(Zanella et al., 2014)

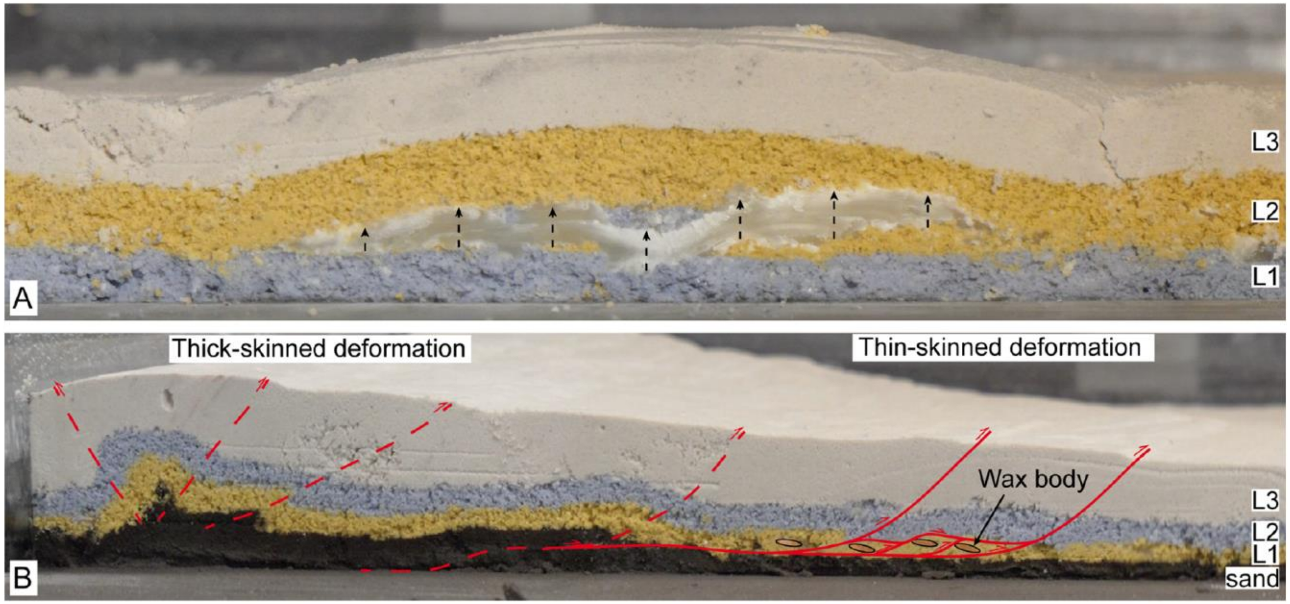

Figure 9. Close-up views of two models, illustrating structural details. A. Central part of cross-section number 16, Experiment 4 – Series II (no applied horizontal deformation). Main wax sill (white) is clearly visible (centre) and attests to tensile opening (arrows) of horizontal hydraulic fracture. Upward bulging of white and yellow layers corresponds to opening of fracture. Basal blue layer has compacted, due to collapse of solid framework, as wax melted and migrated upwards. However, area of compaction is wider than length of main wax body. B. Part of model near piston, after horizontal shortening (Experiment 5 – Series II). Deformation is thick-skinned, near piston (left) and thin-skinned, away from piston (right). Flat-lying detachment is visible at base of yellow source layer. This layer also contains an imbricate thrust zone and several gently dipping wax bodies, which we interpret as having formed during horizontal simple shear (top to right). (For interpretation of the references to colour in this figure legend, the reader is referred to the web version of this article.)

(Zanella et al., 2014)

Physical experiment with horizontal shortening before the wax had started to melt : Fore-thrusts and back-thrusts developed across all of the layers near thepiston, producing a high-angle prism. In contrast, as soon as the wax melted, overpressure developed within the source layer and a basal detachment appeared beneath it. As a result, thin-skinned thrusts propagated further into the model, producing a low-angle prism. In some experiments, bodies of wax formed imbricate zones within the source layer.

It is the transformation, from solid to liquid wax, that led to chemical compaction, overpressure development and hydraulic fracturing within a closed system. Load transfer from the overburden to the fluid, due to collapse of the solid load-supporting framework (this process being mechanically analogous to chemical compaction) was the main mechanism, but volume changes also contributed, producing supra-lithostatic overpressure and therefore tensile failure of the mixture, with hydraulic fractures filled with molten wax.

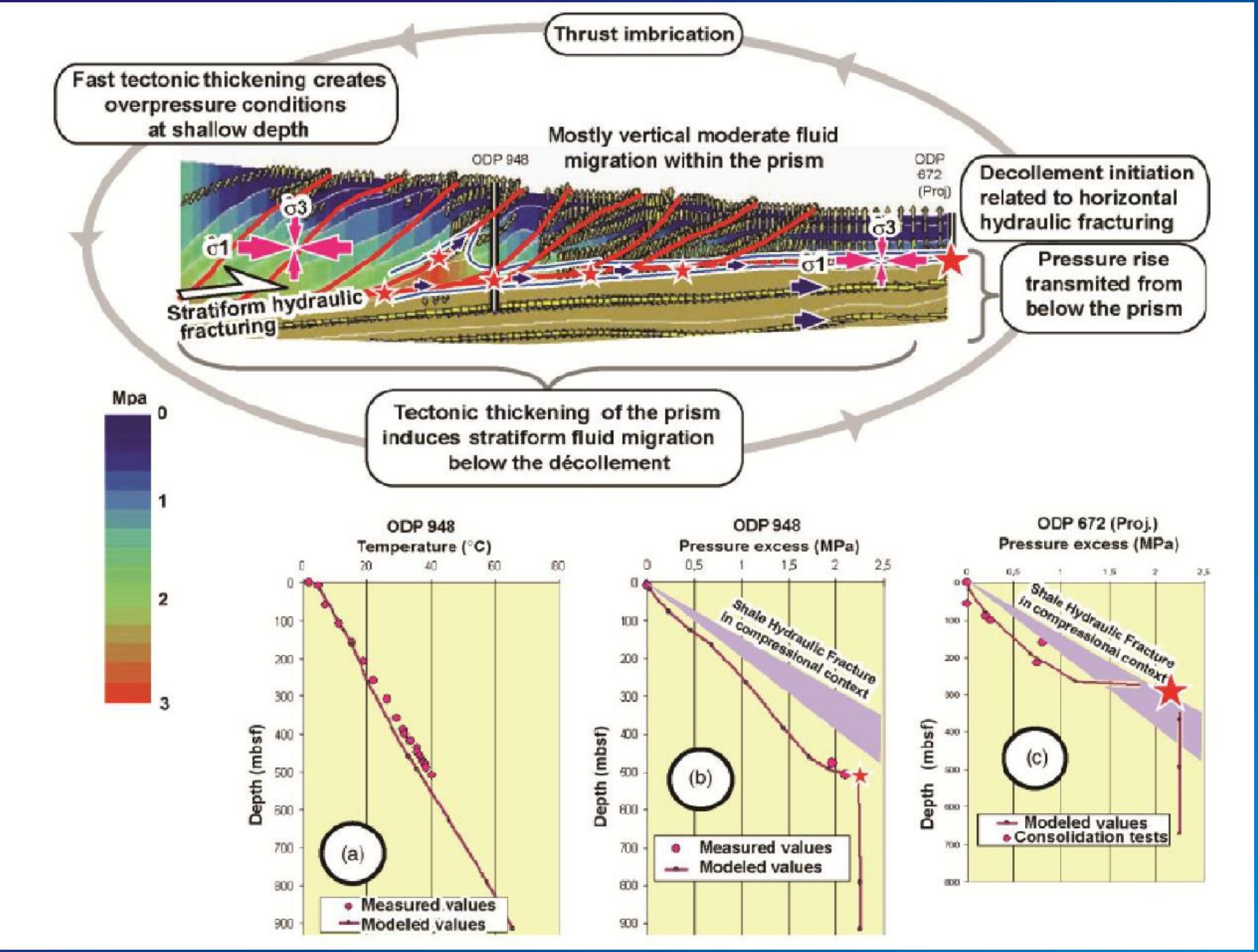

An overpressured horizon in the foreland strongly decreases the mechanical coupling and friction between deeper and shallower horizons, thus helping the localizing and propagating forelandward of the deformation front.

Fluid overpressures and reservoir quality

Viking graben area, Northern North Sea
- Two wells “A” and “B”, 5 km apart
- Same reservoir, middle Jurassic sandstone
- Same burial depth, 3.5 km
- **Very contrasting reservoir quality**

Well	Burial Depth	Present-day Pressure	φ	K
A	3560 m	60 MPa	18%	300 mD
B	3610 m	70 MPa	25%	1200 mD

WHY?

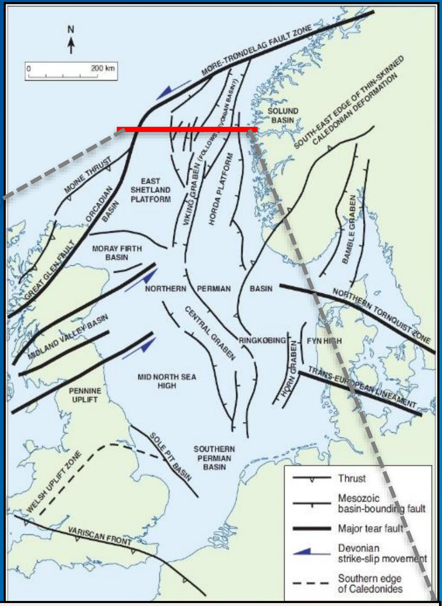

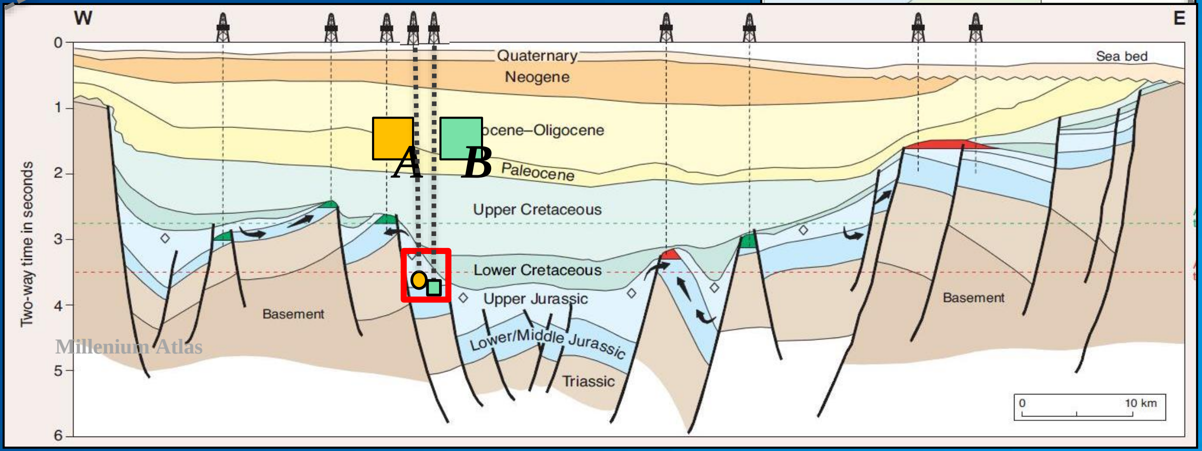

Example of microfractures in quartz grain visible via SEM-CL image from a polished thin sections of well A and well B. FQGR of the samples was quantified using manual grain counting method. FQGR is higher in well A than in well B.

Well	FQGR	GS	Ductile	Sorting
A	49%	300µm	4%	Well
B	32%	250µm	2%	Well

(Merhkian, thèse, 2016)

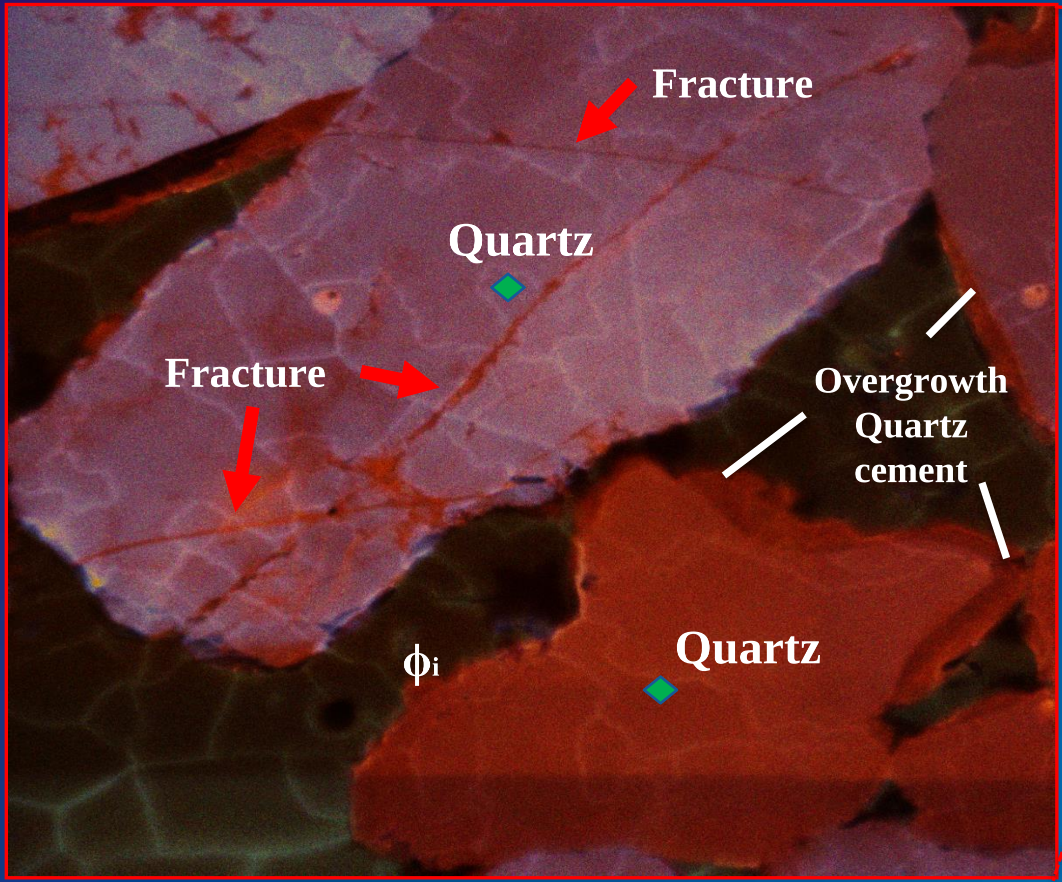

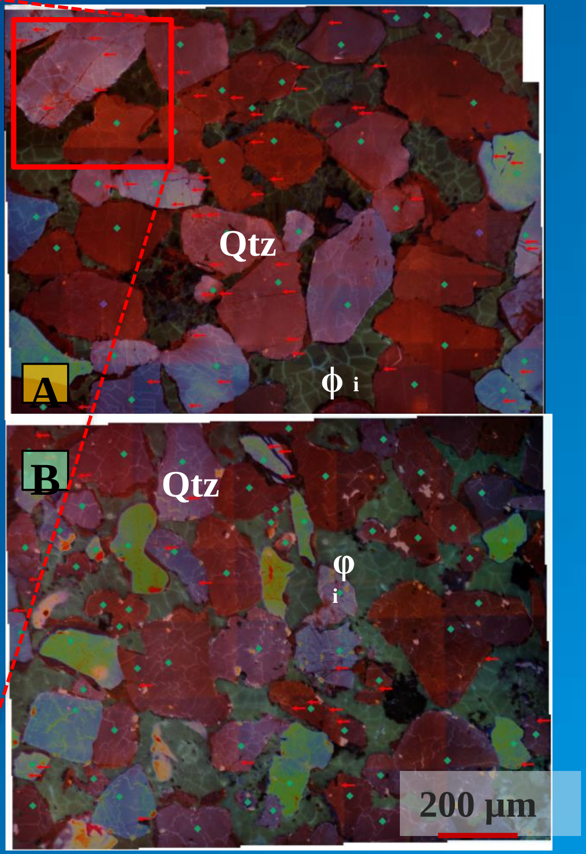

To understand the cause of this difference, normal petrographic studies have been done on thin sections from the plugs of the two wells. Studies consist of point counting of more than 300 point per thin section and SEM-CL imagery of each thin section.

(Merhkian, thèse, 2016)

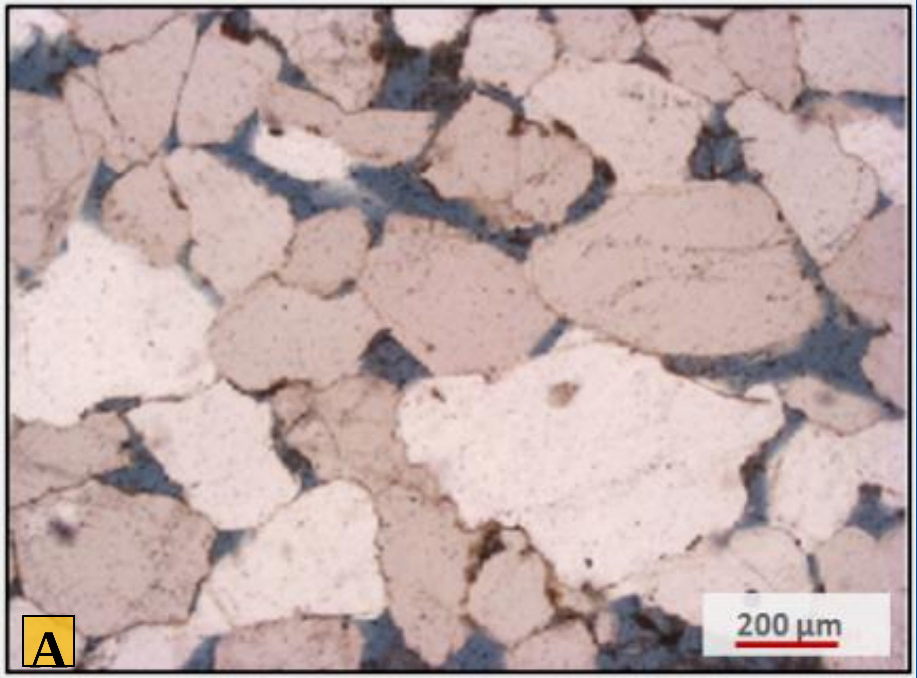

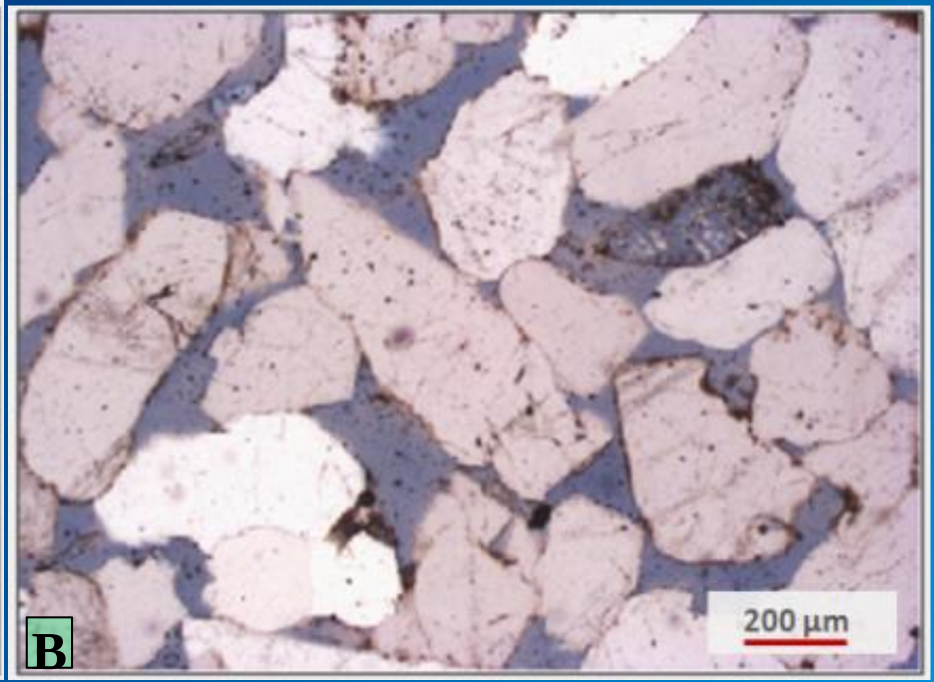

Higher rate of pressure dissolution in quartz grains is obvious in sample from well A. In contrast sample from well B shows more porosity

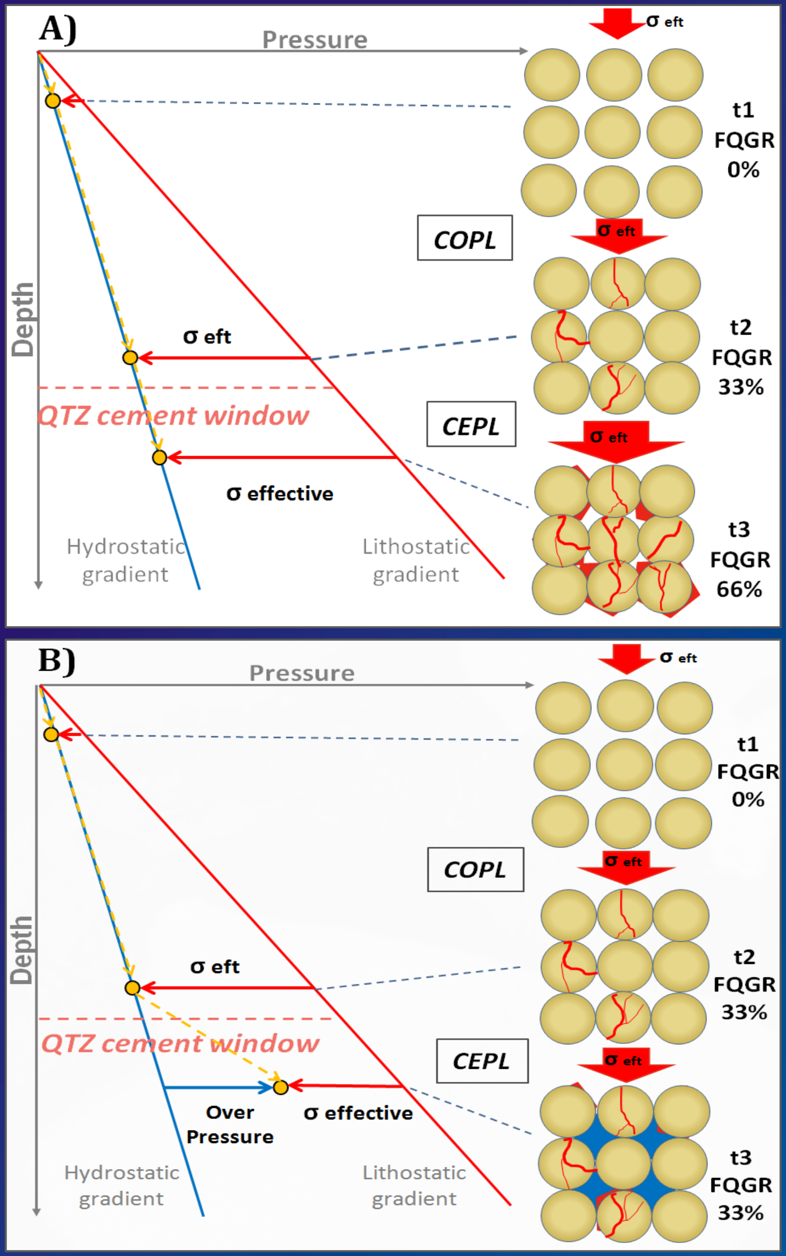

Mechanical compaction in response to effective vertical stress increase consists of rearrangement and ductile/brittle deformation (microfracturing) of framework grains.

Effective stress (burial) ~> microfracturing in brittle grains

In normal hydrostatic conditions, effective stress will progressively increase with burial depth. In petroleum reservoirs, overpressure is commonly observed, resulting in a decrease of effective stress.

We suggest that the ratio of fractured grain in a sealed reservoir is recorded when the Effective stress reaches its highest level in the reservoir and it is quantified as Fractured Quartz Grain ratio (FQGR). By comparing the FQGR of a sealed reservoir with its hydrostatic equivalent, one could deduce the onset of overpressure build up (Maximum effective stress).

(Merhkian, thèse, 2016)

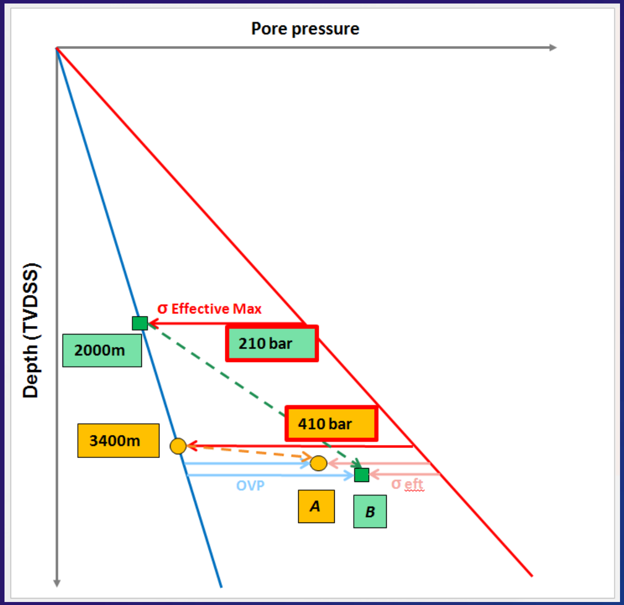

We consider that the maximum effective stress is the onset of overpressure (OVP). The value of **maximum effective stress** will provide the **depth** in which the system has left the hydrostatic gradient (**OVP onset**).
Furthermore, using a basin model, it is possible to obtain the **age** of this event.

In well B, the age of OVP onset occurs slightly before the beginning of hydrocarbon generation; therefore early OVP buildup contributed to inhibit compaction and to favor better reservoir quality in well B.
OVP build-up occurred later in well A.

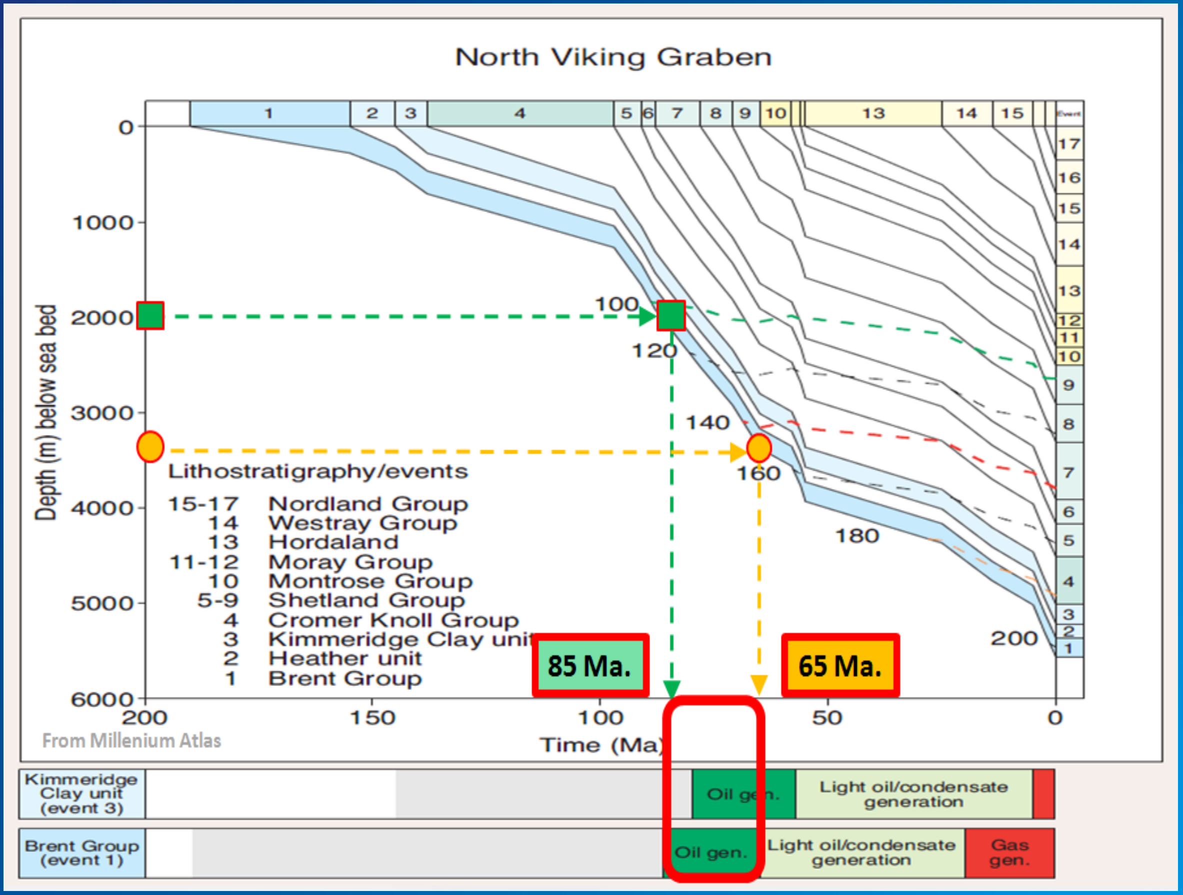

(Merhkian, thèse, 2016)

The Pô Plain case study

From 1973 to 1984, hydrocarbon exploration of the Mesozoic carbonates developed through investigation of both overthrust structures developed during Alpine orogenesis and drilling of Mesozoic structural highs formed by Triassic–Liassic rifting.

Both types of targets proved to be successful and led to the discovery of four major hydrocarbon fields, namely the Malossa, Cavone, Gaggiano and Villafortuna fields. The latter is one of the largest oil fields in continental Europe and has produced 226 MMbbl (million barrels) of light oil to date from a record depth of 6000 m bsl.

Po Valley Hydrocarbons Modelling

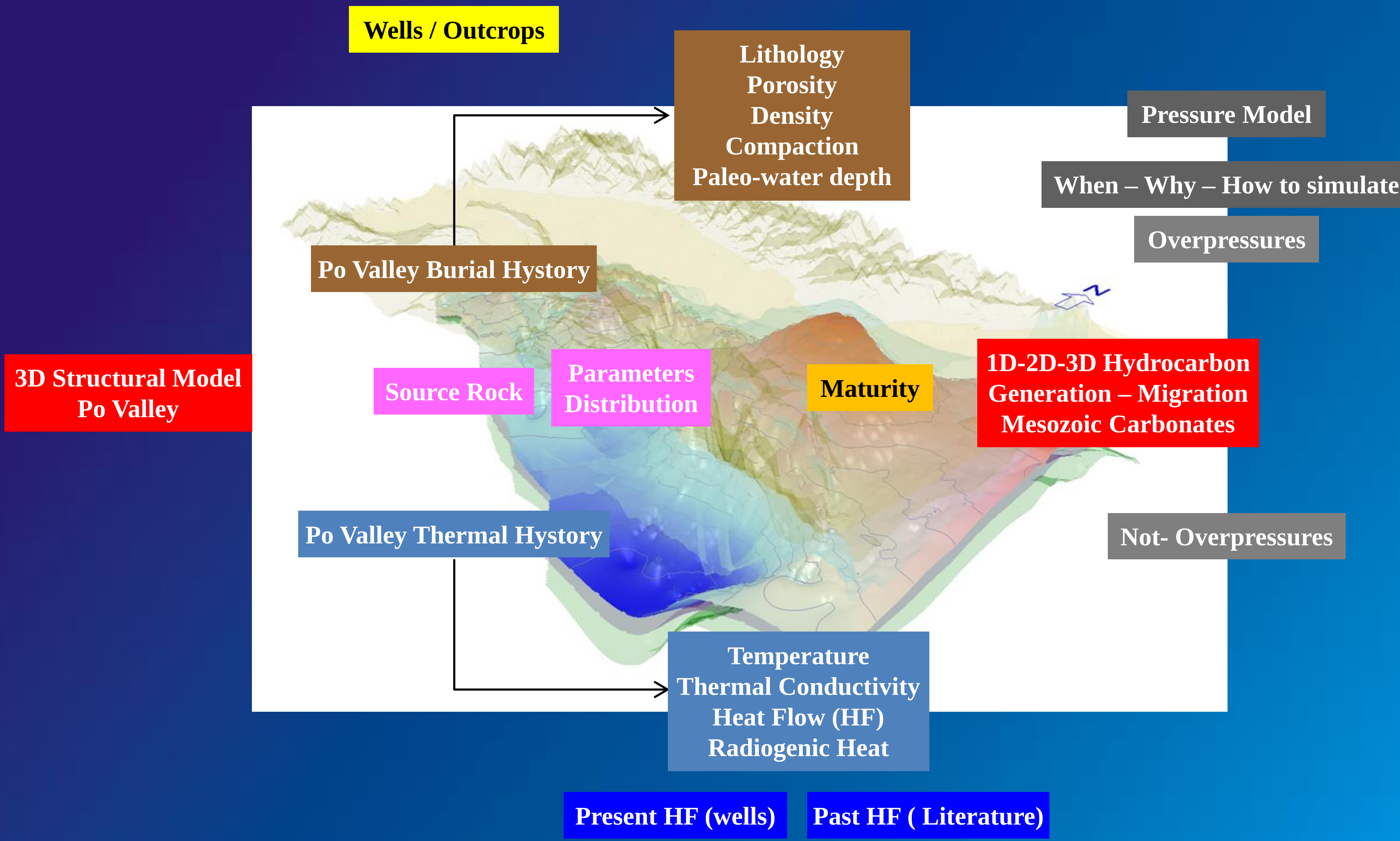

Modelling at basin-scale !!

(Turrini, thèse, 2016)

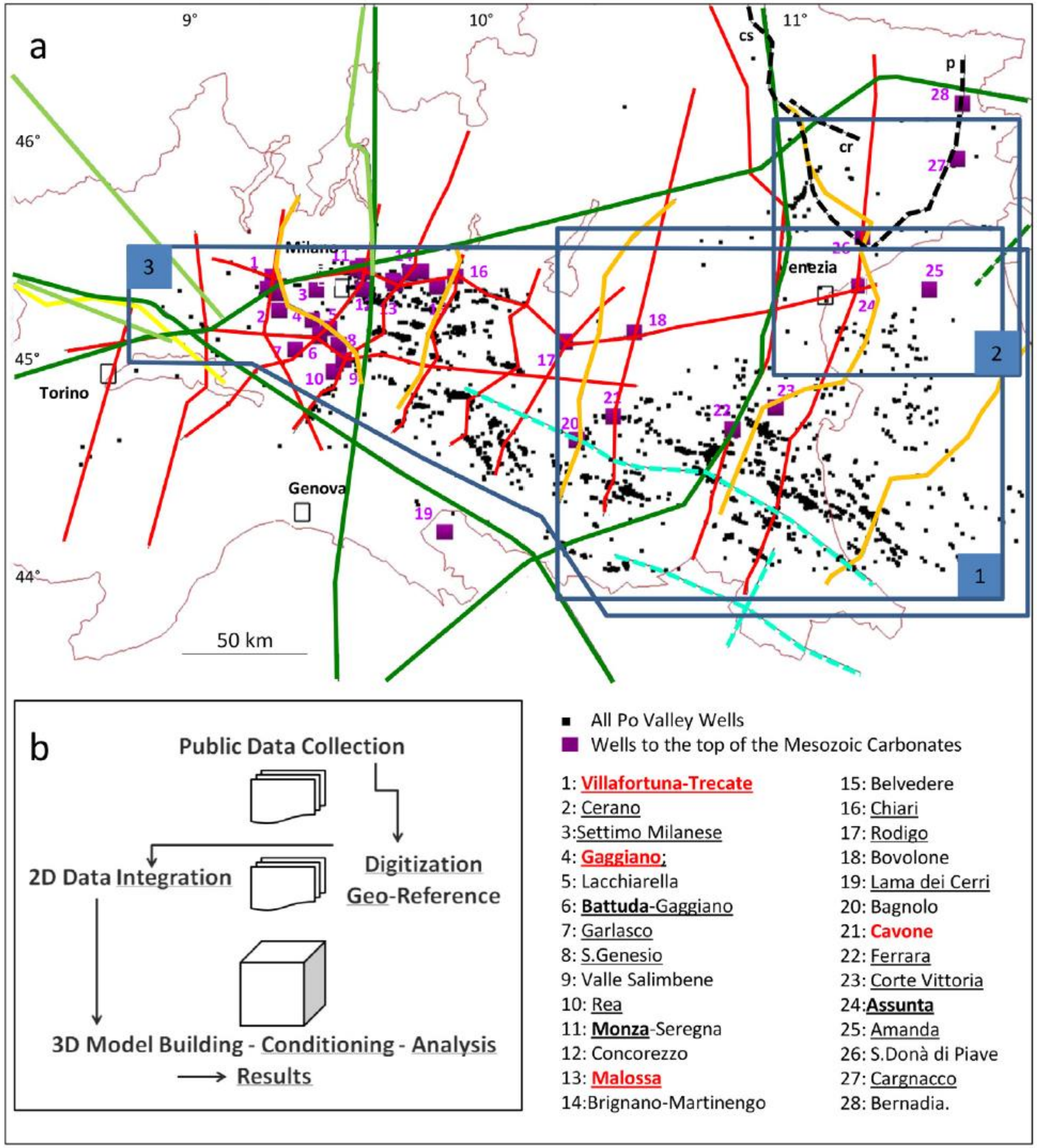

a
9°
10°
11°
46°
45°
44°
cs
cr
p
Milano
Torino
Genova
enezia
50 km
1
2
3
b
Public Data Collection
Digitization
Geo-Reference
2D Data Integration
3D Model Building - Conditioning - Analysis
Results
All Po Valley Wells
Wells to the top of the Mesozoic Carbonates
1: Villafortuna-Trecate
2: Cerano
3:Settimo Milanese
4: Gaggiano;
5: Lacchiarella
6: Battuda-Gaggiano
7: Garlasco
8: S.Genesio
9: Valle Salimbene
10: Rea
11: Monza-Seregna
12: Concorezzo
13: Malossa
14:Brignano-Martinengo
15: Belvedere
16: Chiari
17: Rodigo
18: Bovolone
19: Lama dei Cerri
20: Bagnolo
21: Cavone
22: Ferrara
23: Corte Vittoria
24:Assunta
25: Amanda
26: S.Donà di Piave
27: Cargnacco
28: Bernadia.

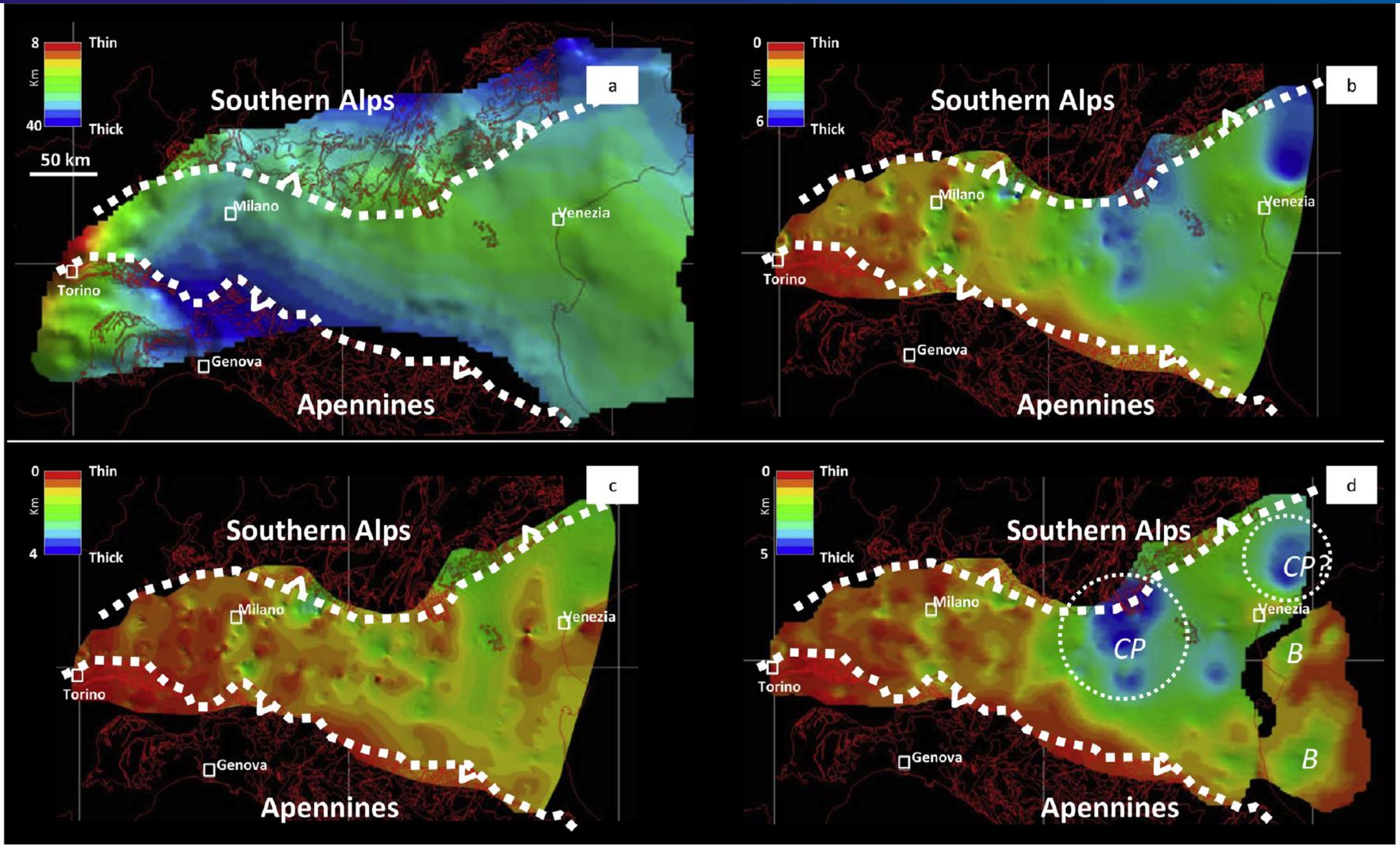

(a) Isopach map of the crust in the Po Valley basin. (b) Isopach map of the Mesozoic sedimentary successions in the Po Valley basin. (c) Isopach map of the Cretaceous–Jurassic sedimentary successions in the Po Valley basin. (d) Isopach map of the Triassic sedimentary successions in the Po Valley basin. (CP) Carbonate Platform facies from outcrops and wells; (B) Triassic basins from 3D seismic data (Franciosi and Vignolo, 2002); Outcrops, coast-line & northern Italy state boundaries in red. Grid in all maps is 200 km. (For interpretation of the references to colour in this figure legend, the reader is referred to the web version of this article.)

(Turrini et al., 2014)

Base Pliocene

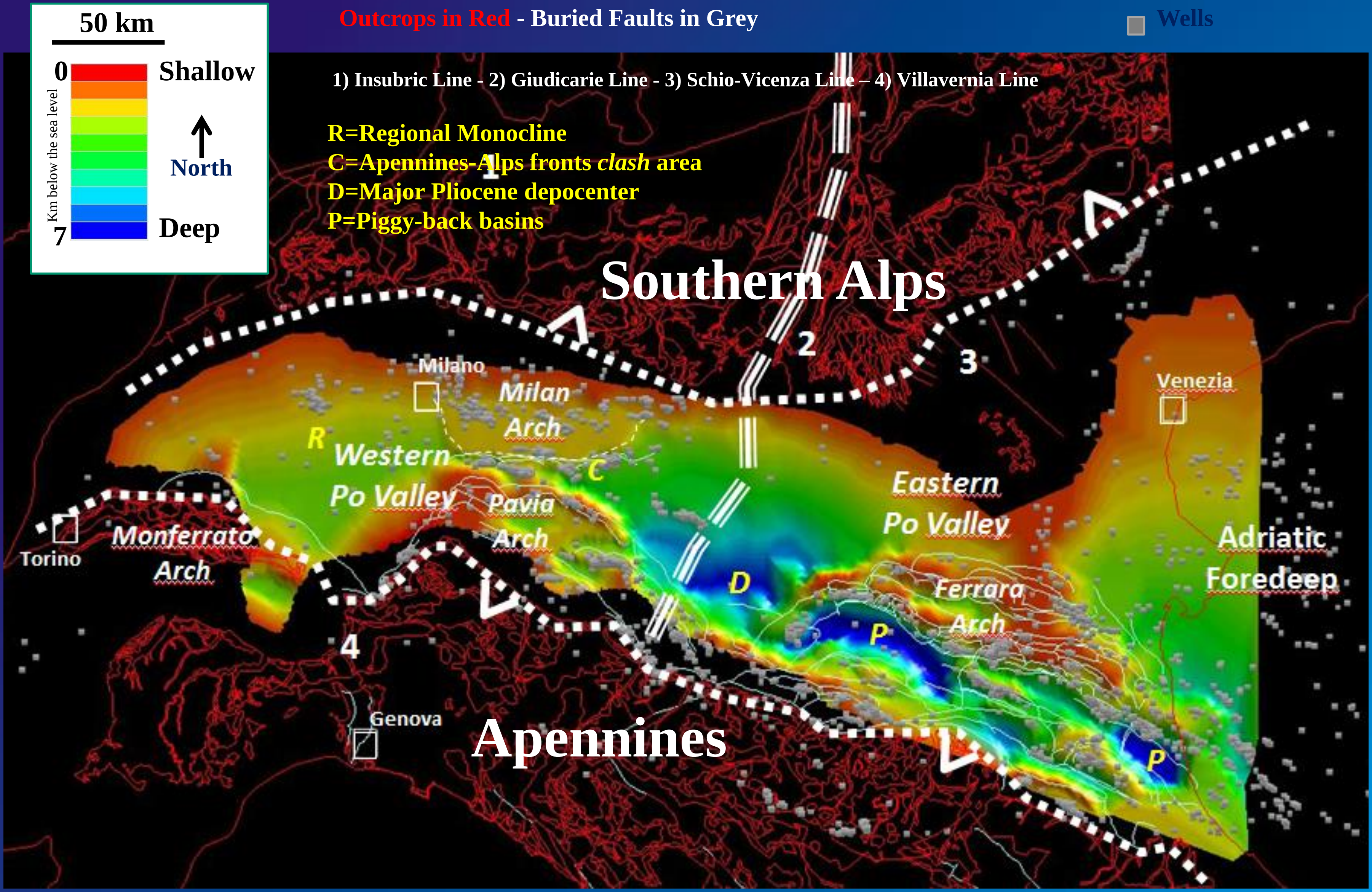

(Turrini et al., 2014)

Top Mesozoic

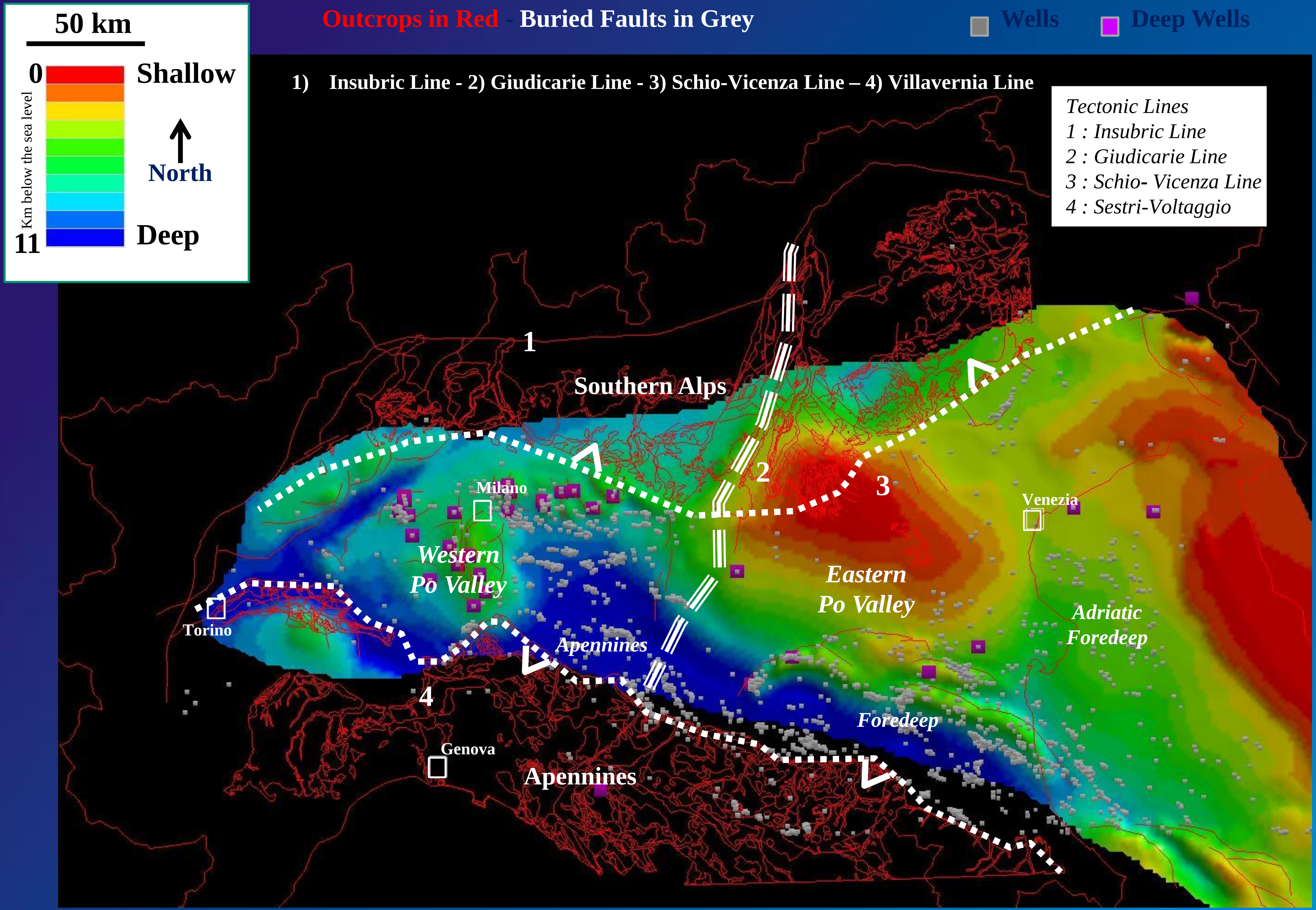

(Turrini et al., 2014)

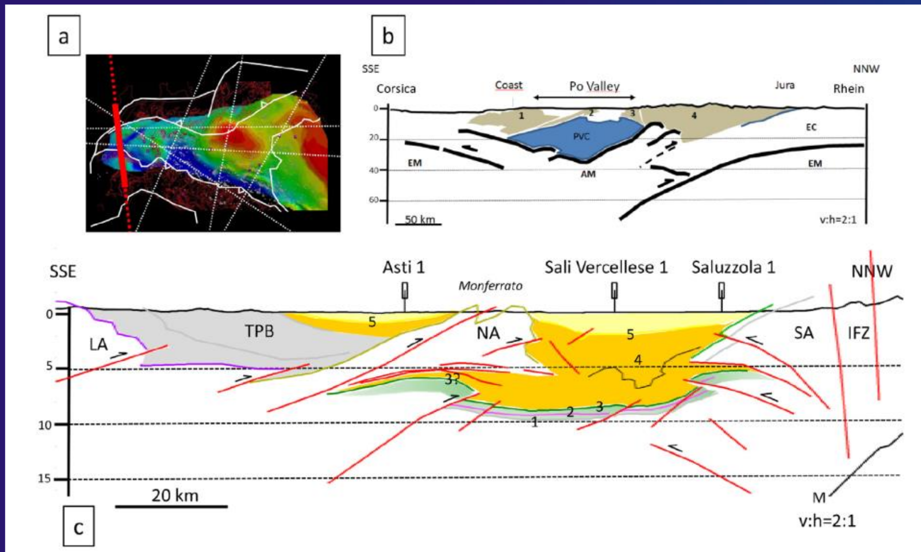
a
b
SSE
NNW
Corsica
Coast
Po Valley
Jura
Rhein
PVC
EM
AM
EC
50 km
v:h=2:1
SSE
Asti 1
Monferrato
Sali Vercellese 1
Saluzzola 1
NNW
LA
TPB
NA
SA
IFZ
M
20 km
c
v:h=2:1
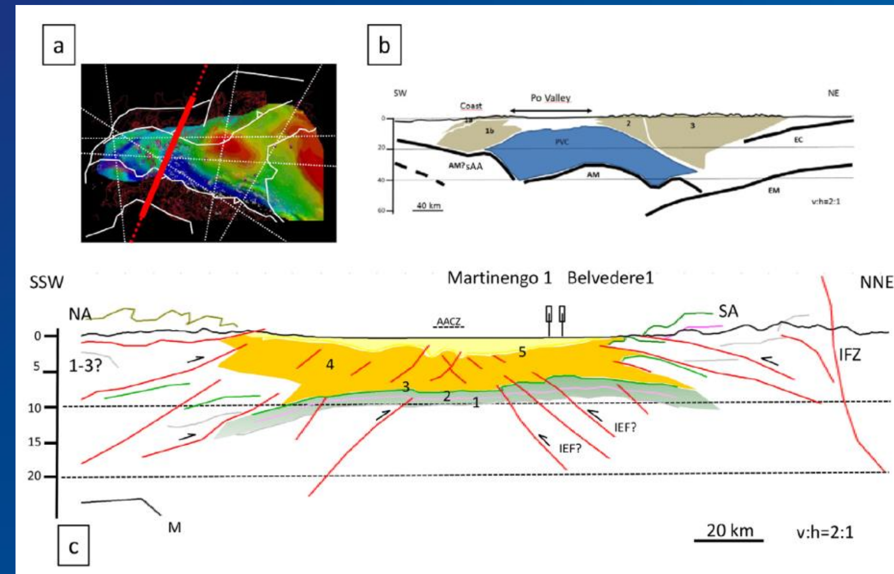
a
b
SW
NE
Coast
Po Valley
PVC
AM
EC
EM
40 km
SSW
Martinengo 1
Belvedere1
NNE
NA
AACZ
SA
1-3?
IFZ
IEF?
IEF?
M
20 km
v:h=2:1
c
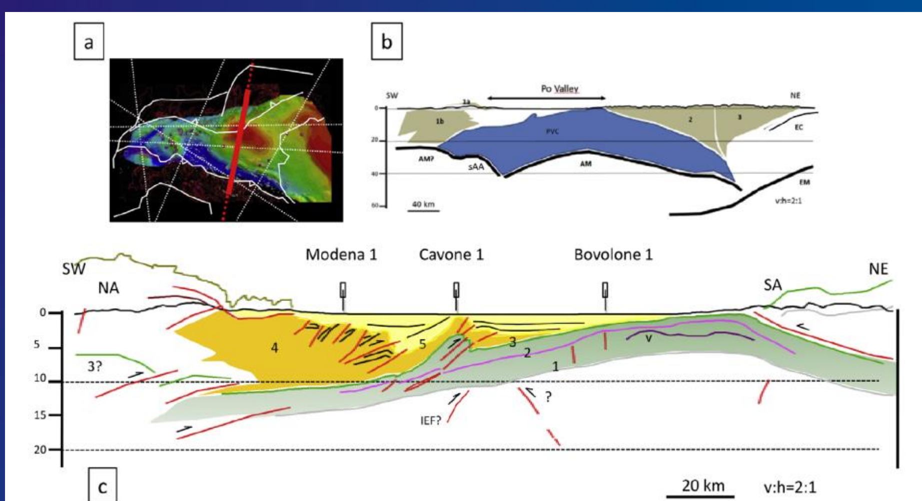
a
b
SW
NE
Po Valley
PVC
AM
sAA
AM?
EC
EM
40 km
SW
Modena 1
Cavone 1
Bovolone 1
NE
NA
SA
3?
IEF?
20 km
v:h=2:1
c
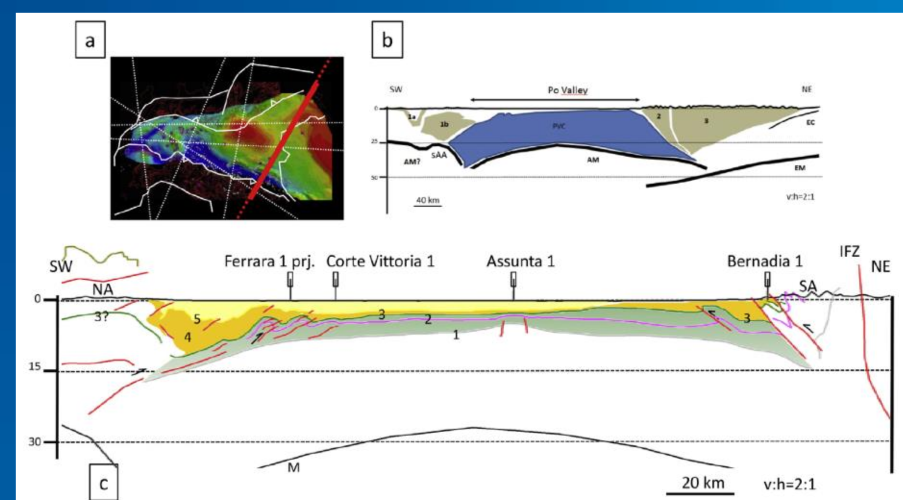
a
b
SW
NE
Po Valley
PVC
AM
sAA
AM?
EC
EM
40 km
SW
Ferrara 1 prj.
Corte Vittoria 1
Assunta 1
Bernadia 1
IFZ
NE
NA
SA
3?
M
20 km
v:h=2:1
c

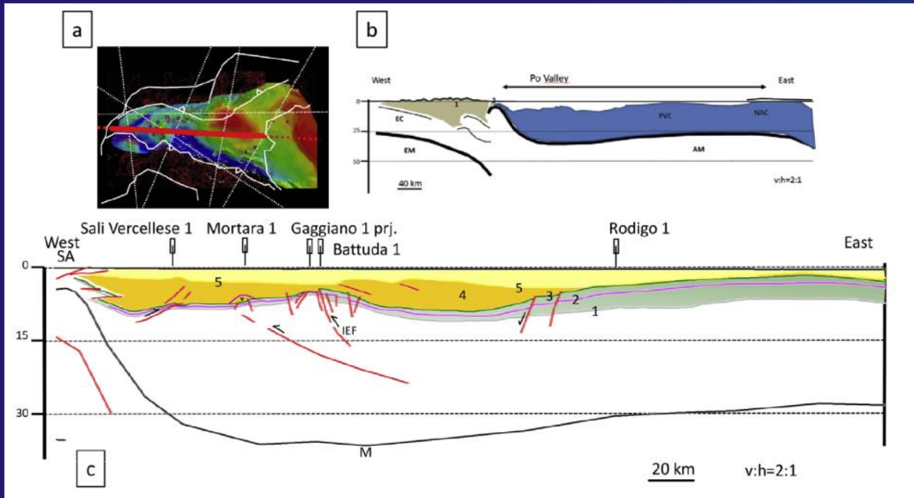
a
b
West
Po Valley
East
EC
EM
PVC
NAC
AM
40 km
v:h=2:1
Sali Vercellese 1
Mortara 1
Gaggiano 1 prj.
Battuda 1
Rodigo 1
West
SA
East
0
15
30
5
4
5
3
2
1
IEF
M
c
20 km
v:h=2:1

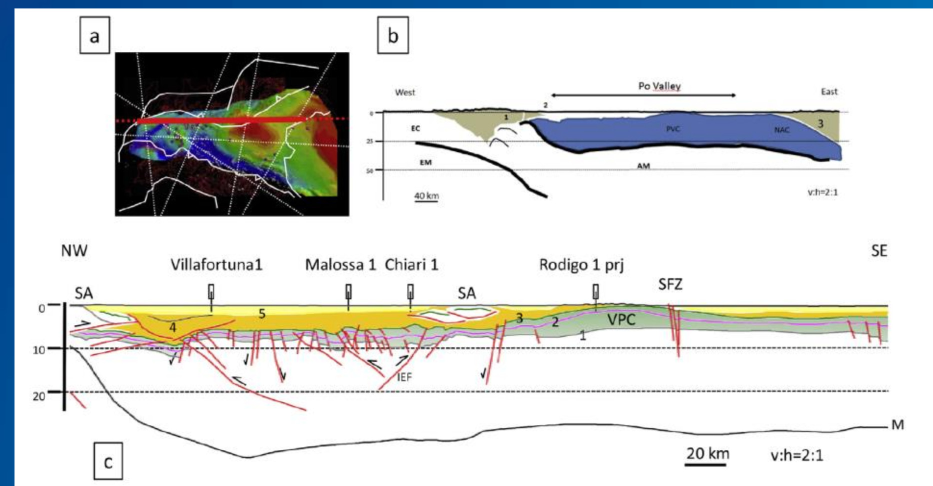
a
b
West
Po Valley
East
EC
EM
PVC
NAC
AM
40 km
v:h=2:1
NW
SE
Villafortuna1
Malossa 1
Chiari 1
Rodigo 1 prj
SA
SA
SFZ
0
10
20
4
5
3
2
1
VPC
IEF
M
c
20 km
v:h=2:1

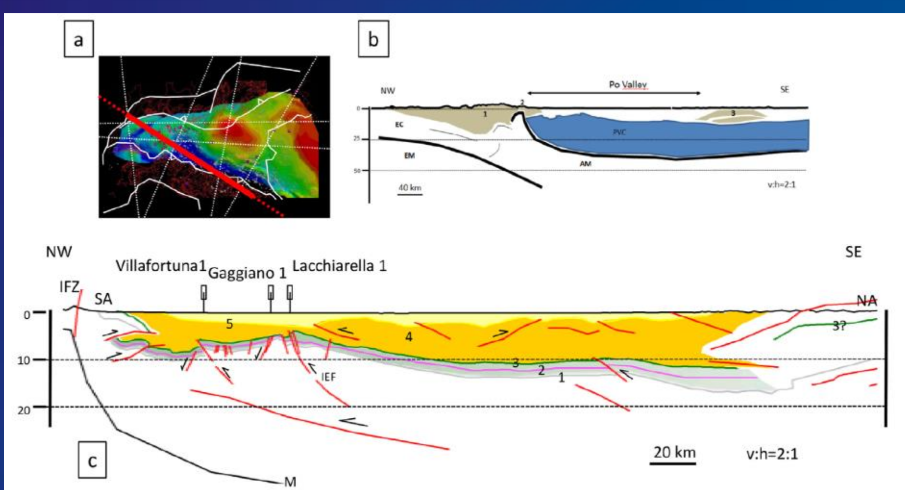
a
b
NW
Po Valley
SE
EC
EM
PVC
AM
40 km
v:h=2:1
NW
SE
IFZ
SA
Villafortuna1
Gaggiano 1
Lacchiarella 1
NA
0
10
20
5
4
3?
3
2
1
IEF
M
c
20 km
v:h=2:1

Turrini et al., 2016

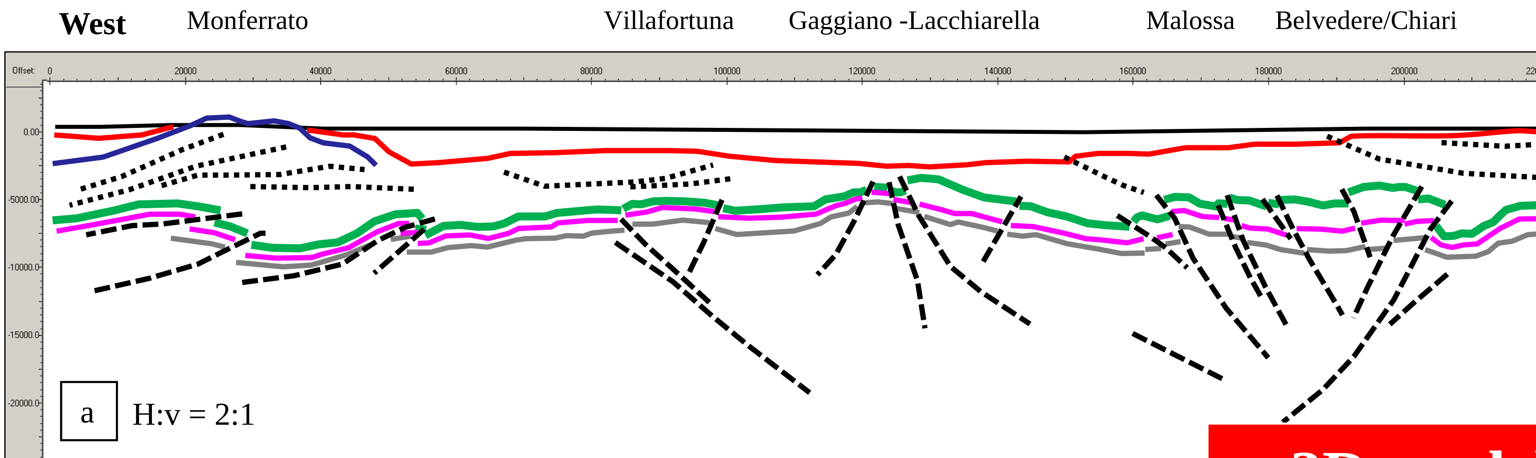

3D model Vertical Slicing

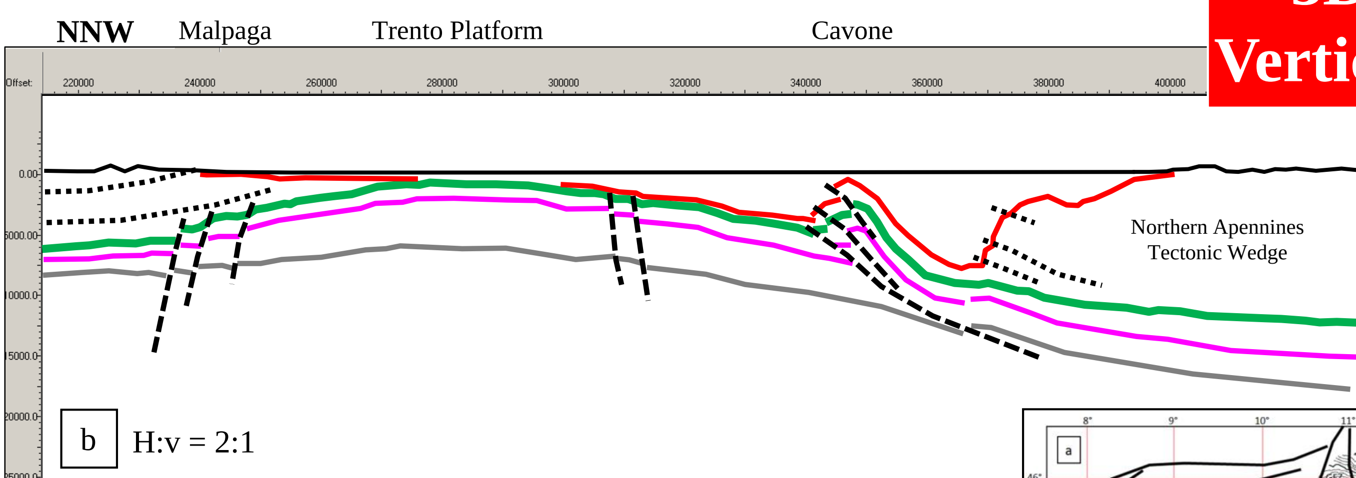

Faults
- Base Pliocene (Messinian Unconformity)
- Top Mesozoic Carbonates (Maiolica)
- Top Triassic
- Top Basement

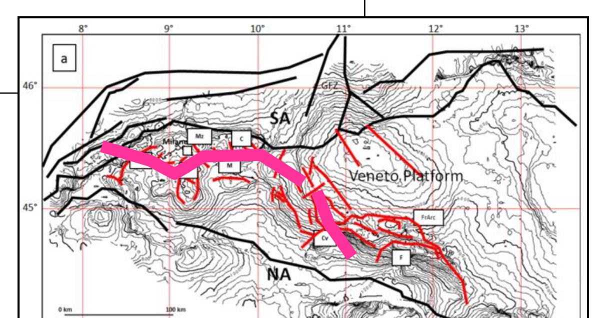

Mesozoic vs Alpine tectonics

Turrini et al., 2016

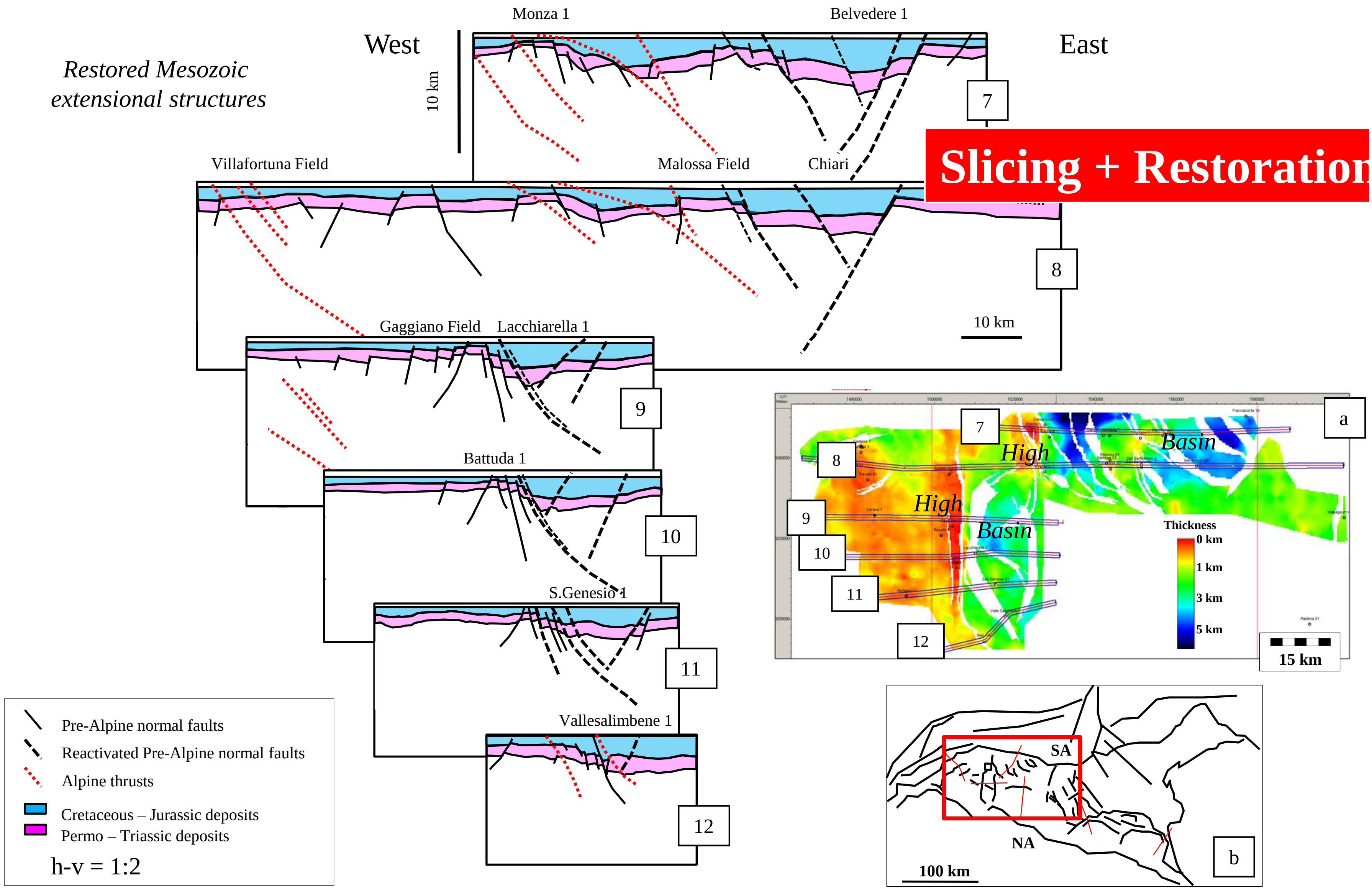

(Turrini et al., 2018)

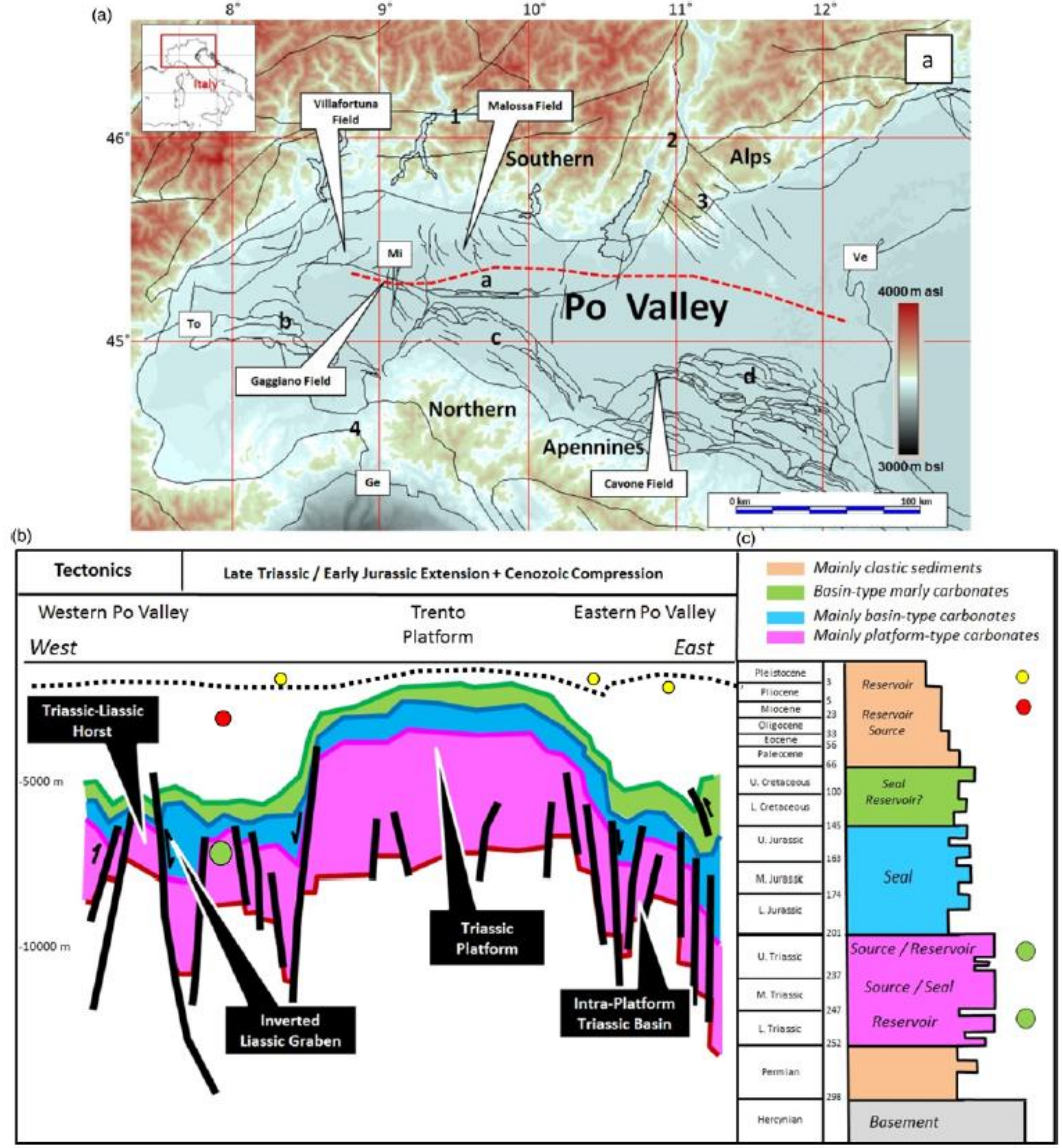

Fig. 1. Regional setting, tectonostratigraphic framework and petroleum system of the Po Valley Basin. (**a**) Location map of the study area , major oil fields at the Mesozoic level and major cities (Mi, Milano; To, Torino; Ge, Genova; Ve, Venezia); a, Milan tectonic arc; b, Monferrato arc; c, Emilia arc; d, Ferrara arc; 1, Insubric line; 2, Giudicarie line; 3, Schio-Vicenza line; 4, Sestri-Voltaggio line. (**b**) Structural cross-section (red dashed line in a) through the study area showing present-day geometries of main structural elements and hydrocarbon distribution. (**c**) Major stratigraphic units, stratigraphy and hydrocarbon distribution: the yellow circle is mainly biogenic gas; the red circle is thermogenic oil in Tertiary successions; the green circle is thermogenic oil and condensate in Triassic carbonates.

Petroleum systems in the Po Valley

Triassic–Liassic petroleum systems have produced gas, condensate and light oil from deep Mesozoic carbonates. The reservoir consists of dolomitized carbonate platform units of middle Triassic–Early Jurassic age, charged by middle–late Triassic carbonate source rocks deposited in intra-platform lagoons and basins. Traps are mostly provided by Mesozoic extensional structures locally inverted during the Cenozoic compression. The Cretaceous–Jurassic pelagic carbonates provide the regional seal.

The Oligo-Miocene petroleum system produces thermogenic gas with secondary quantities of oil from the foredeep successions that are detached and thrust over the carbonates and belong to the Northern Apennine belt. The system is composed of thick turbidite sequences that supply both the reservoir and the source and seal elements, and the traps are usually structural.

The Plio-Pleistocene petroleum system contains large volumes of biogenic gas notably at the buried external fronts of the Apennine thrust belt.
The system consists of sand-rich turbidites in which thick-bedded sand lobes and thin-bedded, fine-grained basin plain/lobe fringe deposits are the main reservoir facies associations.
Interbedded clays are both the source rock and the effective top seal.
Traps are most commonly structural, yet stratigraphic traps also occur, mainly related to the onlap of turbidite reservoirs onto the flanks of thrust propagation folds or against the foreland ramp.

Top Mesozoic structures & Hydrocarbons

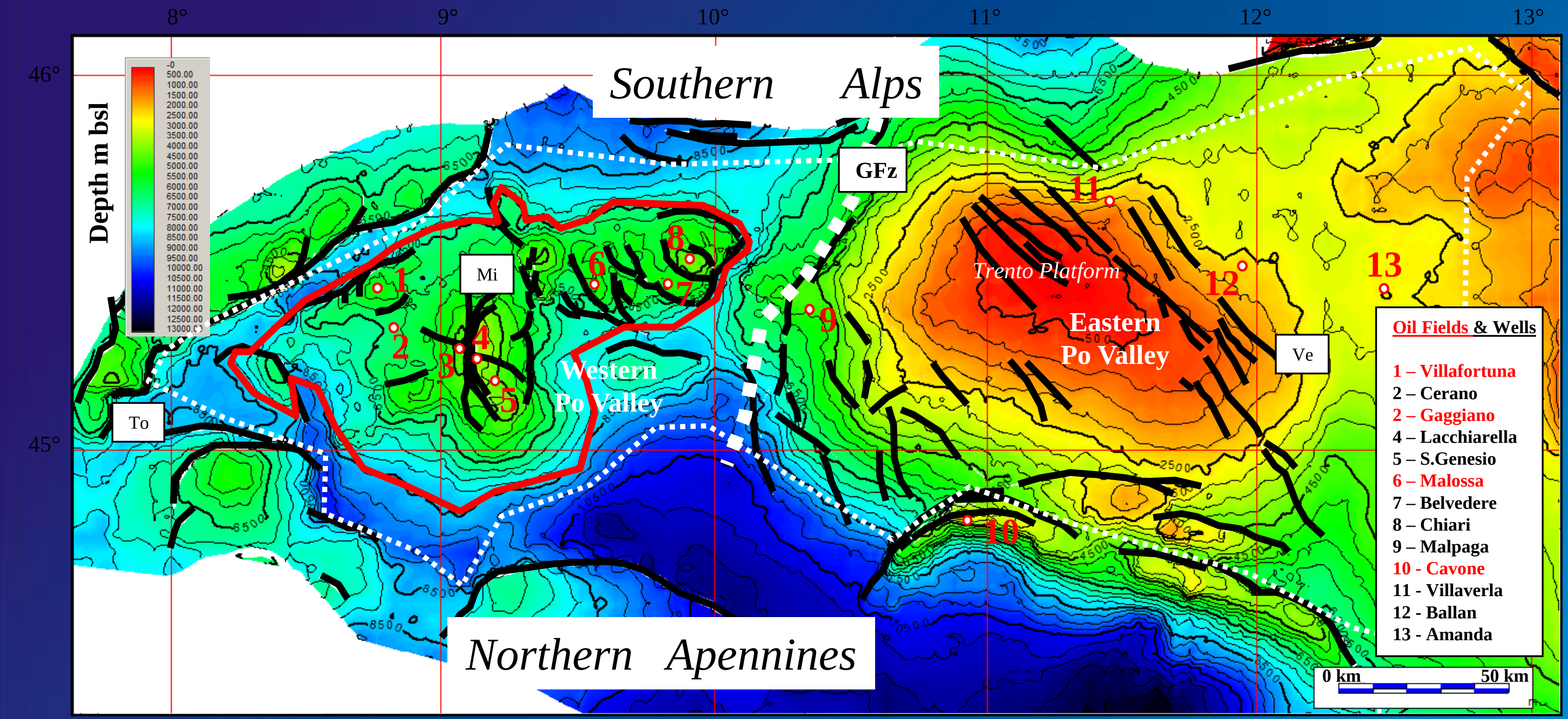

(Turrini et al., 2018)

Po Valley Oil Fields

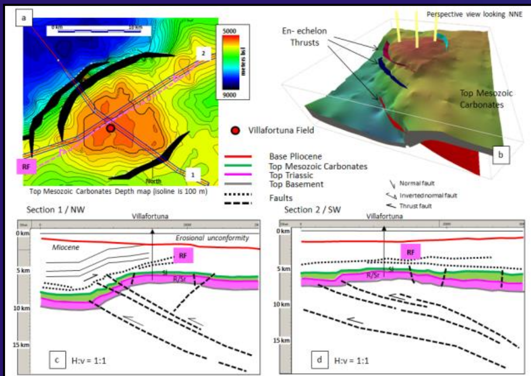

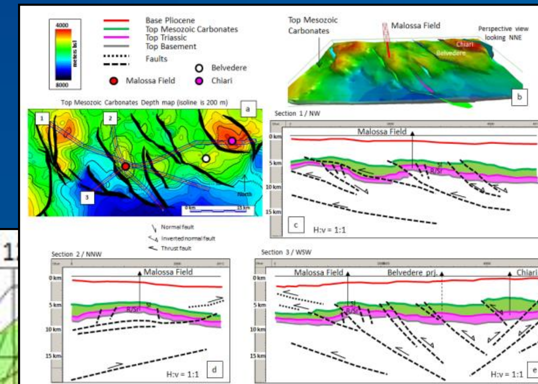

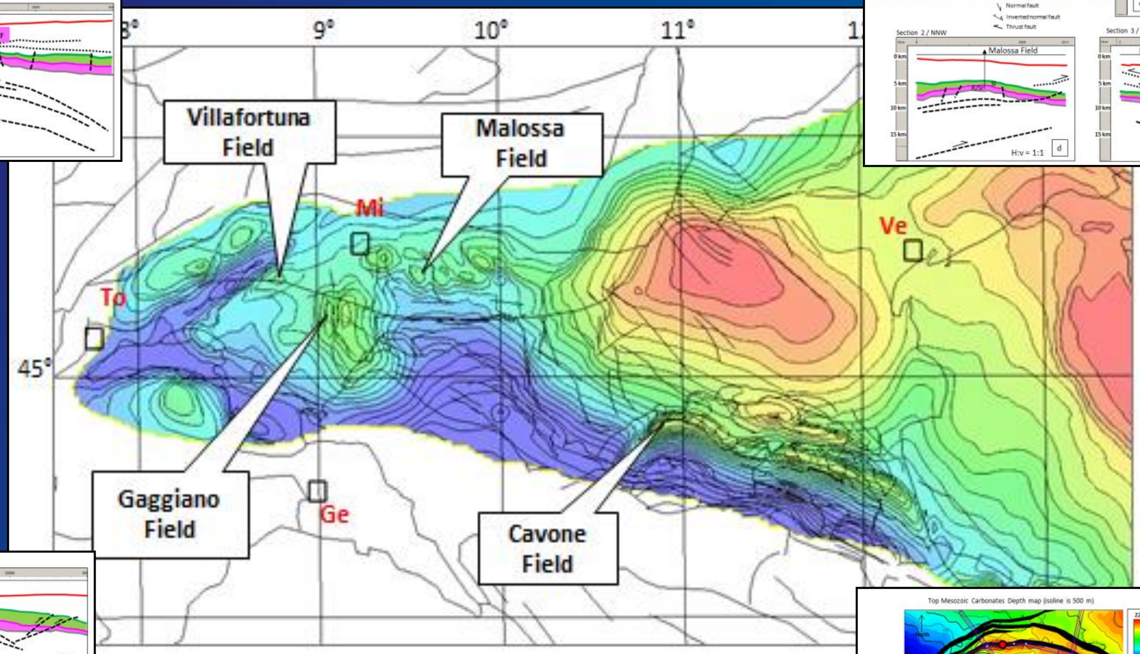

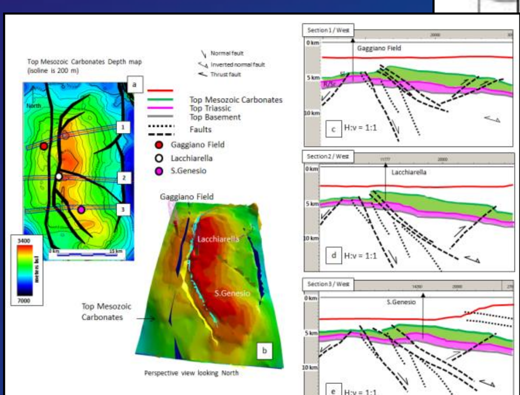

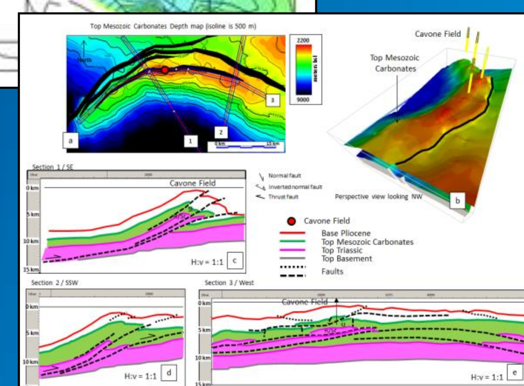

(Turrini, thèse, 2016)

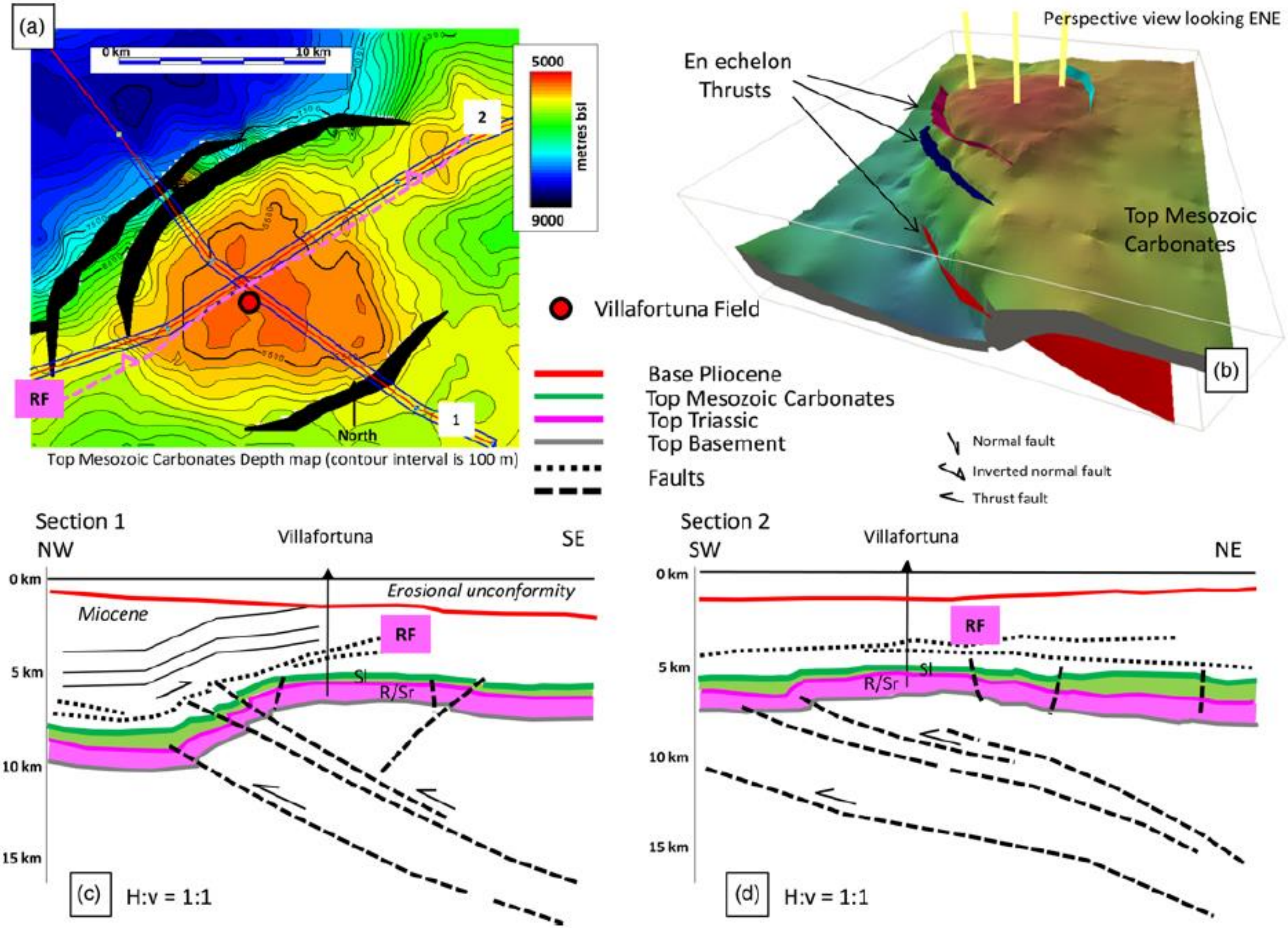

Fig. 4. The Villafortuna oil field structure (see the location in Figs 1 and 2): (**a**) top Mesozoic depth grid; RF, Romentino thrust front; (**b**) 3D structural model of the field structure; and (**c**) & (**d**) cross-sections through the 3D model. R/Sr, reservoir and source; Sl, seal; RF, Romentino thrust front. Note: the Romentino unit geometry within the Oligo-Miocene section in (**c**) & (**d**) is sketched from Pieri & Groppi (1981), Cassano *et al.* (1986) and Bello & Fantoni (2002).

(Turrini et al., 2018)

(Turrini et al., 2018)

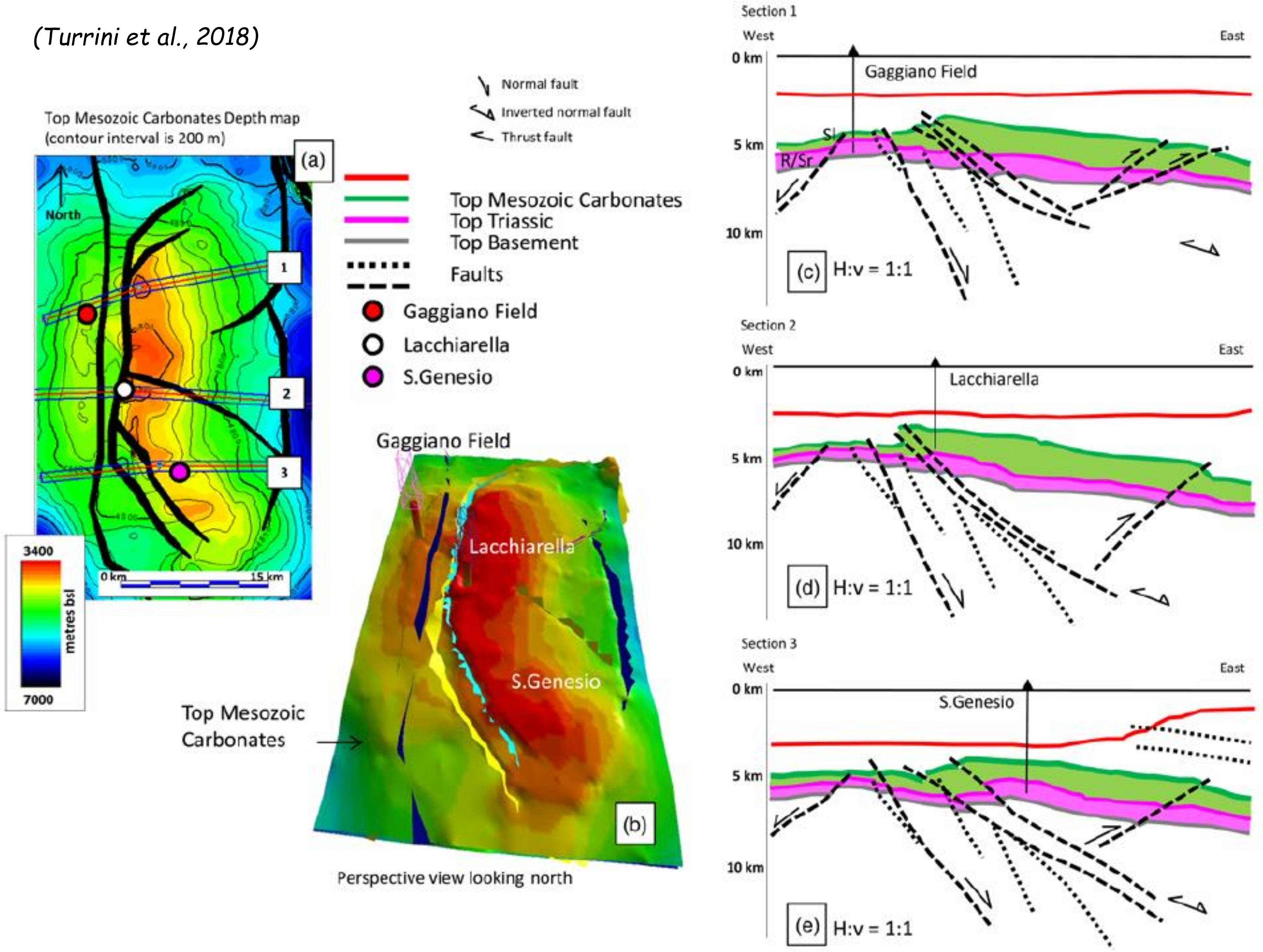

Fig. 5. The Gaggiano oil field and the Lacchiarella structure (see the location in Figs 1 and 2): (**a**) top Mesozoic depth grid; (**b**) 3D structural model of the field and the surrounding structures; and (**c**)–(**e**) cross-sections through the 3D model. R/Sr, reservoir and source; Sl, seal. Note: the extensional terraces in the footwall of the Lacchiarella inverted fault (dotted lines) are sketched based on Cassano *et al.* (1986), Bongiorni (1987) and Fantoni *et al.* (2004).

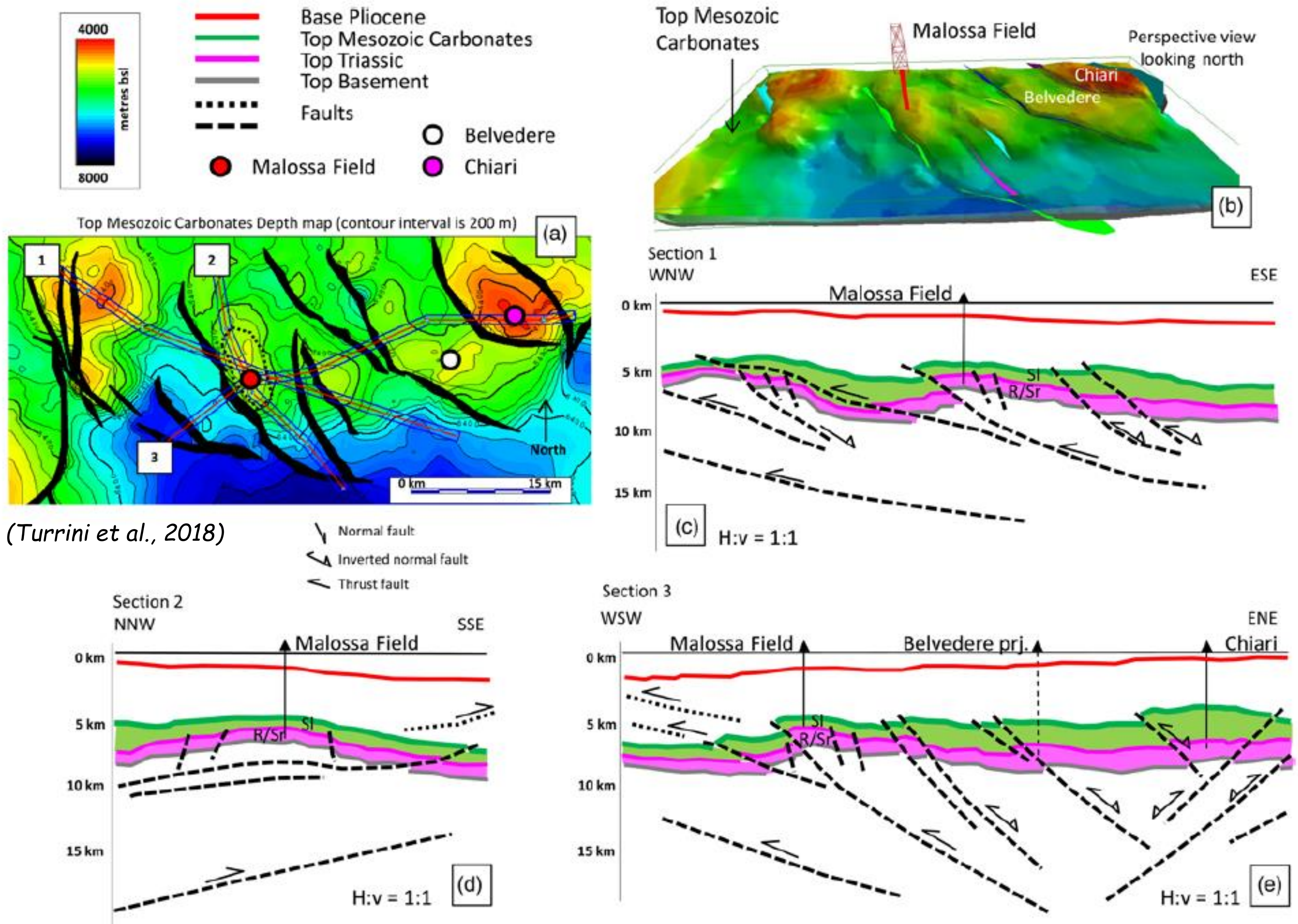

Fig. 6. The Malossa oil field region (see the location in Figs 1 and 2): (**a**) top Mesozoic depth grid; (**b**) 3D structural model of the field and the surrounding structures; and (**c**)–(**e**) cross-sections through the 3D model. R/Sr, reservoir and source; Sl, seal. Belvedere well is projected onto section.

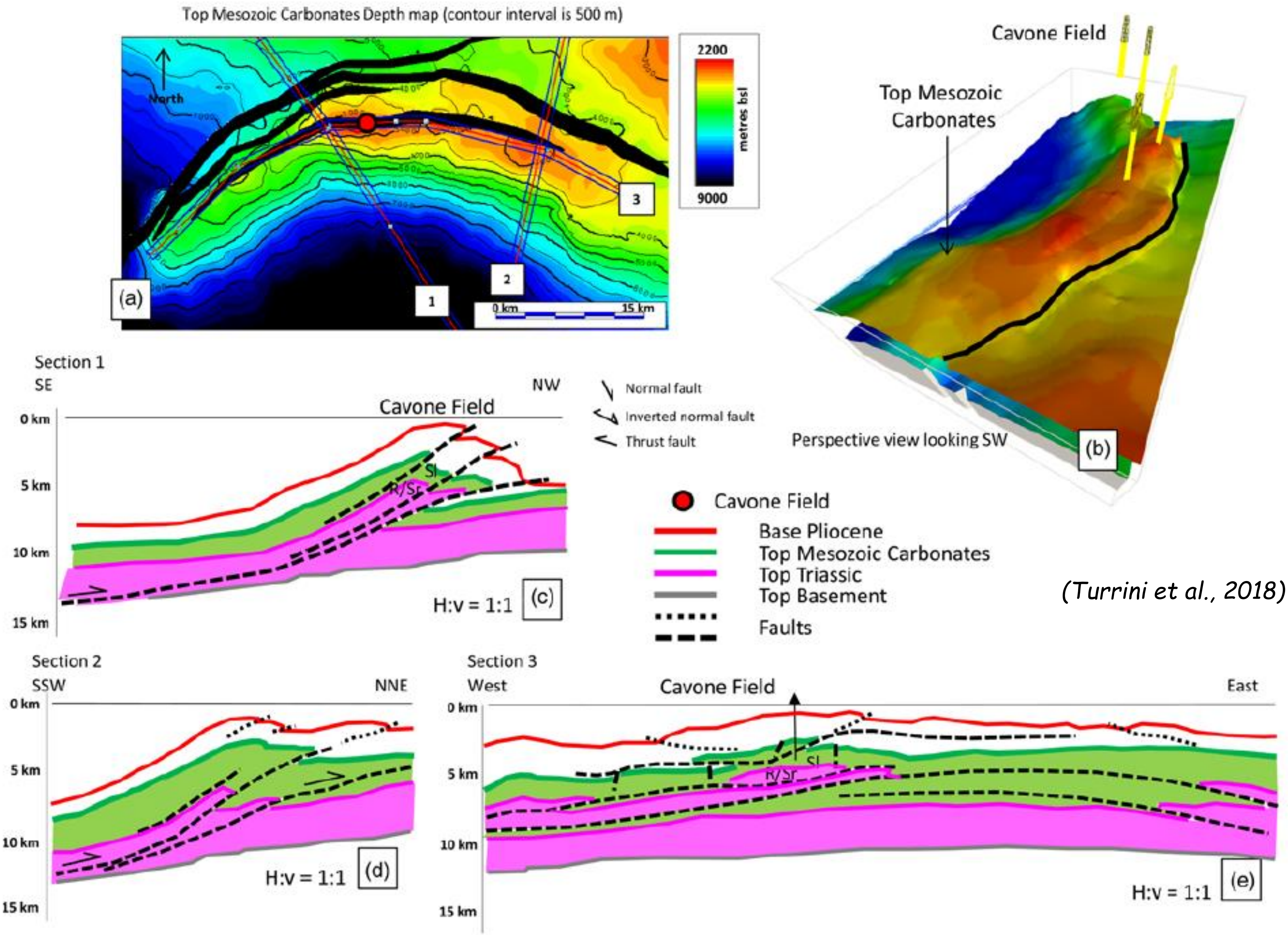

Fig. 7. The Cavone oil field structure (see location in Figs 1 and 2): (**a**) top Mesozoic depth grid; (**b**) 3D structural model of the field and the surrounding structures; and (**c**)–(**e**) cross-sections through the 3D model. R/Sr, reservoir and source; Sl, seal. Note: the stippled segments inside the Cavone thrust-related stack are cross-faults sketched from Nardon *et al.* (1991).

The Genesis and Trinity 3D modelling software from Zetaware Inc. used in this study does not incorporate algorithms that include the overpressure effect.

The most appropriate modelling strategy was therefore to approximate the overpressure effect in the software by applying a reduced heat flow, given that overpressure appears to delay maturation

(Turrini et al., 2018)

Po Valley 3D basin-modelling workflow and associated working phases

Phase 1 – 1D model building:

- reference well and pseudo-well chrono- and lithostratigraphy, back-stripping parameters, thermal parameters, source rock parameters, temperature and maturity data loaded into Genesis (http://www.zetaware.com/);
- definition of geological heat flow and overpressure models, primarily based on the available literature;
- collation of information about palaeowater depth and palaeo-sediment–water interface temperature.

Phase 2 – 1D model calibration and outputs:

- calibration of rock properties and present-day heat flow model against temperature data;
- calibration of back-stripping and heat flow models by forward modelling of thermal maturity and comparison against available maturity data;
- 1D modelling of hydrocarbon generation from key source intervals.

Phase 3 – 3D model building and simulation:

- 3D stratigraphic grids exported from the Kingdom package into the Trinity software, with additional grids generated by interpolating between imported grids as necessary, particularly to define source rock intervals;
- further definition of source intervals within the model, including lateral distribution from gross depositional environment (GDE) maps, thickness and kerogen type as described in the literature;
- definition of 3D palaeotemperature model by calibration against 1D models for key wells and pseudo-wells;
- 3D hydrocarbon maturation/generation/migration history modelling across the Po Valley and analysis of kitchen areas associated with key traps.

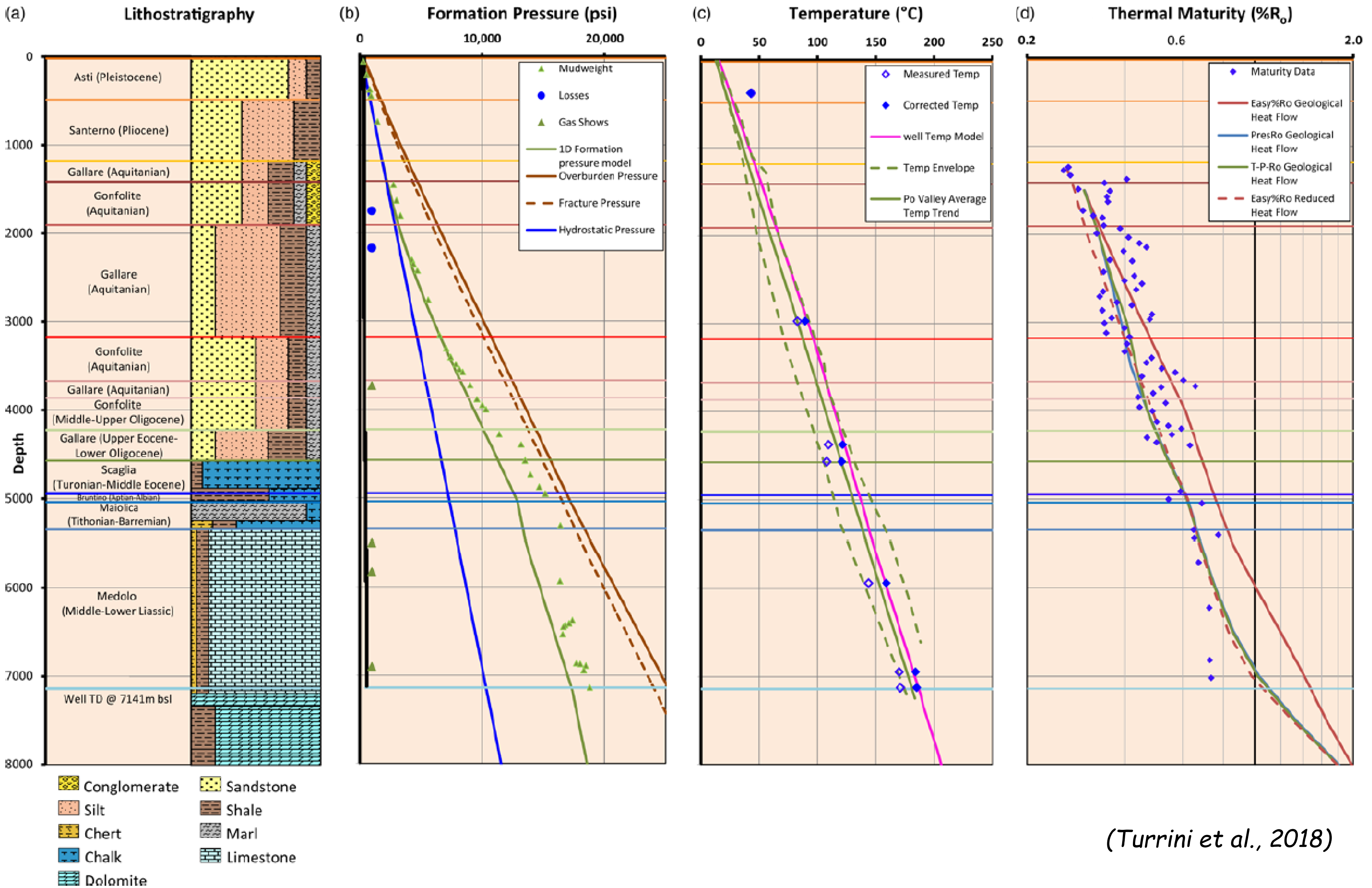

(Turrini et al., 2018)

Formation pressure model shows a significant increase in overpressure below 2000 m through the Tertiary foredeep clastics and basinal carbonates into the highly overpressured deep carbonate aquifer consisting of Liassic and Triassic platform limestones and dolomites

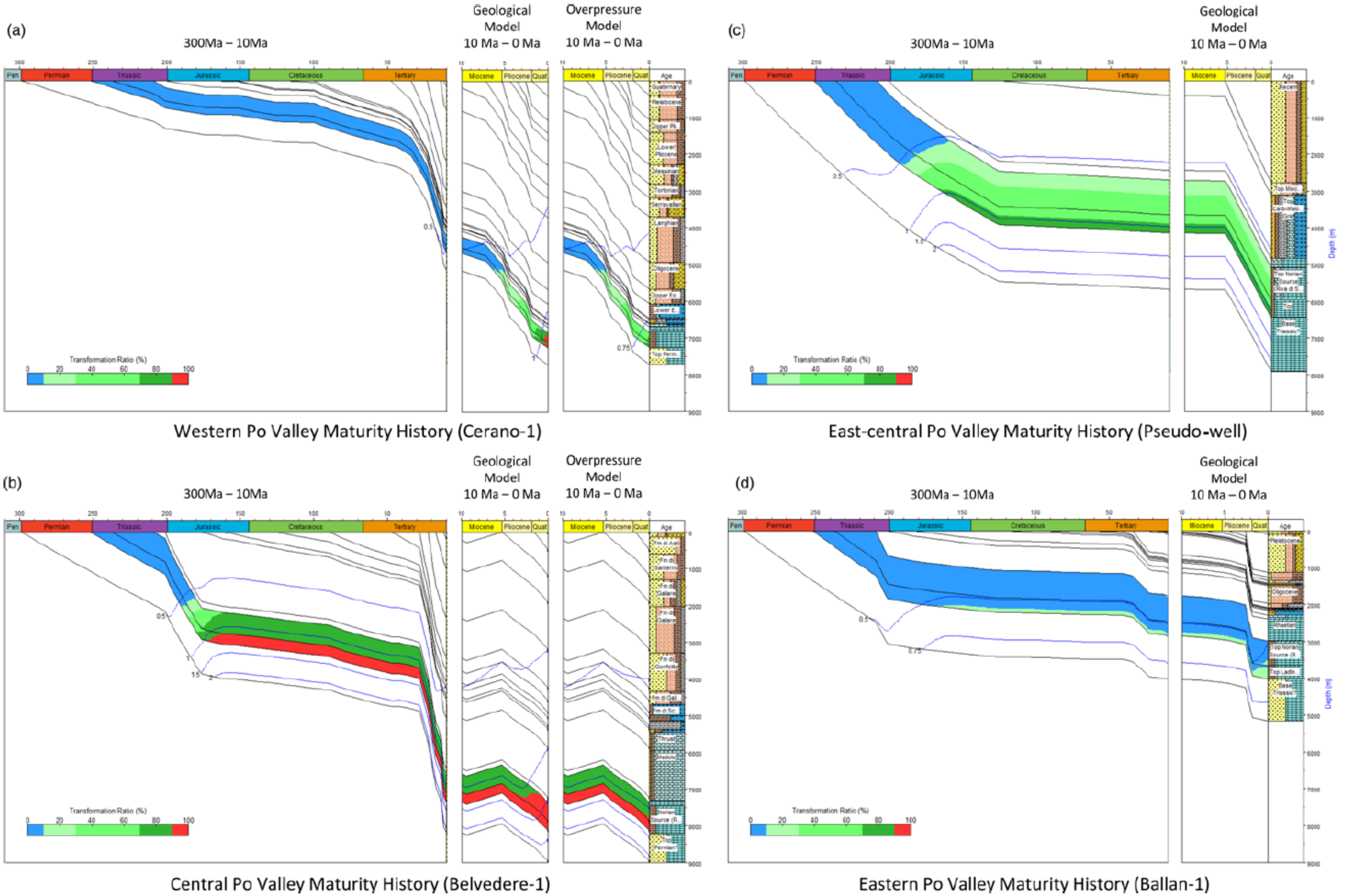

Fig. 11. 1D transformation ratio (TR) maturity histories for four wells from the Po Valley based on initial source rock parameters outlined in Table 1 (the TR scale is 0 – 100): (**a**) Cerano-1 from the western Po Valley; (**b**) Belvedere-1 from the central Po Valley; (**c**) a pseudo-well from the east-central Po Valley; and (**d**) Ballan-1 from the eastern Po Valley (see Fig. 2 for the well locations). Vitrinite reflectance maturities are shown as blue lines (note that for wells in a & b, two histories are shown for the last 10 myr: one based on the geological heat flow and one based on reduced heat flow from end Miocene times to replicate the effect of overpressure; wells in c & d lie outside of the overpressure cell; see the text for explanations).

(Turrini et al., 2018)

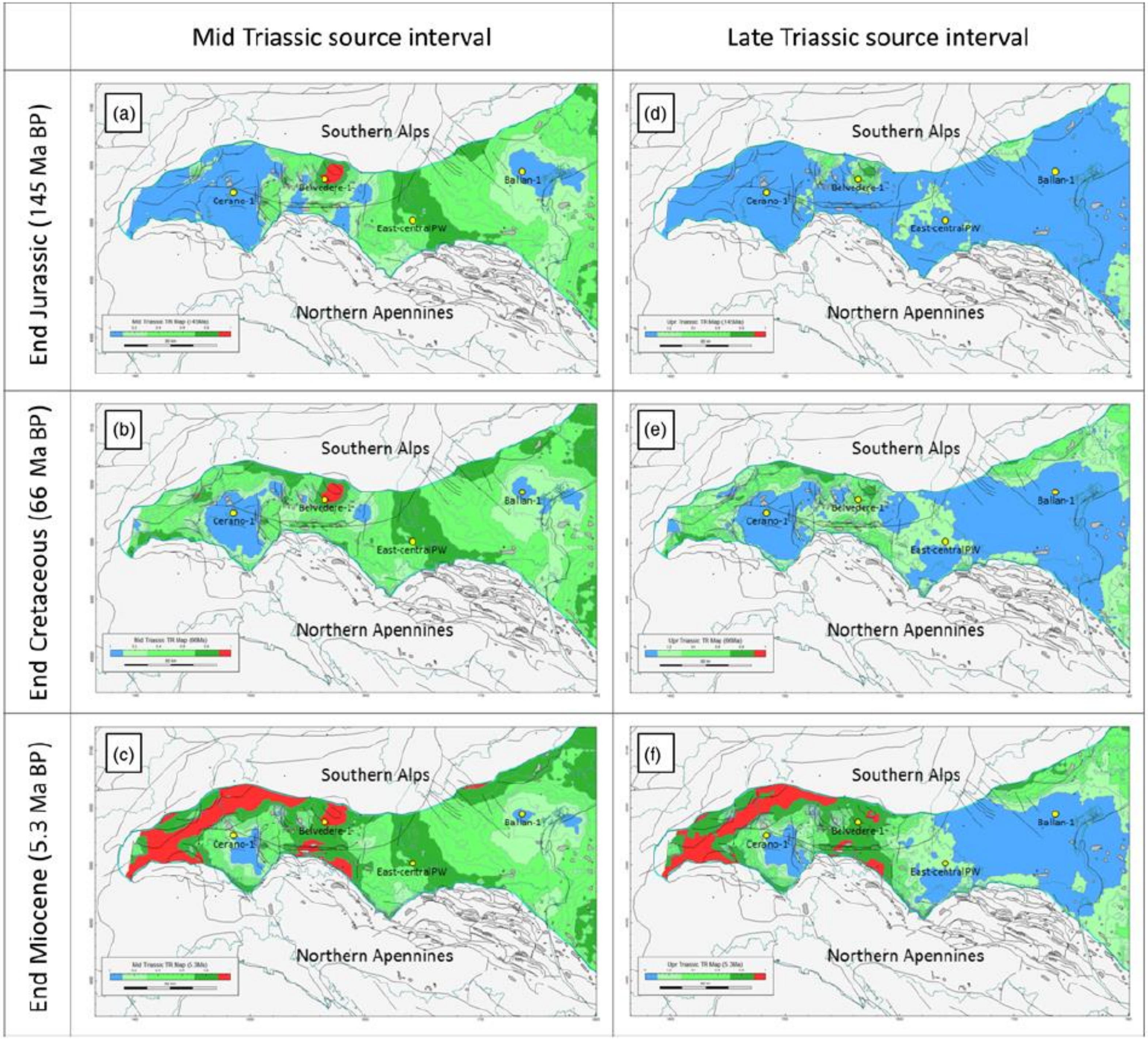

(Turrini et al., 2018)

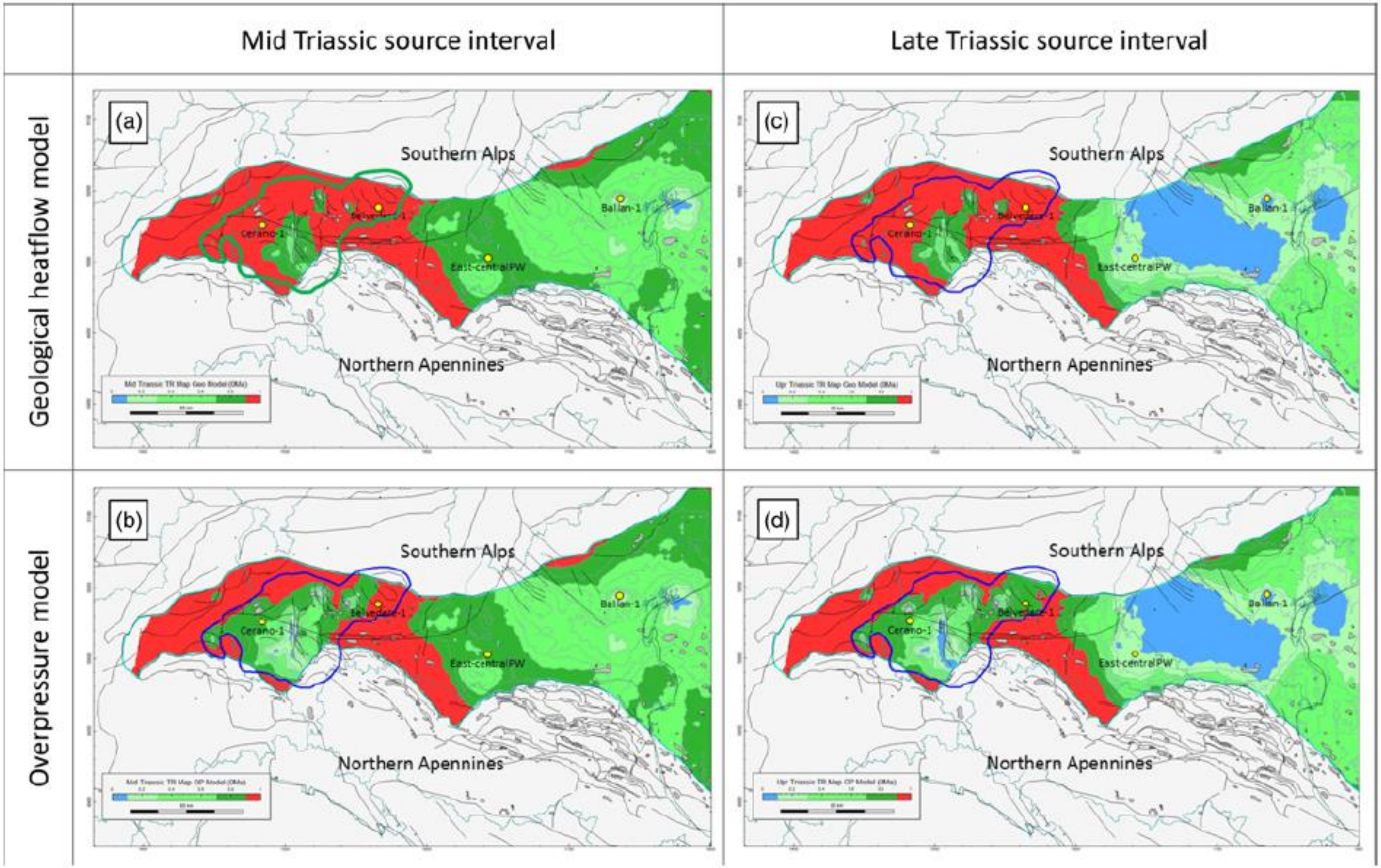

Fig. 13. Present-day transformation ratio (TR) maturity maps (the TR scale is 0 – 1) for the middle Triassic **(a)** & **(b)** and the late Triassic **(c)** & **(d)** source intervals. (a) & (c) show the results of geological heat flow model with (b) & (d) showing the results for the overpressure model, based on the application of reduced Plio-Pleistocene heat flow as described in the text.

In middle–late Miocene times, the deep carbonate aquifer in the western Po Valley became isolated and the Triassic source intervals started to experience overpressure.

The high Plio-Pleistocene sedimentation rate resulted in increased maturity throughout the Po Valley; however, as expected, within the western Po Valley overpressure cell, the increase in maturity is substantially less for the overpressure model than for the geological heat flow model

(Turrini et al., 2018)

(Turrini, thèse, 2016; Turrini et al., 2018)

Hydrocarbons vs Structure timing

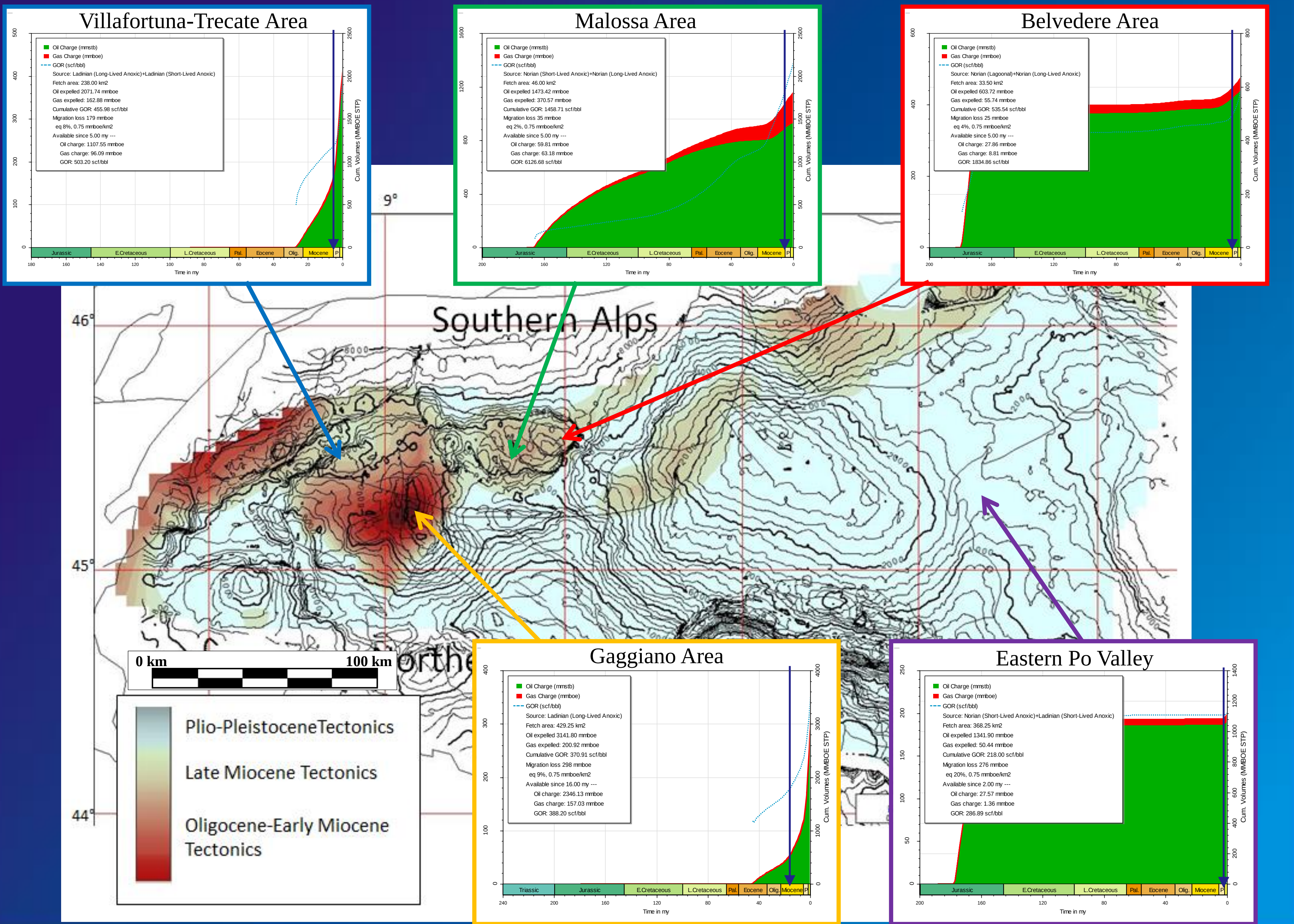

From a hydrocarbon exploration point of view, the timing of hydrocarbon maturation is favorable for exploration in the western Po Valley. Trap formation is likely to have occurred during the Oligocene–late Miocene, along with significant post-Miocene hydrocarbon generation and expulsion (migration?).

In contrast, in the eastern Po Valley, timing is less favourable as traps (Plio- Pleistocene in age) tend to either post-date the main hydrocarbon generation phase or they formed when generation was not advanced enough for migration to occur, or for traps to be filled.

The 3D basin model of the Po Valley provides important insights into the geometry and structural evolution of hydrocarbon-bearing traps, and into the generation and migration of hydrocarbons into these traps.

Hydrocarbon generation is likely to have occurred in two phases: a Jurassic phase and an Alpine Tertiary phase, the latter occurring mainly during the last 5–10 Ma.

Results emphasize the impact that Mesozoic and Tertiary Alpine tectonics had on the development of a successful petroleum system in the Po Valley :

- the Mesozoic extensional phase controlled reservoir and source distribution, trap formation (e.g. the Gaggiano oil field), and the early phases of hydrocarbon maturation in subsiding half-graben associated with high heat flows and substantial synrift to early post-rift sediment accumulation.
- the Tertiary compressional phase controlled trap formation, either by generating new traps (the Cavone oil field) or by reactivating older ones inherited from the Mesozoic extensional phase (the Villafortuna-Trecate and Malossa oil fields).

Clearly, regional hydrocarbon maturation and expulsion/migration are related to rapid foredeep burial ahead of the evolving Southern Alpine and Northern Apenninic thrust belts.

Successful modelling of the effect of overpressure in delaying hydrocarbon maturation

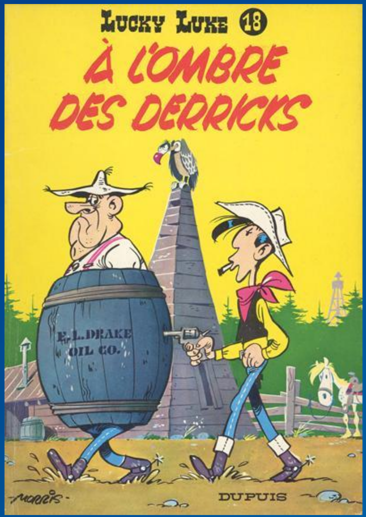

Thank you for your attention